PhD Thesis

Screening and characterization of plant physiological traits using photosynthetic and phenotyping tools

Submitted by

Kenny Paul

Institute of Plant Biology, Biological Research Centre- HAS

Supervisor: Prof. Imre Vass, Director of Plant Biology Institute, BRC-HAS

In partial fulfillment of the requirements

For the Degree of Doctor of Philosophy

Faculty of Science and Informatics, University of Szeged,

Szeged, Hungary

2016

TABLE OF CONTENTS

ACKNOWLEDGEMENTS

I would like to express my sincere thanks and deepest gratitude and appreciation to my supervisor **Prof. Imre Vass** for providing me excellent guidance, support and encouragement throughout my Ph.D. His classic and precise approach in answering scientific questions has been always inspiring to me. The experience I obtained in his group under his guidance will always help me in the future.

I would also like to thank **Dr. Deák Zsuzsanna** for all her guidance and trainings with the fluorescence techniques and useful discussions. I want to thank **Prof. Dénes Dudits** (BRC-HAS) for his guidance, support, and encouragement. I would like to thank **Prof. János Pauk** (Cereal Research Institute, Szeged) and **Dr. Ádam Solti** (Eötvös Loránd University) for all the support and guidance.

I'am thankful to **Dr. Péter Kós, László Sass , Ms. Gabriella Fleit** (Bencuska) and **Mihály Dobó** for all the help and support extended to me. I would like to thank all the past and present members, my colleagues **(István, Sándor, Petra, Ateeq, Sandeesha, Daniel, Leyla, Csaba, Gyula and Éva)** from the **Molecular stress and Photobiology group** for their kind support and care extended to me. I would like to thank all BRC administrative staff who helped me and arranged all necessary documents for my smooth stay at Hungary.

I would like to express my deepest love to my **parents**, my siblings and in-laws for their unconditional love, encouragement, and support all through my life, and to my wife **Shilpa** for her support and patience. I am grateful to **Mrs. Treasa Paily** for all the prayers and spiritual guidance throughout.

Kenny Paul

LIST OF FIGURES AND TABLES

LIST OF ABBREVIATIONS

A	Net CO_2 assimilation rate
AWC	Actual water content
Area	The area above the chlorophyll fluorescence curve between Fo and Fm (reflecting the size of the plastoquinone pool)
CEF	Cyclic electron flow
Chl	Chlorophyll
DFI	Drought factor index
DPWS	Days post water stress
DT	Drought tolerant
DS	Drought sensitive
E	Transpiration/ Evaporation
ETR(I)	Electron transport rate of photosystem I
ETR(II)	Electron transport rate of photosystem II
F_o	Initial fluorescence yield measured at dark adapted state when reaction centres are open
F_m	Maximal fluorescence yield measured at dark adapted state when reaction centres are closed
F_v/F_m	Maximal quantum yield of photosystem II photochemistry
F_v/F_o	Ratio of variable and initial fluorescence yield
g_s	Stomatal conductance
LHC	Light harvesting complex
NPQ	Non-photochemical quenching
PI_{Abs}	Performance index (potential) for energy conservation from photons absorbed by PSII to the reduction of intersystem electron acceptors; ABS is for absorption flux

PPFD	Photosynthetic photon flux density
PSII	Photosystem II
PSI	Photosystem I
PQ	Plastoquinone
Q_A	Primary quinone acceptor of photosystem II
RC/ABS	The amount of active reaction centers per absorption
RWC	Relative water content
SRC	Short rotation coppice
SRF	Short rotation forestry
ST	Salt tolerant
SS	Salt sensitive
$(1-V_j)/ V_j$	Probability of electron transport out of Q_A where $V_j = (F_{2ms} – F_o)/F_v$
Y(I)	Effective quantum yield of photosystem I
Y(II)	Effective quantum yield of photosystem II
Y(NA)	Quantum yield of non-photochemical energy dissipation in PS I due to acceptor side limitation.
Y(ND)	Quantum yield of non-photochemical energy dissipation in PS I due to donor side limitation.
Y(NO)	Quantum yield of nonregulated energy dissipation in PSII
Y(NPQ)	Quantum yield of regulated energy dissipation in PSII
WS	Water stress
WW	Well watered

1. INTRODUCTION AND LITERATURE REVIEW

1.1. Introduction

Plant growth is affected by various factors. Stress is an important challenge which triggers various physiological, molecular and cellular responses in plants. Environmental stresses are the main factors limiting the world's plant production. They are also significant barriers to the introduction of crop plants in noncultivated areas. Plants have to deal with various complex types of interactions involving numerous environmental factors such as temperature, light intensity, water availability and soil composition**.** When the environmental factors extend beyond an optimal range which is characteristic for a particular species, the plant will be subjected to a varying level of stress. There are stress sensitive and resistant plants based on the effectiveness of the protective responses caused by stress. The resistance of the plant to withstand various stress factors plays a vital role for its growth and development. The most important concept of agricultural plant breedings is to gradually form stress resistant crops from stress sensitive cultivars. So breeding of plants for tolerance to various environmental stresses drought, salinity, temperature and desiccation needs proper understanding of physiological characteristics and natural variations.

1.1.1. Theories of drought responses

Drought is a complex environmental stress factor, which can occur at different periods in the growth and development of the crop cycle with different intensities. Water deficit is a multidimensional stress affecting plants at various levels of their organization (Yordanov 2000). Increasing the tolerance to abiotic stresses such as drought is therefore essential for future global food security. The effects of drought

are expected to increase with climate change and increasing water shortage. Drought involves a decrease in environmental water potentials (ψ_w); water flows out of plant cells driven by the potential gradient and cellular dehydration arises as result of osmotic stress. Intracellular water loss damages membrane bilayer structure, disrupts cellular metabolism (Mahajan 2005), inhibits photosynthesis and leads to accumulation of reactive oxygen species (ROS). In addition, stomatal closure reduces CO_2 uptake and photosynthetic activity during drought and prevents further water loss by transpiration (Flexas 2004; Kusumi 2012). Plants have evolved specific acclimation and adaptation mechanisms in order to cope with short- and long-term limitation of water availability. These mechanisms depend on species, genotypes and the co-occurrence with other stresses, such as high temperature or evaporative demand. Analysis of these protective mechanisms can be a key for improved understanding of the molecular background of drought stress tolerance and resistance (Harb 2010; Berger 2010). Drought limits plant growth, affects plant function and reduces the productivity of the land, alters and modifies the physiology, anatomy and morphology of plants (Boyer 1982). Stomatal closure due to drought stress reduce the amount of productive foliage and shortens the vegetative growth period by decreasing the photosynthesis per unit of leaf area (Van Loon 1981; Bradford and Hsiao 1982).

Drought tolerance on the other hand is the ability of plants to utilize limited amount of water, leading to low tissue water potential, with higher efficiency regarding growth, biomass accumulation and reproduction (Ingram & Bartels, 1996). Plants under drought stress accumulate compatible solutes and thrive on by maintaining cell turgor and reducing evaporative water loss (Yancey 1982). Plants can respond to limited soil water availability by various strategies including drought escape, which is described as the ability of plants to complete their life cycle before

severe stress sets in. Besides the escape strategy plants can resist water scarcity conditions via drought avoidance, or drought tolerance (Levitt 1980; Price 2002). Drought avoidance is classified as the ability of plants to maintain high tissue water potential despite soil water deficit. This can be achieved via improved water uptake under stress. The capacity of plant cells to hold acquired water and reduce water loss also confers drought avoidance. Plants can survive water stress by improved root traits, decreasing stomatal conductance, leaf area and radiation absorptivity (Price 2002). On the contrary, stress tolerance mechanisms programme each plant to resist and fight stress by changing their physiology as long as stress exists (Bray, 2000; Taiz, 2010) as in the case of regulation of stomatal aperture and synthesis of osmolites during water deficit stress (Hoekstra, 2001).

In different species it has been shown that drought conditions affect the relationship between the carbon content in photosynthetic organs, such as leaves (source), and the carbon content in heterotrophic organs, such as seeds and roots (sink), indicating that the processes related to carbon partitioning are sensitive targets of drought stress (Cuellar-Ortiz 2008). These alterations cause the abortion of reproductive structures, as well as a decrease in the accumulation of biomass in storage organs, causing losses in crop production (Boyer & Westgate, 2004; Marcelis 2004).

Understanding the biochemical, biophysical, and physiological bases for impairment of photosynthesis in plants which experience internal water deficits becomes of major interest in order to improve plant responses to environmental stresses (Brestic 2013). We studied the effect of drought on the biomass accumulation and grain yield in sensitive Cappelle Desprez and tolerant Plainsman V wheat cultivars.

1.1.2. Salinity responses

Salinity is the concentration of all soluble salts in water or in the soil. Soil salinization is one of the serious forms of soil degradation, which can arise from natural causes and human-mediated activity, such as irrigation in arid and semi-arid regions (Rengasamy 2006). More than 800 million hectares of land throughout the world are salt-affected, which has important consequences for wheat productivity. Increased soil salt concentrations decrease the ability of a plant to take up water and, once Na^+ and Cl^- are taken up in large amounts by roots, both Na^+ and Cl^- negatively affect growth by impairing metabolic processes and decreasing photosynthetic efficiency (Flowers 1995; Maser 2002). Plant growth in combination of salt stress has damaging effects in the form of nutritional imbalance, specific ion change and low osmotic potential causing drought effect (Ashraf 1994; Marschener 1995).

The response to the NaCl was osmotic rather than Na^+-specific (Rahnama 2010). Osmotic stress inhibits the formation of lateral shoots and reduce the rate at which leaves expand. Reduction in shoot biomass is mainly due to the decrease in the number of tillers formed rather than development of individual leafs (Nicolas 1993). Plant growth responds to salinity in two phases: a rapid, osmotic phase that inhibits growth of young leaves, and a slower, ionic phase that accelerates senescence of mature leaves.

Salt tolerance may be defined as a sustained growth of plants in a highly saline environment. Crops vary significantly in their threshold limits of drought/salt tolerance. Screening of crops for tolerance can strengthen the breeding programs by identifying genotypes with high salt tolerance and yield potential. Plant species and varieties vary in their tolerance to salinity and this tolerance also varies with the stage of growth (Rengaswamy 2010). Studies proved salinity causes reduction in number of

tillers in cereals. Salinity tolerance studies aim to increase the ability of plants to decrease the effect of salinity in growth and yield (Roy 2014). To behave salt tolerant there should be considerable biomass production, which is not decreased significantly due to salinity in the soil (Munns and James, 2003). The tolerance of a species to environmental stresses can be studied considering variations in relative growth parameters (Ashraf and Ali, 2008).

Drought and salinity are two widespread environmental abiotic stresses in many regions leading to low water availability and salinization of more than 50% of all arable lands by the year 2050 (Wang 2003). Plant growth in combination of salt stress has damaging effects in the form of nutritional imbalance, specific ion change and low osmotic potential causing drought effect (Ashraf 1994, Marschener 1995). Apart from ion transport processes, the metabolic and hormonal responses are similar between water and salt stress. They increase the concentration of abscisic acid within one hour of treatment (Bensen 1988; He & Cramer, 1996). In the time scale of minutes to days, photosynthetic responses also decrease in both salt and water stress (Munns 2002). The physiological status of stressed plants is usually assessed by the suppression of photosynthesis. To investigate the processes that give rise to tolerance of salt, as distinct from tolerance of osmotic stress, it is necessary to design experiments that distinguish between tolerance of salt and tolerance of water stress and avoid treatments that induce cell plasmolysis.

1.1.3. Desiccation tolerance

Desiccation is the process of extreme drying of plant tissues during which they lose most of their water content. Anhydrobiosis is an astounding strategy that allows certain organisms to survive almost total dehydration. Most higher plants are unable

to survive desiccation to an air-dried state (Bartels 2005). Desiccation tolerance cannot be considered similar to drought tolerance (Alpert, 2005). In desiccation tolerance, plants can survive drying lower than (< 50%) relative humidity (RH) and maintain low intracellular water concentrations. In contrast drought tolerant plants survive low environmental water availability while high internal water contents is required. A small group of vascular angiosperm plants termed "resurrection plants" possess vegetative tissues that are able to tolerate severe desiccation (Gaff 1971). They could dry to equilibrium with the air humidity but resume normal function upon rehydration (Alpert 2005). Resurrection plants can be categorised into two types: poikilochlorophyllous and homoiochlorophyllous. Poikilochlorophyllous lose chlorophyll (Chl) and the thylakoid membranes are at least partially degraded during water loss, while homoiochlorophyllous recover rapidly after desiccation restore photosynthetic activities within 24 hours of rehydration and retain Chl (Bernacchia 1996). The poikilochlorophyllous plants take longer to recover their photosynthetic activity. *Haberlea rhodopensis* is a homoiochlorophyllous poikilohydric plant species which preserves most of the Chl content and photosynthetic apparatus during desiccation in their leaves (Toldi 2009). Haberlea exposed to severe drought or desiccation, and subsequent rehydration showed complete recovery with no signs of damage or severe oxidative stress compared to untreated control plants (Gechev 2013).

Previous studies have shown that *H. rhodopensis* plants growing in a deep shadow in natural conditions were very sensitive to photoinhibition (Georgieva and Maslenkova 2006). Desiccation at irradiance of 350 μmol photon m^{-2} s^{-1} induced irreversible changes in the photosynthetic apparatus, and mature leaves did not recover after rehydration (Georgieva 2008). On the other hand, an unexpected

ecological plasticity of *H. rhodopensis* was found in natural habitats (Daskalova 2011). Besides the shady habitats (‘shade’ plants), several habitats of high irradiance, where plants grow on rocks more exposed to the sunlight (‘sun’ plants), out of the forest coverage and with low air humidity, were also discovered. The high irradiation ecotype is acclimated to a stressful environment thus this pre-conditioning also contributes to the survival of the desiccation under high irradiation conditions.

Cyclic electron flow (CEF) has been well defined as a crucial process for preventing Photosystem I (PSI) from excess light stress through alleviating the over-reduction of PSI acceptor side (Munekage 2004; Huang 2012). The CEF would contribute to producing additional ATP. Another function of CEF is enhancement of the NPQ, through generating the electrochemical potential difference of H^+ across the thylakoid membrane (Munekage 2002). Since CEF is a protectant of PSI against photoinhibition, we studied the severe desiccation and rehydration induced alterations in the electron flow in low and high light acclimated ecotypes to reveal the role of electron transport alterations in desiccation tolerance.

1.1.4. Biomass production

Production of a climate-neutral renewable energy source that does not increase greenhouse gas emissions into the atmosphere gains increasing significance. Biomass is a term for all organic material that is produced by plants (including algae, trees and crops). The use of biomass as renewable energy sources is becoming increasingly necessary to counter the impacts of global warming (McKendry 2002). Energy crops offer clear ecological advantages over fossil fuels, such as a positive carbon balance (due to the photosynthesis of the biomass used as raw material), which contributes to the reduction of greenhouse gas emissions and the low sulphur content, which

contributes to reduced emission of acidifying gases (Gosse, 1995). The type of biomass required is largely determined by the energy conversion process and the form in which the energy is required (McKendry 2002). The carbon dioxide (CO_2) removed from the atmosphere during photosynthesis is converted into organic carbon and stored in biomass, such as trees and crops. When harvested and combusted, the carbon in the biomass is released as CO_2, thus completing the carbon cycle. The carbon in biomass will return to the atmosphere regardless of whether it is burned for energy. Overall, biomass CO_2 neutrality is an inherent property of biomass based on the natural carbon cycle (Johnson 2009). The cultivation of short rotation coppice (SRC), and perennial grasses for heat and power generation can also make a substantial contribution to agricultural bioenergy production. A large number of annual and perennial crops have been investigated for their potential use as energy crops in Europe (Eppler and Petersen 2007). Short Rotation Coppice plantations are characterized by a very short rotation of between 2 and 4 years. Species related to SRC are mainly willow and poplar, but Black locust may also be used. Due to the flexibility associated with harvest time and a variety of inherent logistical benefits, the production of SRC willow for heat and power has made considerable progress. Through alternative silvicultural systems, improved breeding and biotechnology, short-rotation coppice forestry can produce high yields (Hinchee 2009). If high productivity is expected as an anticipation of higher levels of future demand for wood biomass, the most effective strategy is to manage forest for a harvestable crop which will encourage increased investments in forests for biomass energy (Sedjo 2013).

Shrub willow (*Salix spp.*) is a short-rotation woody crop that produces large amounts of harvestable biomass. Willows are considered as plants with high

degree of hybridization, a large genetic variability and impact on morphological variability. Willows are representatives of the population r-strategy with rapid growth, particularly at early seedling stage. In terms of life forms they belong into the shrub or tree phanerophytes. They grow quickly on locations with water-logged soils (Milovanovic 2012).

Advanced cropping technologies and genetic potential of cultivars are considered significant for biomass production of shrub willow plants. Genome size controls the organ structure and function of energy willow for biomass productivity. Genome duplication or tetraploidization has been observed to be a positive approach to enhance the genetic potential of willow cultivars for increasing growth characteristics (Dudits 2016). Among the new "Poli Plusz, PP-E" tetraploid lines, which were produced by Prof. Dénes Dudits and his coworkers, genotypes were identified with improved biomass production whose photosynthetic characeristics were investigated.

1.2. Photosynthesis as a physiological indicator

The light reactions in photosynthesis convert light energy into chemical energy in the forms of ATP and NADPH. The reactions involve two types of electron flow in the thylakoid membrane. While linear electron transport generates both ATP and NADPH, cyclic electron transport around PSI is exclusively involved in ATP synthesis without the accumulation of NADPH (Fig. 1).

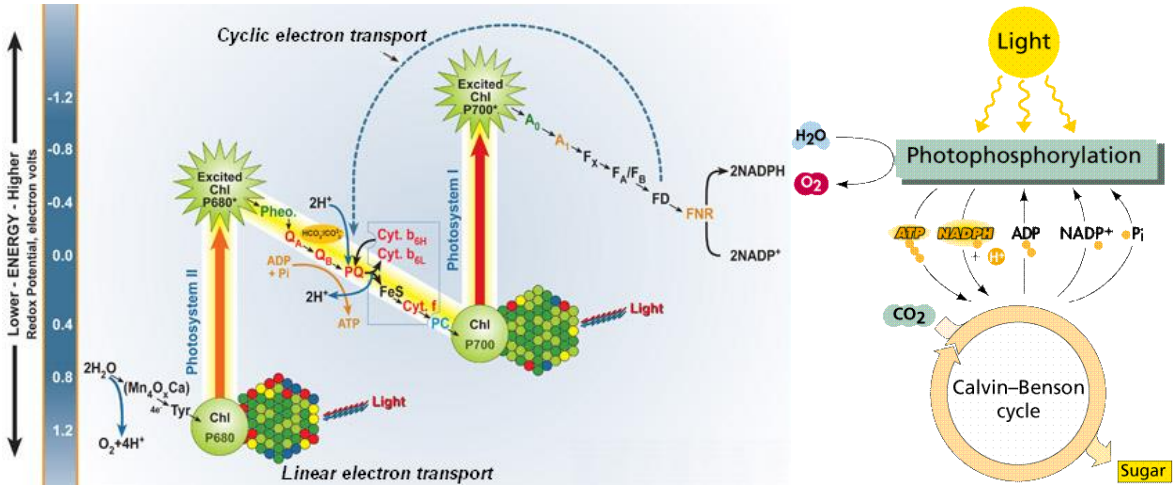

Figure 1. The Z scheme illustration of photosynthetic electron transport chain. Linear electron transport chain in the chloroplasts of plants consisting of both PSII and PSI converts light energy into the chemical forms ATP and NADPH (Govindjee and Wilbert Veit 2010). Cyclic electron transport route is exclusively involved in ATP synthesis by cycling electrons from PSI to plastoquinone via ferredoxin (FD) generating a pH gradient across thylakoid membrane (ΔpH) (Joliot and Johnson 2011). In the Calvin-Benson cycle, free energy of ATP and NADPH are used to fix and reduce CO_2 to form sugar.

ATP and NADPH generated by light reactions are utilized primarily in the Calvin-Benson cycle and photorespiratory cycle (Munekage 2004; Kono 2014 and Yamori 2015) (Fig. 1). From mild drought to severe dehydration stresses, functions of cyclic electron transfer pathways through PSI are activated which have been documented for higher plants (Golding and Johnson 2003; Johnson 2011).

1.2.1. Effect of drought on photosynthesis

The measurement of modulated Chl fluorescence simultaneously with PSI transmittance is able to detect the rates of photochemistry of PSI and PSII with high accuracy. In general the method is applicable to and capable of characterisation of all types of factors affecting the interplay between the photosystems (Pfündel 2009), e.g. different types of stresses and physiological growth reponses. This will increase

reliability of the results and provide very complex information about photosynthetic processes with new possibilities into plant research (Brestic 2013).

At the whole plant level the effect of drought stress is usually perceived as a de**c**rease in photosynthesis and growth. However, photosynthetic responses to drought stress are complex, involving the interplay of different structural levels at different time scales in relation to plant development (Chaves 2009). One of the most frequently used fluorescence parameters in plant physiological research is the maximum quantum yield of PSII photochemistry (F_v/F_m). It is mostly because this parameter is very easy to measure and it is generally well accepted measure of photosynthetic status (Brestic 2013). Mild water stress showed no effects on the maximal quantum yield of PSII photochemistry (F_v/F_m), the rapid fluorescence induction kinetics, and the polyphasic fluorescence transients in dark-adapted leaves, indicating that less severe water stress had no significant effects on the primary photochemistry of PSII (Brestic 2013; Lu and Zhang, 1999). However, in light-adapted leaves, water stress reduced the efficiency of excitation energy capture by open PSII reaction centres (F'v/F'm) and the quantum yield of PSII electron transport (Φ_{PSII}), increased the non-photochemical quenching (qN) and showed no effects on the photochemical quenching (qP) (Lu and Zhang, 1999).

Under mild water deficit the stomatal closure is a first event, followed by changes of photosynthetic reactions (Cornic and Briantais 1991). Stomatal responses are more closely linked to soil moisture content than to leaf water status. This suggests that stomata are responding to "non-hydraulic" chemical signals (Yordanov 2003). This chemical signal has been shown to be abscisic acid (ABA) synthesized in the roots in response to soil drying (Davies and Zang 1991). Stomata often close in

response to drought before any change in leaf water potential and/or leaf water content is detectable (Medrano 2000).

During mild to severe dehydration stresses, functions of cyclic electron transfer pathways through PSI are activated, which have been documented for non-desiccation tolerant higher plants (Golding and Johnson, 2003; Johnson 2011). Cyclic electron flow (CEF) has been well defined as a crucial process for preventing PSI from excess light stress through alleviating the over-reduction of PSI acceptor side (Munekage 2004; Huang 2012). The CEF would contribute to producing additional ATP. Another function of CEF is enhancement of the NPQ, through generating the electrochemical potential difference of H^+ across the thylakoid membrane (Munekage 2002).

1.2.2. Effect of salinity on photosynthesis

Salt stress induces stomatal closure, which affects CO_2 fixation. Exposed to salt and water stresses over days cause reduction in photosynthesis (Munns 2000; Paul and Foyer 2001). In addition to reduced CO_2 diffusion through the stomata, both stresses also result in an apparent reduced CO_2 diffusion through the leaf mesophyll, i.e. in a reduced mesophyll conductance to CO_2 (gm; reviewed in Flexas 2004, 2007). Reduced rate of photosynthesis induces production of ROS, which can cause strong photoinhibition and interrupt photochemical processes in thylakoids (Sairam and Tyagi, 2004).

Analysis of chlorophyll fluorescence showed that applied salt doses did not disturb the light phase of photosynthesis in all cultivars under study (Plazek 2013). Maximal PSII quantum yield (F_v/F_m) which reflects efficiency of PSII electron transport was unaffected in salt stressed condition (Plazek 2013).

1.2.3. Effect of desiccation on photosynthesis

Light exposure together with the retained photosynthetic pigment content and inhibition of photosynthetic electron transport during dehydration is one of the main challenges in desiccation tolerance. Previous results showed that the membrane integrity of sun ecotype *Haberlea* plants was well protected so that desiccation of high light plants did not cause more oxidative damage regardless of the higher malondialdehyde content measured in the well-hydrated *H. rhodopensis* sun plants compared to shade ones (Georgieva 2012). The activity of superoxide dismutases proved to be higher in sun ecotype compared to shade one under desiccation (Solti 2014a). As a result of these protective mechanisms, the inactivation of Photosystem II (PSII) reaction centres (Solti 2014b) and the accumulation of malondialdehyde (Solti 2014a) remained significantly lower compared to the shade ecotype under desiccation. Increased synthesis of phenolics during desiccation of *H. rhodopensis* leaves may also contribute to drought resistance and recovery (Georgieva 2007).

The higher photosynthetic activity of well-hydrated sun plants reduced the susceptibility to photoinhibition. In addition, a significantly lower proportion of light was allocated to photochemistry during desiccation at high irradiance due to the different protective mechanisms (Solti 2014b). Strasser (2010) described that in the shade ecotype, the protection of the photosynthetic machinery is mainly based on a PSII inactivation and excitation energy quenching of inactive reaction centres. This PSII inactivation was triggered even by the initial water loss. Solti (2014) indicated that in the initial stage of water loss, the maximal quantum efficiency of PSII reaction centres decreased gradually in both shade and sun leaves. Nevertheless, the shade ecotype could not perform a significant antennae-based excitation energy quenching, thus the PSII inactivation was faster and more pronounced.

The maximal quantum efficiency of PSII was shown to decrease gradually in both shade and sun ecotype during dehydration. Shade ecotype leaves are not able to increase antennae-based quenching, thus inactivated PSII take part in quenching of excess irradiation (Solti 2014b). As antennae-based non-photochemical quenching increases in parallel with desiccation in sun ecotype, this ecotype seems to be pre-conditioned to quench excess light (Solti 2014b). The reversible modifications in PSII and the enhanced probability for thermal energy dissipation during desiccation also contribute to drought resistance of *H. rhodopensis* and its fast recovery after rehydration (Georgieva 2007).

1.2.4. Photosynthesis and biomass production

The hypothesis that higher leaf photosynthetic rates is necessary for increased yields is a well known theory (Elmore 1980). A strong positive correlation was found between net photosynthesis rate of different tree species and their Chl content or biomass production as described in Naidu (1995). Several factors such as light intensity, ambient CO_2 concentration water, mineral nutrition, growth hormones, pests, weeds and regulation technologies are known to affect leaf photosynthesis also affect yield in the same direction (Moss and Musgrave 1971).

In the natural succession process, they are gradually pushed away by shade trees, which overgrow and overshadow them. Ecological demands of willows to light are high. They have maximum requirements for sun exposure; they are so called heliophytes (light-demanding species). Shade restricts their growth. From an economic and production point of view, all *Salix* species demand year-round available soil moisture. Lack of water during the growing season reduces their height increases, but also resistance to biological impacts (Jurekova 2011). Requirements for soil

moisture are specific to particular willow species. Selection of a suitable site, based on knowledge of ecological requirements of *Salix* is an essential step to ensuring optimal production and economic use of this woody crop. The system of willow biomass production should be implemented in order to achieve maximum biomass production while maintaining good soil quality and ensuring nutrient cycle (Jurekova 2011; Milovanovic 2012).

Biomass productivity of shrub willows is largely dependent on coppicing capability, early vigorous growth, shoot growth rate, size of root system, photosynthetic efficiency, formation and composition of woody stems. Improvement of physiological traits by autotetraploidization is a novel approach for maximizing biomass yield. The present study was designed to quantify the pattern of biomass accumulation, photosynthetic electron flow efficiency and gas exchange activities at different growth stages of tetraploid willows in comparison to diploid ones.

1.3. Phenotyping

1.3.1. Plant Phenotyping

For optimizing cereal crop productivity under drought stress it is highly important to characterize and understand the relationship between the responses induced by water limitation at the level of green biomass accumulation and seed production. Phenotyping has revolutionized plant breeding up to the level of trait predictions. Precision phenotyping is a rapidly growing field of plant sciences, which provides excellent tools for quantitative characterization of the adverse consequences of various stress effects including drought (Berger 2010; Golzarian 2011).

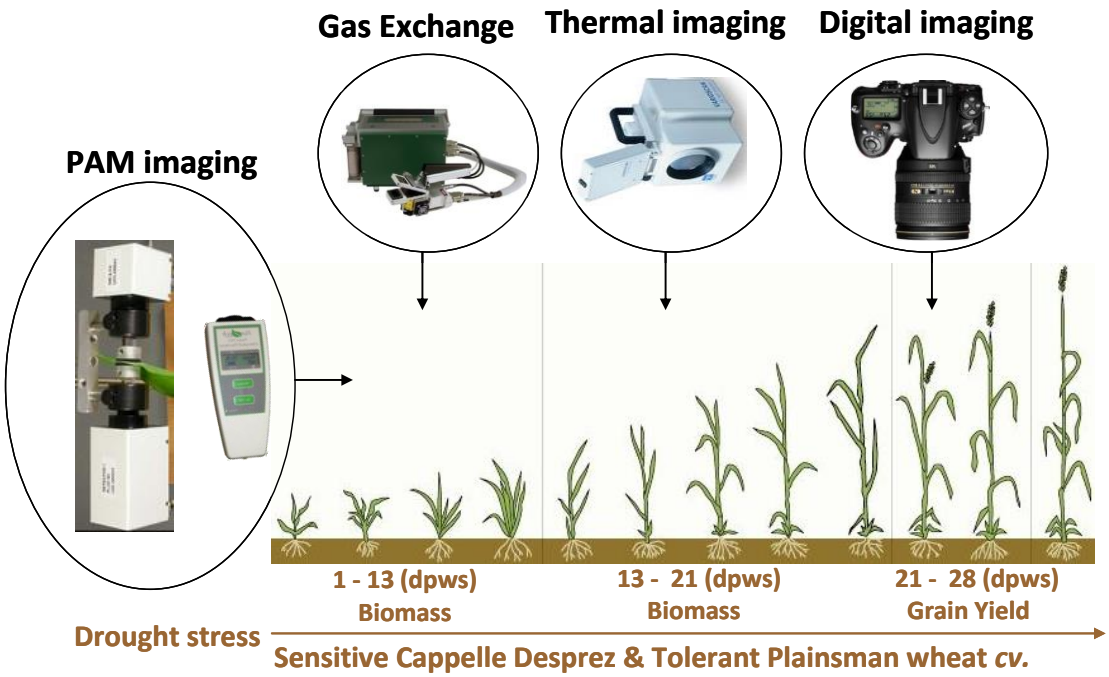

Figure 2. A scheme of sampling prototype used in plant phenotyping for studying drought stress.

Phenotyping approaches vary from manual platforms to complex robotic systems with automated data acquisition and measurement workflows. They usually comprise non-invasive measurements at a spatial resolution stretching from the sub cellular level to canopy stands, and temporal resolutions ranging from seconds to entire growing seasons (Dhondt 2013). Despite the obviously very high potential of plant phenotyping to characterize the consequences of stress-induced effects, there is a highly important and often overlooked question in the case of cereal crops: whether the most easily quantified phenotypic parameters such as the above ground green biomass, can predict correctly the grain yield, or not?

1.3.2. Non-invasive plant phenotyping tools

Nowadays, with the availability of various non invasive photosynthetic phenotyping tools, it is possible to correlate and characterise plants under different abiotic and biotic conditions.

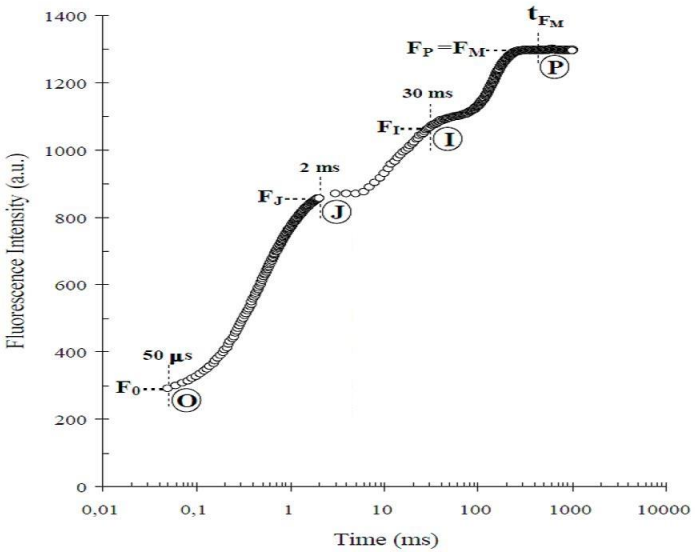

Figure 3. A typical Chl *a* polyphasic fluorescence rise O-J-I-P, exhibited by higher plants. The transient is plotted on a logarithmic time scale from 50 µs to 1 s. The characteristic parameters are: the fluorescence intensity F_O (at 50 µs); the fluorescence intensities F_J (at 2 ms) and F_I (at 30 ms); the maximal fluorescence intensity, $F_P = F_M$ (at t_{FM}) (Strasser 2004).

Measurement of the *OJIP polyphasic fluorescence* rise is widely accepted technique to monitor the accumulation of the reduced form of the primary quinone acceptor Q_A (i.e. the reaction center's closure), which is the net result of Q_A reduction due to Photosystem II (PSII) activity and Q_A^- reoxidation due to Photosystem I (PSI) activity (Strasser 2000). The polyphasic OJIP fluorescence transient was used to evaluate PSII function. Drought and re-watering had little effect on the maximum quantum yield of primary photochemistry F_V/F_M (Lu and Zhang 1999). The photosynthetic performance index (PI) is the product of an antenna, reaction center and electron transport dependent parameter, which revealed differences between wheat varieties as a function of drought and re-watering (Zivcak 2008; Brestic and Zivcak 2013). For screening for drought stress tolerance, changes in the PI during a 2-week drought stress treatment were analysed and a new parameter was defined: the drought factor index (Oukarroum 2007). The drought factor index (DFI) of the tested

varieties correlated with their drought tolerance. The recorded chlorophyll a fluorescence transients were analysed by the so-called JIP-test that translates stress-induced alterations in these transients to changes in biophysical parameters quantifying the energy flow through PSII (Strauss 2006). The performance index (PI_{ABS}) parameter is a multi-parametric expression that combines the three main functional steps taking place in PSII (light energy absorption, excitation energy trapping, and conversion of excitation energy to electron transport) (Strauss 2006).

Measuring *gas exchange* is the most commonly utilized technique at present for commercial and research purposes in order to measure photosynthesis of individual leaves, whole plants or plant canopy. Gas exchange measurements provide direct measure of the net rate of photosynthetic carbon assimilation (Long 1996). Net photosynthesis and stomatal conductance were significantly lower in the unirrigated wheat leaves (Marco 1988).

Simultaneous measurements of variable *chlorophyll fluorescence and P700 absorbance* changes represent a powerful tool to monitor PSI and PSII functions in parallel. P700 provides analogous information on PSI electron transport as chlorophyll fluorescence provides on PSII. Based on a highly innovative pulse-modulation technique, absorbance changes of P700 (reaction center chlorophyll of PSI) can be measured with a similar signal/noise ratio as chlorophyll fluorescence. Saturation pulses are applied for assessment of energy conversion efficiency in PSI and PSII. Differences between quantum yields, Y(I) and Y(II) and between apparent electron transport rates, ETR(I) and ETR(II), may be related to cyclic electron flow, differences in energy distribution and/or PSI/ PSII ratio.

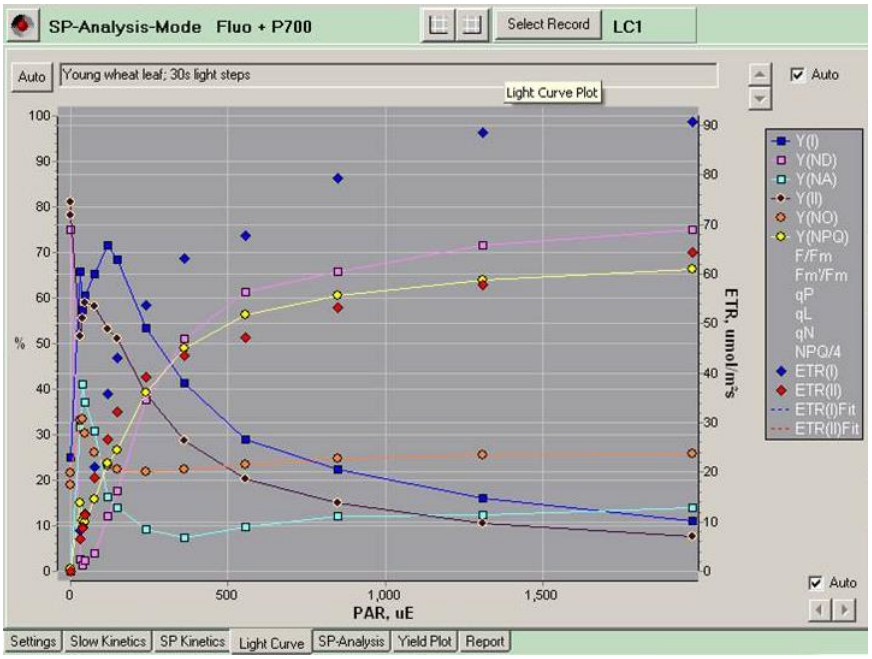

Figure 4. Simultaneous recording of Chl fluorescence and P700 light response curves of 30s light steps in a young wheat leaf. (http://www.walz.com/downloads/manuals/dual-pam-100/Dual-PAM_1e.pdf).

Thermoimaging – a highly sensitive and non-invasive method of leaf temperature measurement could be used to correlate the effect of evaporation and stomatal closure (Grant 2006). In the absence of evaporative cooling through the stomata, leaf temperature is increased (Kana and Vass, 2008). Prolonged transpiration rate is a secondary associated mechanism during drought stress (Evans 1972).

Digital phenotyping of plants, which is based on digital imaging and image processing have revolutionized plant phenotyping and are now a major tool for phenotypic trait measurement (Dhondt 2013). The applicability of freely accessible softwares, like ImageJ, in digital phenotyping plays a vital role for accessing traits like biomass production (Hartmann 2011). Determination of the area covered by green leaves and shoots has proven to be a very useful approach for monitoring plant growth non-destructively under various stress conditions (Kacira and Ling 2001).

In the Plant Biology Institute of BRC a greenhouse-based stress diagnostic system has been developed during the last ten years by using semi-automatic leaf area determination, which could be used to analyse the responses of different wheat genotypes by modelling drought and salt stress (Majer 2008, Cseri 2013, Feher-Juhasz 2014).

1.4. Research approach and perspectives

The productivity and distribution of plants are affected to a large extent by environmental conditions, due to the immobile nature of plants. Wheat (*Triticum aestivum* L.) is one of the main agricultural crops cultivated in different environments. Grain yield is the most important parameter of the wheat genotypes, which are cultivated for grain production. Growth and yield are functions of a large number of metabolic processes, which are affected by environmental and genetic factors. Studies of growth pattern and its understanding not only tell us how plant accumulates dry matter, but also reveals the events which can make a plant more or less productive (Ahad, 1986). The need to bridge the gap between genotype and phenotype, correlate gene function, discover plant performance, mechanisms and adaptations of plant responses to the environment could be solved by using fast and high resolution plant phenotyping tools (Furbank 2009). Mining natural variations of plant physiological growth and correlate aspects of ’agronomical and morphological’ traits provides a powerful tool for optimising crop productivity. This approach is based on the prediction of physiological parameters which correlate with stress tolerance and can be used to study several physiological questions of environmental stresses which can facilitate the breeding process of wheat.

1.5. Objectives of the thesis

Our research group has been working for years in the development of a complex stress diagnostic system which could be used for studying and characterising plant growth and development under various stressfull conditions. Our primary interest here was to correlate natural variations of physiological responses using photosynthetic and phenotyping tools. By considering these main objectives, our aims were:

1) To characterise key physiological and economically important traits 'biomass and grain yield'using our complex stress diagnostic protocols.
2) To compare the yields of biomass and grain production based on the phenotypic and photosynthetic parameters obtained during biomass accumulation and grain filling period.
3) To evaluate prediction of biomass and grain yield based on the photosynthetic measurements taken from *'secondary leaves'* of vegetative phase and *'flag leaf'* of grain filling reproductive phase in sensitive and tolerant wheat varieties under severe drought and salinity stress conditions.
4) To monitor the synergistic effects of drought and salt stress in various wheat cultivars of different geographic origin. To explain the effects of high salt stress on energy absorption and energy dissipation on the basis of various parameters from fluorescence induction curves.
5) To deduce electron flow responses under desiccation and rehydration of the resurrection plant *Haberlea rhodopensis* grown in different natural ecotypes.
6) To determine the photosynthetic efficacy of tetraploid willow plants for enhanced growth and biomass production.

2. MATERIALS AND METHODS

2.1. Plant material and experimental conditions

2.1.1. Drought experiment

Vernalization of one-week old seedlings was carried out for 6-week, at 4^{o}C in a cold chamber, under continuous dim light. Vernalized plantlets of the Cappelle Desprez and Plainsman V (Guóth 2009) (http://genbank.vurv.cz/wheat/pedigree) winter wheat (*Triticum aestivum* L.) varieties were planted in a soil-sand-peat mixture (3:1:1, v/v/v). Plants were regularly irrigated and grown in controlled green-house conditions for two weeks before starting the drought stress treatment. Photosynthetically active radiation (PAR) within controlled environment was maintained with a 14 h photoperiod at a PPFD of 400 – 500 µmol m^{-2} s^{-1}, 22-25 °C and ca. 45–55% relative humidity.

Drought stress was induced on the above mentioned seedlings (4- 5 leaf stage) by limiting irrigation to ensure 10% field capacity of the soil using the computer-controlled water supply system of our phenotyping platform (Cseri 2013) for a period of 35 days. The well watered control plants were irrigated to keep 60 % field capacity of the soil. Biomass accumulation in the vegetative phase, i.e. in the first 3 weeks of the drought treatment, was monitored from the younger fully developed leaves, which are denoted as '*Secondary leaves'.* While in the reproductive grain filling phase, in the 4th-5th week of the drought treatment, the measurements were performed on the last fully developed leaf, denoted as *'flag leaf'*. Six replicates of each treatment were used for the study in three separate experimental trials conducted in August-September 2012, April- May and July- August 2013 respectively.

2.1.2. Salinity and drought experiment

The experiment was conducted with 14 wheat (*Triticum aestivum* L.) cultivars from Serbia (5), Austria (4) and Azerbaijan (5), which were chosen on the basis of data available for their salt and drought tolerance. Serbian wheat cultivars used were Balkan, NS 40S (DT), NS Avangarda, Suboticanka (DS), Renesansa. (Babic 2011, Dencic 2000, Dimitrijevic 2009). Austrian wheat cultivars used were Donnato, Midas (DT), Gallio, Capo (DT) (Teizer 2010). Azerbaijani wheat cultivars used were Tale 38 (DS), Azamatli-95 (DT), Giymatli-2/17 (DS), Gobustan (DT), Gyrmyzy gul- 1 (DS) (Babyev 2013, Huseynova 2007, Talai 2010).

Plants were grown under four different water/salt treatment (T) conditions:

T1- Well watered (60 % water capacity) and no salt (NaCl) added (control 1),

T2- Water limited (20 % water capacity) and no salt (NaCl) added (control 2),

T3- Well watered (60 % water capacity) and saline conditions (0.2% NaCl or 2g /kg soil),

T4- Water limited (20 % water capacity) and saline conditions (0.2% NaCl or 2g /kg soil).

Watering was done automatically by a plant mover system including a balance in connection with a computer- mediated peristaltic pump. As pots had a radiofrequency identifier, watering data could be stored automatically by computer. PAR levels within controlled greenhouse environment was maintained with a 14 h photoperiod at a PPFD of 400 – 550 μmol m^{-2} s^{-1}. The daytime temperatures were 8-15°C for young plants at seedling stage, 16-22°C for the growing phase, and 23-28°C after heading. The night time temperatures were ca 5°C lower than the daytime minimum temperatures, but did not drop below 5°C even in case of the young plants at seedling stage.

Biomass accumulation in the vegetative phase, i.e. in the first 3^{rd} / 4^{th} weeks post treatment imposition, was monitored from the younger fully developed leaves, which are denoted as '*Secondary leaves'*. While in the reproductive grain filling phase, the measurements were performed on the last fully developed leaf, denoted as *'flag leaf'* in the 5^{th} / 6^{th} week post treatment.

At 4- 5 leaf stage, irrigation was limited to 20% field capacity of the soil using the computer-controlled water supply system of our phenotyping platform (Cseri 2013). Experiments with 14 different wheat cv. were monitored for 13 weeks post treatment. The control well watered plants were irrigated to keep 60 % field capacity of the soil. At the end of the experiment grain production parameters (above ground biomass, plant height, yield/main spike, yield/side tillers and total grain yield weight etc.) were measured. Five replicates of each treatment were used for the study.

2.1.3. Desiccation experiment

Haberlea rhodopensis Friv. tufts were collected in the Rhodope Mountains (Bulgaria) at two neighbouring natural habitats. Low-light-adapted ecotype (Shade) plants were collected at an altitude of 1000 m, from rocks below trees where the average daily irradiance was very low (20–30 μmol m^{-2} s^{-1} PPFD), the daytime temperature and relative humidity, measured in June were 21–25 °C and 40–45%, respectively. High-light-adapted ecotype (Sun) plants were collected at an altitude of 1200 m, where the light intensity measured in the midday in June was 1300–1700 μmol m^{-2} s^{-1} PPFD, the temperature at leaf level and the relative humidity were 30–37 °C and 15–30%, respectively. Plants were cultivated under controlled environments referring to the natural conditions until the measurements. Leaves of adult rosettes

from the same ecotype and of similar size and appearance were selected for the experiments.

Detached three leaf replicates of sun and shade ecotypes were kept in partially closed transparent glass petri plates at room temperature of low light laboratory conditions in each replication. Leaf weight was monitored daily using analytical weighing balance. Recovery was done by keeping the leaf samples in the wet chromatograph paper kept inside the closed petri plates. Photosynthetic measurements were carried out daily in the morning 9–11 am timings.

2.2. Relative water content (RWC)

The relative leaf water content (RWC) was calculated as 100*(SW-DW)/FW, where DW= dry weight, FW= fresh weight and SW= saturated weight. SW was measured after saturating the water content of leaf discs for 24 hours. DW was measured after desiccating leaf discs at 60 °C to air-dry state.

2.3. Pigment content estimation

Sampling was done on the sixth or seventh fully opened leaves from the top. Pigment extraction was done using dimethylformamide (Jacobsen 2012). Leaf discs of 0.8 cm were immersed in 1mL of dimethylformamide for 48 h. The spectral determination of chlorophylls a and b, as well as total carotenoids, was carried out according to Wellburn (1994): Car(x + c) mg/cm^2 = total leaf carotenoids [xanthophyll (x) plus carotenes (c)].

2.4. Proline content

0.1g of fresh leaf samples (*fully developed leaf below flag leaves*) were

collected in liquid nitrogen from all the wheat cultivars which are subjected to various treatment conditions. Leaf proline content was analyzed at the 10^{th} week post stress treatment. The content of free proline in wheat leaves was determined as described by (Bates 1973). Samples were homogenized in 3% (w/v) sulfosalicylic acid to precipitate protein, and centrifuged at 14,000xg for 10 min. The reaction mixture contained 2 mL glacial acetic acid, 2 mL ninhydrin reagent (2.50 % w/v ninhydrin in 60 % v/v 6 M phosphoric acid) and 2 mL of supernatant. The incubation lasted for 1 h at 90°C then, after stopping the reaction with ice, 4 cm^3 of toluene was added and mixed by vortex. The upper toluene phase was decanted into a glass cuvette and absorbance was measured at k = 520 nm. The concentration was assayed using proline as the calibration standard. Each assay was performed in five replicates representing five leaves from different plants for each treatment. The content of proline was expressed as mg proline/ (g of leaf fresh weight).

2.5. Gas exchange measurements

Gas exchange parameters: CO_2 uptake rate, transpiration, stomatal conductance and intercellular CO_2 concentration were measured by using a Li-6400 gas analyzer (Licor, Lincoln, Nebraska, USA). Two to three selected leaves of secondary as well as flag leaf from plant replicates under respective drought regime were inserted into the gas cuvette for individual measurements. The gas cuvette conditions were set to 400 ppm CO_2, ambient temperature and 400 µmol m^{-2} s^{-1} growth light intensity.

2.6. Fluorescence measurements

2.6.1. OJIP chl *a* fluorescence

OJIP chlorophyll *a* fluorescence transients were measured using a Plant Efficiency Analyzer (Pocket Pea, Hansatech, Norfolk, UK). The transients were induced by red light from an LED source (627 nm, up to 3500 μmoles m^{-2} s^{-1} intensity) for drought and salt stress experiments while OJIP test for desiccation experiment on *Haberlea* leaves (2 s saturating pulse at 639 nm) were measured by a double-modulation FL 3000 Fluorometer (Photon Systems Instruments Ltd., Brno) at room temperature kept in cuvette.

Prior to measurements performed on the adaxial surface, leaves were dark adapted for 20 min using light tight leaf-clips. The OJIP-test (Strasser 2000) was used to analyze the chlorophyll *a* fluorescence transients and the following original data were acquired: O (F_o) initial fluorescence level (measured at 50 μs), P (F_m) maximal fluorescence intensity, as well as the J (at about 2 ms) and the I (at about 30 ms) intermediate fluorescence levels. From these specific fluorescence features the following parameters of photosynthetic efficiency were calculated: Maximal PSII quantum yield, F_v/F_m; The ratio of variable fluorescence to initial fluorescence, F_v/F_o where $F_v = F_m - F_o$; Probability of electron transport out of Q_A**,** $(1-V_j)/ V_j$ where $V_j = (F_{2ms} - F_o)/F_v$; Total complementary area between the fluorescence induction curve and F_m of the OJIP curve, Area; Q_A reducing reaction centers per PSII antenna chlorophyll, $RC/ABS = (F_V/F_M) . (F_J - F_0) /[4. (F_{300\mu s} - F_0)]$ (Campos 2014; Strasser 2004); Performance index (potential) for energy conservation from photons absorbed by PSII to the reduction of intersystem electron acceptors, PI_{Abs} (Zivcak 2008; Campos 2014).

$$\mathbf{PI_{abs}} = \frac{\mathbf{1-(F_o/F_m)}}{\mathbf{M_o/V_j}} \mathbf{x} \frac{\mathbf{F_m - Fo}}{\mathbf{F_o}} \mathbf{x} \frac{\mathbf{1-V_j}}{\mathbf{V_j}}$$

where M_o= 4* ($F_{300\ \mu s} - F_o$)/ ($F_M - F_o$) represents initial slope of fluorescence kinetics.

For screening of drought stress tolerance a further parameter, the so called drought factor index (DFI) was used, which is derived from PI values measured after 1 or 2 weeks of drought treatment, and reflects the ability of plants to tolerate sustained drought stress conditions (Oukarroum 2007).

$$\mathbf{(DFI)=\log (PI_{week1}/ PI_{control})+ 2 \log (PI_{week\ 2}/ PI_{control})}$$

2.6.2. Flash induced Chl *a* fluorescence relaxation

Photosystem (PS) II activity in detached *H. rhodopensis* leaves during and after desiccation treatments and recovery periods was assessed by measuring the changes of variable Chl a fluorescence values, using the initial amplitudes of the flash-induced fluorescence signals ($F_v = F_m - F_o$) as an indicator of the amount of functional PSII centers. Changes in chl fluorescence yield induced by a 20 μs saturating flash (1020 μmol m^{-2} s^{-1} actinic light at 639 nm) were measured by a double-modulation FL3000 fluorometer (PSI, Brno, Czech Republic) range as described in (Vass 1999).

The flash-induced Chl *a* fluorescence measurements were performed with an FL 3000 Fluorometer (Photon Systems Instruments Ltd., Brno) (Trtilek 1997). The instrument contained red LEDs for both actinic (20 μs) and measuring (8 μs) flashes, with measuring delay of (7 μs). By using the double-modulation technique, fluorescence yield changes can be measured in a very broad time range, from 100 μs to 100 s, and study reoxidation processes of Q_A by both forward and back reactions (Vass 1999). Measurements were repeated on three biologically different samples at

preset time points. The data were visualized and evaluated using the Fluorwin software, version 3.6.3.11 and Origin 2015.

Analysis of the fluorescence relaxation kinetics was based on the widely used model of the two-electron gate. According to this model, the fast (few hundred microseconds) decay component reflects Q_A^- reoxidation via forward electron transport in centers which contain bound PQ (in the oxidized or semireduced form) at the Q_B site before the flash. The middle (few milliseconds) phase arises from Q_A^- reoxidation in centers which had an empty Q_B site at the time of the flash and have to bind a PQ molecule from the PQ pool. Finally, the slow (few seconds) phase reflects Q_A^- reoxidation via back reaction with the S_2 state of the water oxidizing complex. The fast and middle phases are generally described by exponential components. In contrast, the slow decay of Q_A^- via charge recombination has been shown to obey hyperbolic decay kinetics corresponding to an apparent second-order process.

2.7. Simultaneous measurements of P700 redox state and Chl fluorescence

Variable Chl fluorescence from PSII and the amount of oxidized PSI primary Chl electron donor ($P700^+$) was simultaneously measured using a DUAL-PAM-100 system (WALZ, Effeltrich, Germany). From the fluorescence data F_v/F_m and the effective quantum yield of photochemical energy conversion in PSII, $Y(II)= (F_{m'} - F)/ F_{m'}$ (Genty 1989) where F_o, $F_{o'}$ are dark fluorescence yield from dark- and light-adapted leaf, respectively and F_m, $F_{m'}$ are maximal fluorescence yield from dark- and light-adapted leaf, respectively were calculated. The $P700^+$ signal (P) may vary between a minimal (P700 fully reduced) and a maximal level (P700 fully oxidized). The maximum level of $P700^+$ is called P_m in analogy with F_m. It was determined by application of a saturation pulse (300 ms, 10000 μmol $m^{-2}s^{-1}$; 635 nm) after pre-

illumination with far-red light. P_m' is analogous to the fluorescence parameter F_m' and was determined by applying 800 ms saturating pulse of 635 nm red light. The photochemical quantum yield of PSI, Y(I) is the quantum yield of photochemical energy conversion in PSI. It is calculated as $Y(I) = (P_m' - P)/ P_m$. Y(ND) is the quantum yield of non-photochemical energy dissipation in PSI due to donor side limitation, $Y(ND) = P/P_m$. Y(NA) is the quantum yield of non-photochemical energy dissipation due to acceptor side limitation in PSI, $Y(NA) = (P_m - P_m')/ P_m$, and Y(I) + Y(ND) + Y(NA) = 1 (Klughammer & Schreiber, 1994). Non-photochemical quenching NPQ (Bilger & Bjorkman, 1990), was calculated as $(F_m - F_{ms})/F_{ms}$, where F_m represents the fluorescence of a dark-adapted sample and F_{ms} represents a fluorescence of the illuminated sample. Plants were dark-adapted for ~20 min and kinetics were measured after repeated light pulses of 94 PPFD for 300 sec. Leaves were subsequently relaxed in darkness for 240 sec and fluorescence while continuously measuring and recording fluorescence (Szalonek 2015). The electron transport rates through PSII as well as through PSI were determined simultaneously (Miyake 2005; Fan 2007). The apparent rate of electron transport in higher plants were calculated as ETR(II) = Y(II) * PPFD * 0.5 * 0.84 and ETR(I) = Y(I) * PPFD * 0.5 * 0.84 (Genty 1989), where Y(II) and Y(I) are effective quantum yields of PSII and PSI respectively, PPFD is the photon flux density of incident photosynthetically active radiation and two coefficients (0.5 and 0.84 for higher plants; Bjorkman and Demmig 1987; Schreiber 2004).

The ETR(II) in flag leaves during grain filling period of selected wheat cultivars from different geographical origin of salinity experiment were determined by using WALZ Mini-PAM photosynthesis yield analyzer.

2.8. Thermal imaging

Thermal images were taken by using a Thermo Varioscan (Jenoptik, Laser optik, Systeme, GmbH) camera as described by (Kana & Vass, 2008). Thermal images of wheat cultivars under various drought stress treatments were analyzed by using ImageJ software (http://rsbweb.nih.gov/ij/) to select and measure areas based on color. Images were threshold using Hue, Saturation and Brightness (HSB) color space and converted to binary values by defining a color scale cutoff point. Values of evaporative cooled area, represented by pixels below the ambient temperature, become black and those in above become white.

2.9. Digital imaging

Digital images of seedlings in drought experiment were performed by using a Nikon D80 camera equipped with an AF-S DX Zoom-NIKKOR 18-135 mm objective (f/3.5-5.6G ED-IF Lens) and close-up rings. Digital images of plant replicates under various drought stress treatments in drought stress trial were analyzed for green biomass area using ImageJ software. We used colour thresholding to select just the plant green area and exclude the stand, pot, shadows and yellowish leaves (http://rsbweb.nih.gov/ij/).

The shoot growth parameters in salinity trial were analyzed according to the protocols used in Fehér-Juhász (2014) during the whole life cycle of the tested wheat cultivars by using the HAS-SSDS platform of the EPPN in Szeged, Hungary. These measurements provided information on plant height, and total green biomass change during the cultivation period. Water use profiles were recorded at the level of individual plants during the whole cultivation period from which the efficiency of water usage, as well as the effect of NaCl on water utilization was determined.

2.10. Statistical analysis

The comparison of traits of plants of the same variety, which were grown under different treatment conditions/ genetic changes was based on the two-sample Student's *t*-Tests (http://www.physics.csbsju.edu/stats/t-test.html). Welch's t test is an adaptation of Student's t test and is more reliable if the samples have unequal sample sizes or variances. Levels of significance (P values) in differences from means of control and treatment plant samples are indicated in the figure legends.

In photosynthetic studies, the data were visualized and evaluated by the following methods: for ETR(I) and ETR(II) measurements, Dual PAM version 1.18 and Origin 2015; for gas-exchange measurements, LI-6400 OPEN Software version 5.3 and Origin 2015; for chlorophyll fluorescence parameters deduced from OJIP fast kinetics measurements, PEA Plus version 1.00 and Origin 2015.Spider graph values are displayed after normalization to respective values obtained in the controls.

3. RESULTS AND DISCUSSION

3.1. Characterization of biomass and grain yield responses in wheat (*Triticum aestivum* L.) under severe water stress

3.1.1. Phenotyping for biomass accumulation and grain yield

Growth of wheat plants was monitored by digital photography by recording green pixel-based shoot surface area of wheat plants, which was performed during the whole growth period once a week. According to our previous data the green pixel-based shoot surface area correlates with green biomass (Fehér-Juhász 2014). Digital RGB imaging of leaf/shoot area showed that the Cappelle Desprez cv. produces larger

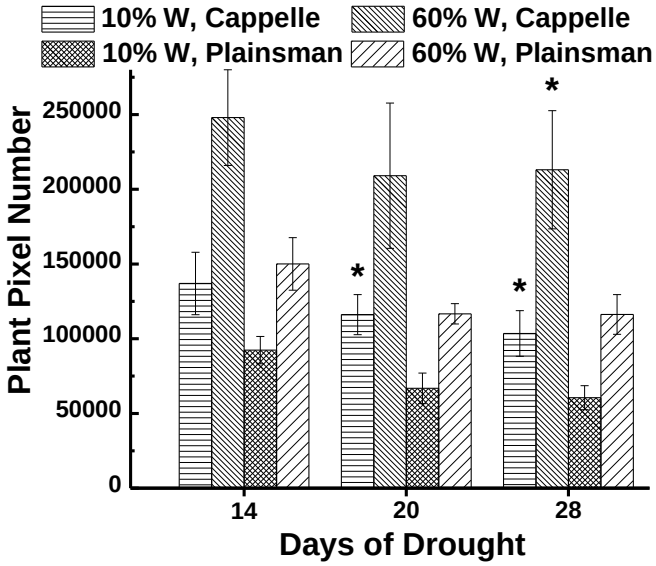

Figure 5. Effect of drought stress on the accumulation of green biomass. A. The area of the green leaves and shoots, which is used as a proxy for the above ground green biomass, was calculated from the analysis of digital photographs for the Cappelle Desprez and the Plainsman V wheat cultivars kept either under well watered (*60% field capacity*) or water limited (*10% field capacity*) conditions. The measurements were performed after 14, 20 and 28 days following the start of the drought treatment, which occurred after two weeks of planting the vernalized seedlings into pots. The means ± SE were calculated from five plants/ treatment. The asterisks indicate significant differences (*: $p \leq 0.05$) between plants of the two different varieties, which were kept at the same soil water content.

above ground green biomass than Plainsman V not only under conditions of water availability but also under water scarcity (Fig. 5).

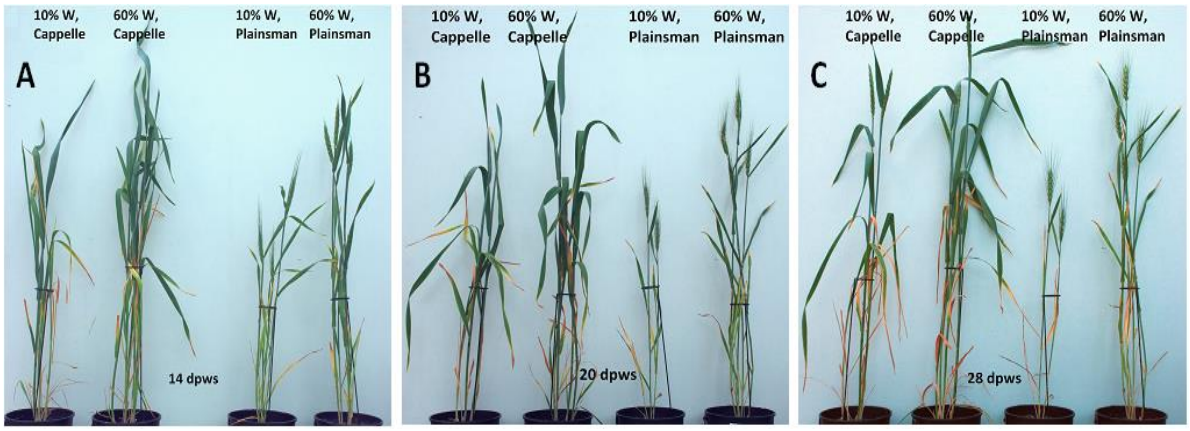

Figure 6. Representative digital images show drought stressed wheat plants Cappelle Desprez and Plainsman V at A. 14; B. 20; and C. 28 days of post water stress (dpws), respectively.

3.1.1.1. Direct measurement of actual mass and growth parameters

We also checked the actual biomass and growth attributes at the end of drought treatment. Although shoot biomass was comparatively higher in drought stressed cv. Cappelle Desprez, significant reduction of shoot fresh weight was observed in both wheat cv. with respect to controls (Fig. 7A). Plant height was significantly higher in Cappelle cv. irrespective of drought (Fig. 7B). But the number of tillers/ plant were higher in cv. Plainsman V which substantiates its better grain yield stability under drought stress (Fig. 7C).

The area of flag and secondary leaves were four fold higher in Cappelle Desprez cv. as that observed in Plainsman V under severe drought (Figs. 7D and 7E). Higher leaf area adapts Cappelle cv. to recieve more quanta of photons in the inactive reaction centers of PSI thereby activating light saturated photosynthesis and enhanced cyclic electron flow under drought. The higher leaf area helps the plant to reduce the soil transpiration and save the soil water for prolonged use.

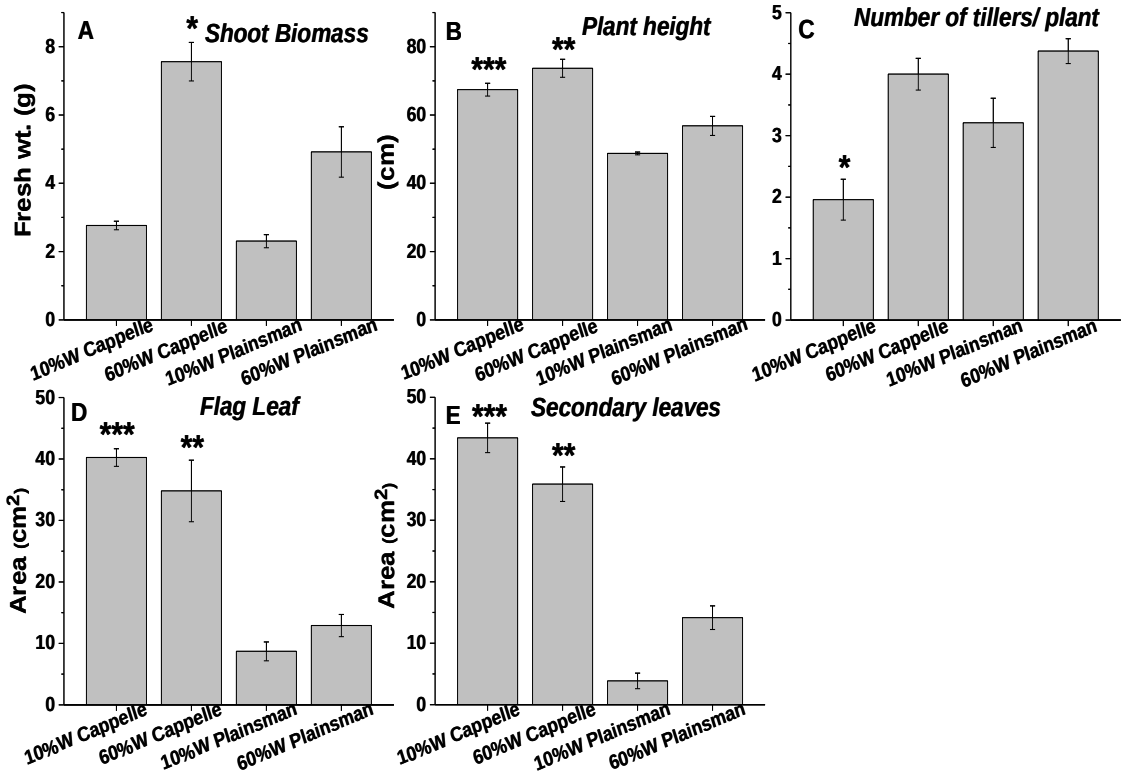

Figure 7. Physical measurements of biomass and growth parameters at the end of the drought stress experiment. A, Shoot biomass; B, Plant height; C, Number of tillers/plant; D, Flag leaf area; E, Average of secondary leaves area. Based on Welch's t test, statistically significant differences (*: $p \leq 0.05$, **: $p \leq 0.01$ and ***: $p \leq 0.001$) between plants of the two different varieties, which were kept at the same soil water content are indicated.

3.1.1.2. Grain yield determination

Table 1. Effect of drought stress on the total grain yield of the experiment and the thousand-kernel weight of Cappelle Desprez and Plainsman V wheat cultivars.

Treatment	Total grain yield/plant[1] (g)	1000 kernel weight[1] (g)
10% W, Cappelle Desprez	0.41 ± 0.01 (** p< 0.01)	19.18 ± 0.32 (*** p< 0.001)
60% W, Cappelle Desprez	1.57 ± 0.12 (* p< 0.05)	41.20 ± 1.47 (*** p< 0.001)
10% W, Plainsman V	0.77 ± 0.06	29.10 ± 1.79
60% W, Plainsman V	1.01 ± 0.07	32.14 ± 0.91
[1] data is average of three replications The * signs indicate the level of significance for the difference between the two cultivars when compared under the same watering conditions		

The grain yield data showed an opposite trend compared to the biomass accumulation, i.e. although grain yield under well watered conditions was higher in the Cappelle Desprez cv., the Plainsman V produced more grains under water limitation, and showed lower grain yield loss (24%) than the Cappelle Desprez (74%) (Table 1).

From grain yield attributes, we can find that the number of grains/ears and spike weight (fresh/dry) of main tiller is significantly higher in Cappelle plants when compared to Plainsman V (Figs. 8A, 8C and 8D). Total number of spikes/plant along with number of tillers/plant during drought stress was increased in drought stressed Plainsman V when compared Cappelle cv. under stress (Fig. 8B). Weight of spikes obtained from side tillers remain the same in both cultivars even though Cappelle cv. had lower number of tillers and spikes/plant (Figs. 8E and 8F).

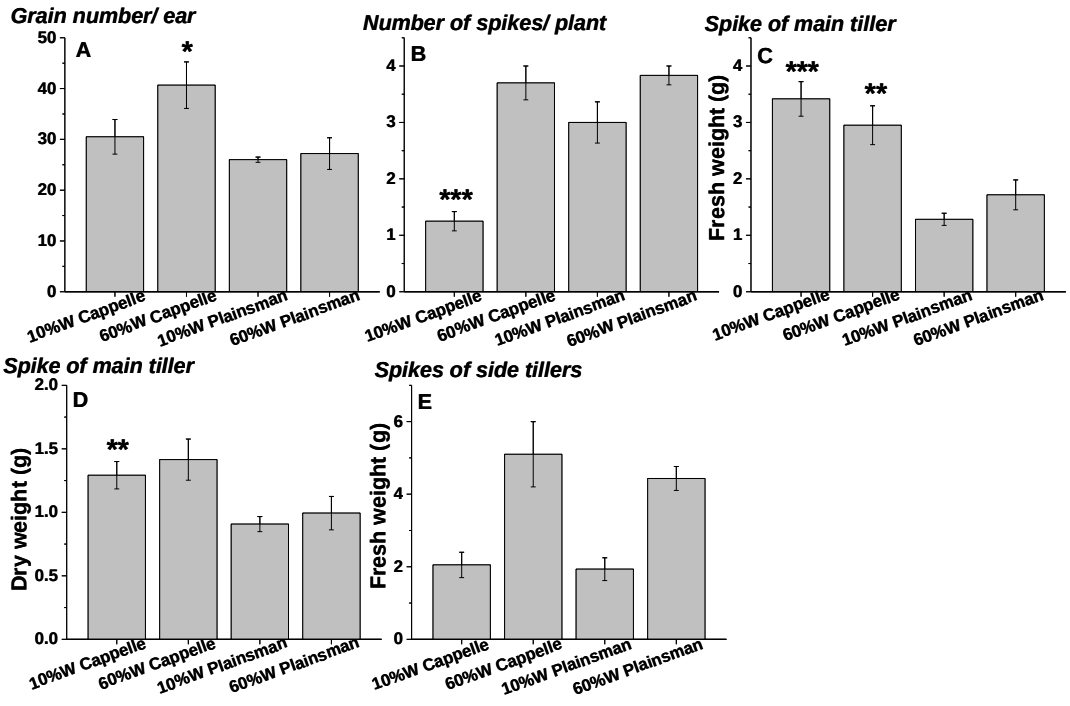

Figure 8. Physical measurements of grain yield attributes at the end of the drought stress experiment. A, Shoot biomass; B, Plant height; C, Number of tillers/plant; D, Flag leaf area; E, Average of secondary leaves area. Based on Welch's t test, statistically significant differences (*: $p \leq 0.05$, **: $p \leq 0.01$ and ***: $p \leq 0.001$) between plants of the two different varieties, which were kept at the same soil water content are indicated.

These findings represent an interesting situation in which green biomass accumulation and grain production respond differentially to water scarcity in different wheat cultivars, i.e. although the "drought sensitive" Cappelle Desprez keeps higher biomass than the "drought tolerant" Plainsman V., the Plainsman V. is able to maintain higher absolute grain yield and grain yield stability under conditions of water limitation. Therefore, phenotyping based only on shoot/leaf area (green biomass) can be largely misleading for drawing predictions about grain yield potential.

3.1.2. Carbon fixation and stomatal functions and water use efficiency (WUE)

The ultimate source of biomass accumulation is CO_2, which is fixed by the photosynthetic apparatus in the form of organic substances. From gas exchange measurements, we could observe that the net CO_2 uptake rate and other gas exchange parameters were not affected in the first week of drought stress. After the second week the net CO_2 uptake decreased in the secondary leaves of water limited plants both in the case of drought sensitive Cappelle Desprez and drought tolerant Plainsman V cv. (Fig 9A). However, the extent of decrease was less for the Cappelle Desprez than for the Plainsman V (Fig. 9A), which agrees with the larger green biomass accumulation in the Cappelle Desprez. Interestingly, in the grain filling period only the Cappelle Desprez cv. responded with decreased CO_2 uptake to the decreased soil water content in case of the flag leaves (Fig. 9A). The CO_2 uptake rate was maintained higher in the Plainsman V than in the Cappelle Desprez cv, which correlates well with the higher grain yield of the drought stressed Plainsman V cv.

The calculated intercellular CO_2 showed decreased levels in the drought stressed Cappelle Desprez plants both in the secondary and flag leaves (Fig. 9C).

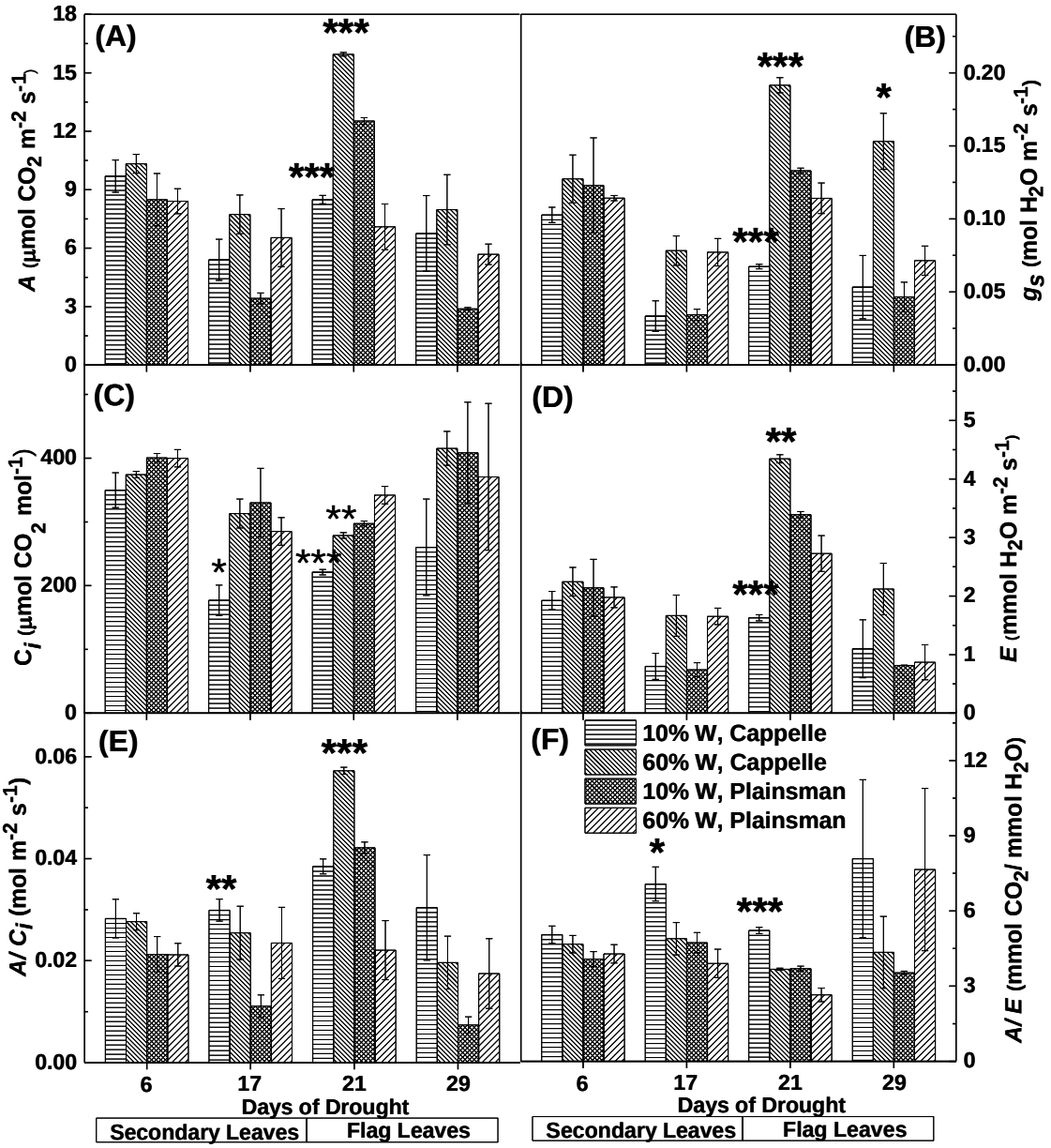

Figure 9. Gas exchange parameters of drought stressed wheat cv. Cappelle Desprez and Plainsman V. A, Net rate of photosynthesis (*A*). B, Stomatal conductance (*g*s). C, Intercellular CO_2 concentration (C_i). D, Transpiration rate (*E*). E, Mesophyl conductance (A/C_i,). F, Water use efficiency (A/E,). Values represent means ± SE of 3-5 plants/treatment. Based on Welch's t test, statistically significant differences (*: p $\leq$0.05, **: p $\leq$0.01 and ***: p $\leq$0.001) between plants of the two different varieties, which were kept at the same soil water content are indicated.

However, in the Plainsman cv. both the secondary and the flag leaves maintained intercellular CO_2 at a similar level in the drought stressed and well watered plants.

CO_2 access to the inner leaf compartments, which determines CO_2 availability for the Calvin-Benson cycle, is limited in the first place by penetration through the stomata. Therefore, stomatal closure, which is a usual response to water limitation, is an important factor for determining the rate of photosynthesis. Stomatal closure occurred under drought stress in the secondary leaves of both cultivars. However, in the grain filling flag leaves only the Cappelle Desprez cv. closed the stomata, while they were kept practically open in the Plainsman V., which again agrees well with the higher grain yield observed in this cultivar.

Regulation of stomatal function is an important mechanism in dealing with the adverse consequences of drought stress. The typical response of plants to water limitation is stomatal closure through which the amount of water loss through evaporation can be decreased. On the other hand, drought induced closing of stomata limits also CO_2 uptake; therefore, it decreases the efficiency of net photosynthesis. The response of stomatal conductance (Fig. 9B) and evaporation rate (Fig. 9D) shows similar pattern to that of CO_2 uptake.

Interestingly, in case of secondary leaves both parameters decreased under drought stress in both cultivars, while in the flag leaves only the Cappelle Desprez cv. showed significant decrease of stomatal conductance and evaporation rate under drought conditions relative to their well watered controls. The Plainsman cv. did not close its stomata in the flag leaves and did not decrease its evaporation rate (Figs. 9B and 9D).

The ability of leaves to achieve optimal photosynthesis relative to the amount of used water, i.e. to conserve water under drought conditions, is characterized by the water use efficiency, which is given by the ratio of the rates of net photosynthesis and transpiration. In a typical plant response to water limitation stomata close and

transpiration decreases in parallel with the decrease of CO_2 uptake and net photosynthesis. Since the extent of decreasing the transpiration rate is usually higher than the decrease of net photosynthesis the water use efficiency increases, and the plants conserve water and increase their chances for survival. This typical response can be observed both in the secondary and flag leaves of the Cappelle Desprez cv. (Fig. 9F). In the Plainsman cv. the WUE (A/E) parameter increased only slightly in the secondary leaves and also in the flag leaves during the grain filling phase of the drought stressed plants, which is consistent with sustained photosynthesis and flag leaf transpiration in order to maintain high grain yield.

After entering into the leaf via the stomata CO_2 is also limited in reaching the chloroplasts, where the Calvin-Benson cycle enzymes are located, by entering through the mesophyll tissue. This phenomenon is characterized by the mesophyll conductance (g_m) parameter, which can be accessed by using A/C_i ratio (calculated from the ratio of the rates of net photosynthesis and intercellular CO_2 concentration) (Harley 1992). During the vegetative phase of biomass accumulation period higher g_m values were observed in the secondary leaves of drought stressed Cappelle Desprez cv. when compared to drought stressed Plainsman V and controls of both varieties (Fig. 9E). These higher g_m values of drought stressed Cappelle Desprez positively correlate with its better WUE (Barbour 2010) (Figs. 9E and 9F). However, in the early phases of grain filling period the flag leaves of drought stressed Plainsman cv. show better g_m in comparison to drought stressed Cappelle Desprez and well watered Plainsman V. This higher g_m value of drought stressed flag leaves of the Plainsman cv. during grain filling period helps the plant to retain grain yield stability. While the higher g_m and WUE values help Cappelle Desprez for delaying senescence (Hafsi 2007; Guóth 2009) and retain biomass yield stability.

3.1.3. Evapotranspiration

The stomata status influences not only CO_2 uptake, but also the efficiency of evaporating water from the leaf tissue, which in turn affects the temperature of the leaves. Leaf temperature can be conveniently monitored by thermal imaging in the infrared spectral range, and drought stress induced leaf temperature changes can be studied.

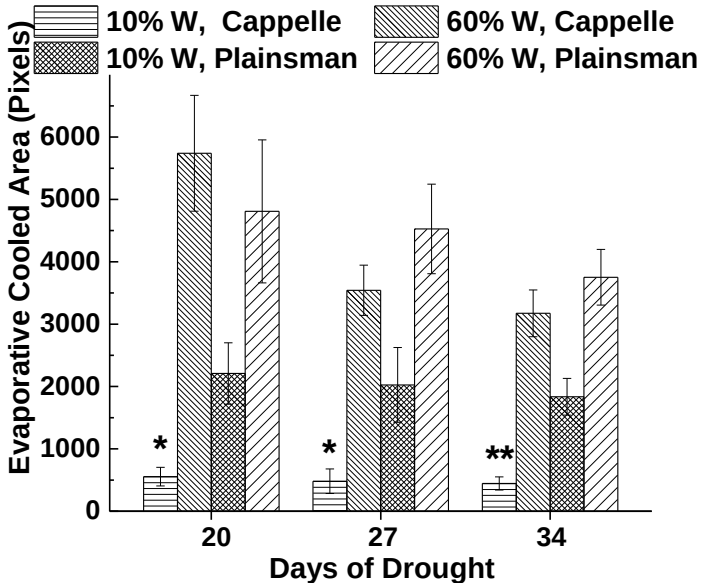

Figure 10. Quantified data from thermal images of drought stressed Cappelle Desprez and Plainsman V wheat plants by using ImageJ software by thresholding evaporative cooled area relative to the temperature of the surrounding air. The presented data were obtained from the average of thermal images taken under conditions of water stress (10% W) and well watered control (60% W) on the 20th, 27th and 34th day of drought stress. The means ± SE were calculated from 5 plants/treatment. The asterisks indicate significant differences (*: $p \leq 0.05$, **: $p \leq 0.01$) between plants of the two different varieties, which were kept at the same soil water content.

Thermal images were quantified based on pixel numbers calculated from thresholded evaporative cooled area relative to ambient background temperature (Vass 2015) (Fig. 10). The data show that the leaf and shoot area, which is cooler than the surrounding air, i.e. cooled by evaporation via transpiration, is small in drought stressed Cappelle Desprez plants indicating low transpiration rate due to stomatal closure (Fig. 10). In contrast, the Plainsman V cv. has larger cooled leaf area not only in the well watered, but also in the drought stressed plants (Fig. 10).

Evaporative cooling is especially pronounced in the spikes of Plainsman V plants (Fig. 11A-C), which is in agreement with the open status of the stomata allowing efficient CO_2 uptake and large net photosynthesis rate for a sustained period during grain filling leading to increased grain yield stability.

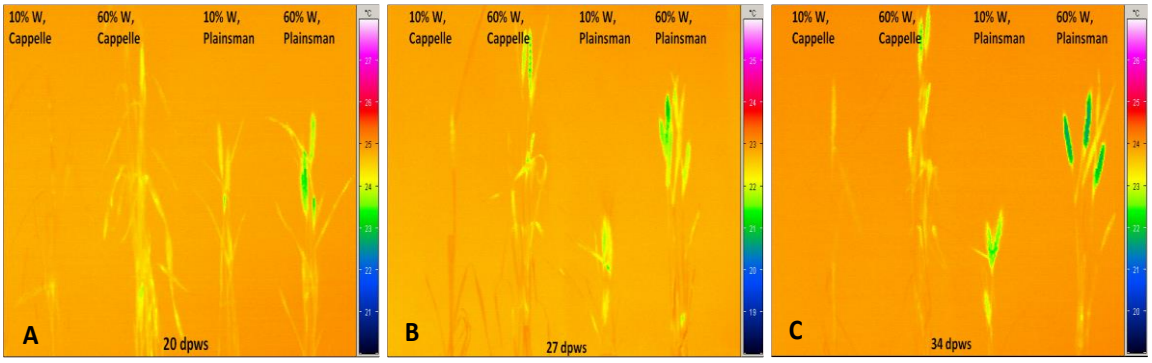

Figure 11. Representative thermal images show wheat plants Cappelle Desprez and Plainsman V under water stress (10% W) and control (60% W) conditions taken after A. 20; B. 27; and C. 34 days of post water stress (dpws), respectively.

3.1.4. Fast kinetics measurements: Chl fluorescence and P700

We observed drought induced changes in photosynthetic electron transport rate from the analysis of fast Chl fluorescence and P700 kinetics measured in dark adapted leaves (Fig. 12). The effects of drought on the initial processes of photosynthesis which take place in the PSII complex were characterized by measuring variable chlorophyll fluorescence induction transients, the so called OJIP curves.

The measurements were performed both on the secondary leaves, which are expected to reflect photosynthetic activity that is responsible for overall green biomass growth, as well as on flag leaves, which primarily support grain development. The I-P amplitude which reflects the size of the electron acceptor pool of PSI showed clear differences in variable fluorescence transients (Schansker 2005; Tsimilli-Michael and Strasser, 2008), and was correlated with a higher PSI activity due to an increased PSI/PSII ratio (Ceppi 2012).

In case of secondary leaves the Cappelle Desprez cv. responded to water withdrawal with only minor changes of the OJIP fluorescence and P700 kinetic transients in the first 2 weeks of the drought treatment (Fig. 12A). After 3 weeks, however, faster rise in Chl fluorescence and P700 oxidation and re-reduction transient was observed in drought stressed Cappelle cv. showing reduction of ferredoxin and increased PSI content (ca. 20%, Fig. 12B) (Schansker 2005; Ceppi 2012).

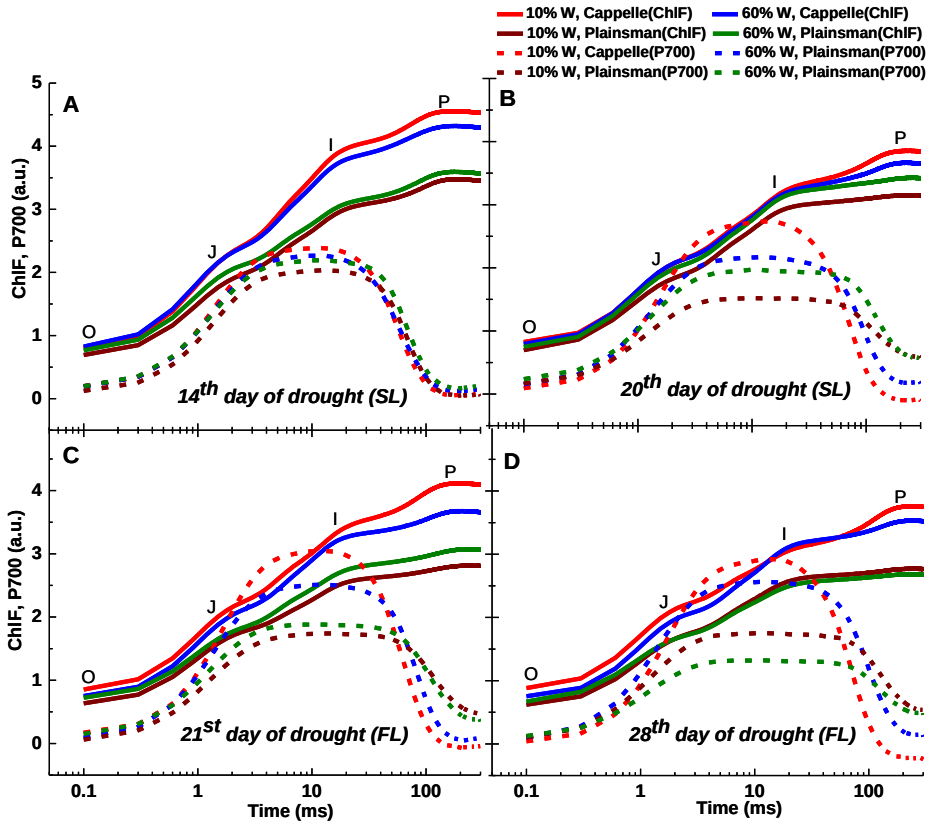

Figure 12. Fast chlorophyll a fluorescence and P700 redox kinetics. The measurements were done in leaves of well-watered (60% W) and drought stressed (10% W) of Cappelle Desprez and Plainsman V cv. wheat plants. Measurements were carried out in early developed secondary leaves (SL) on the A, 14th and B, 20th days of treatment, while on the C, 21st and D, 28th days of treatment in flag leaves (FL). The saturation pulse intensity was 10,000 µmol photons m^{-2} s^{-1} for 0.8 s. The O, J, I and P points represent the standard phases of chlorophyll a fluorescence transients. Curves shown are plotted without any normalization.

In drought stressed Plainsman V we could observe a faster rise of the J-I phase, PSI oxidation was prolonged and PSI re-reduction did not reach normal level. Faster decay of drought stressed Plainsman V shows less functional PSII activity and

smaller PSI content. Well watered controls of both cultivars showed comparable responses in Chl fluorescence and P700 redox kinetics (Fig. 12B).

Kinetically, the I-P phase has been shown to correlate with PSI activity and changes in the I-P amplitude can be used as semi quantitative indicators for (relative) changes in the PSI content of the leaf (Ceppi 2012). During the early phase of spiking (21^{st} and 28^{th} day of drought), 10% W Cappelle Desprez cv. showed similar trend of higher PSI content in the flag leaves with an increase of I-P amplitude in fast chlorophyll fluorescence and $P700^{+}$/ P700 ratio (Fig. 12C and 12D). This effect could be due to enhanced CEF around PSI, which is an important defense mechanism against drought and other abiotic stress factors (Joliot & Joliot, 2002; Kono 2014), as a result of a transient block of electron transfer at the electron acceptor side of PSI under a high [NADPH]/ [$NADP^{+}$] ratio (Hamdani 2015). In drought stressed Plainsman V we could observe a slower rise of J-I phase and I-P amplitude with increased P700 oxidation ending in faster re-reduction decay kinetics (Fig. 12C and 12D). This indicates higher functional PSII activity for drought stressed Plainsman V in the flag leaves during early grain filling phase.

3.1.5. Chl fluorescence parameters to drought stress

Various biophysical parameters derived from Chl *a* fluorescence transient measurements help to understand the energy flow through PSII and provide useful indicators of the development and severity of stress effects, including drought. One of the useful calculated parameters is the so called performance index (PI), which combines the three main functional steps taking place in PSII (light energy absorption, excitation energy trapping, and conversion of excitation energy to electron transport), and was used as measure of drought stress tolerance (Strauss 2006). PI,

which provides useful and quantitative information about the physiological conditions and the vitality of plants (Zivcak 2008), revealed differences among varieties under conditions of drought stress (Oukarroum 2007). Other calculated parameters like Area and RC/ABS also responded for secondary and flag leaves under severe drought stress (Campos 2014).

In case of secondary leaves the Cappelle Desprez cv. responded to water withdrawal with only minor changes in the deduced electron transport parameters in the first 2 weeks of the drought treatment (Fig. 13). In contrast, the Plainsman V. showed a clear tendency for decreasing the PI, the Area reflecting the size of oxidized PQ pool, and the RC/ABS parameters indicating a decreased photosynthetic performance at the level of secondary leaves (Fig. 13).

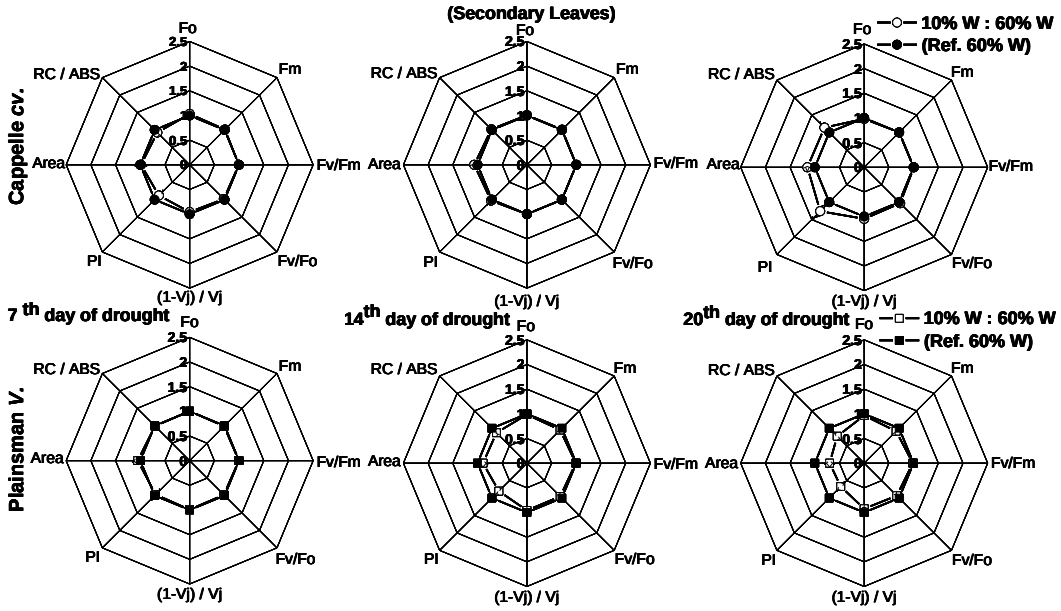

Figure 13. Variable Chl *a* fluorescence characteristic of secondary leaves in Cappelle and Plainsman cv. wheat seedlings after 7, 14 and 20 days of drought stress. Spider graphs represent means ± SE of five plants/ treatment in the drought stressed plants shown after normalization to their respective well watered controls.

Interestingly, the flag leaves, which serve as grain development supporting leaves in the phase of spiking, showed a partially opposite trend in response to water withdrawal. Well watered and drought stressed Cappelle Desprez plants show only

minor differences relative to each other (Fig. 14). As regards deduced fluorescence parameters there was no significant effect of drought stress in either of the developmental stages of the flag leaf of the Cappelle Desprez cv. with the exception of a small increase of PI after 2 weeks of drought stress (Fig. 14). In contrast, the Plainsman V cv. showed a marked increase of the PI parameter with the progress of drought stress with some increase also in the Area, RC/ABS, and Fv/Fm parameters after 4 weeks of drought stress (Fig. 14). These data show that the photosynthetic efficiency of flag leaves during drought stress conditions were less affected in tolerant Plainsman V cv. compared to sensitive Cappelle Desprez variety.

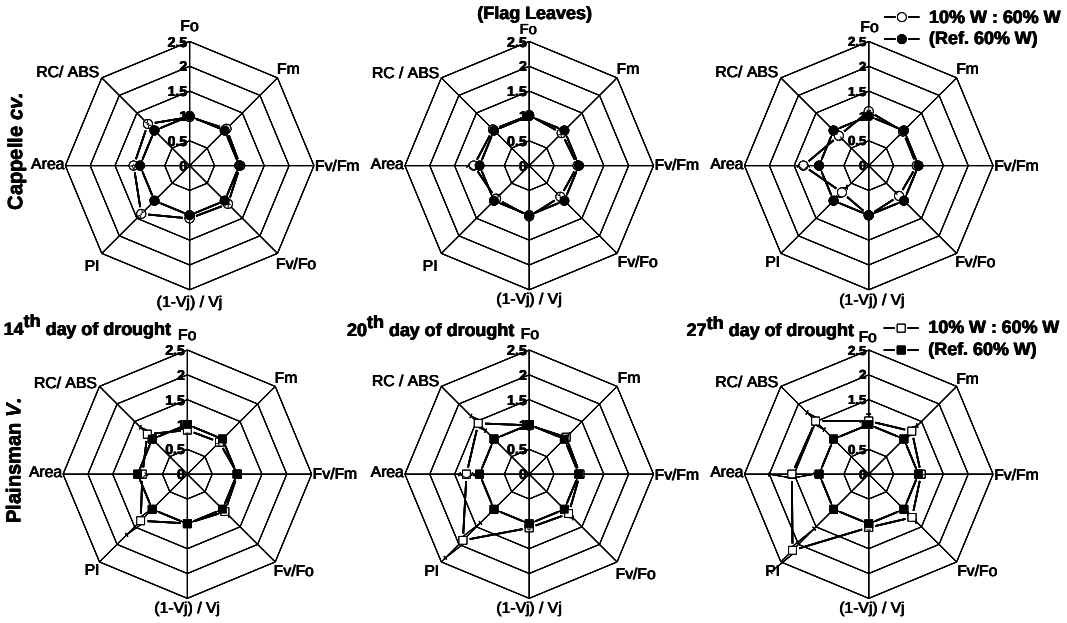

Figure 14. Variable Chl *a* fluorescence characteristic of flag leaves in Cappelle and Plainsman cv. wheat seedlings after 7, 14 and 20 days of drought stress. Spider graphs represent means ± SE of five plants/ treatment in the drought stressed plants shown after normalization to their respective well watered controls.

For the characterization of drought tolerance on the basis of Chl fluorescence data Strasser and coworkers have introduced the so called drought factor index (DFI). This parameter represents the relative decrease of the performance index (PI) during water scarcity and reflects the ability of plants to tolerate long-term drought stress

(Oukarroum 2007). A large positive value of DFI indicates drought tolerance, while a large negative value is characteristic for drought sensitivity. According to Table 2, in the periods of severe drought and senescence the secondary leaves of the Cappelle Desprez and Plainsman V cv. show positive and negative DFI, respectively, which is in agreement with the larger green leaf area and biomass of Cappelle Desprez as compared to that of Plainsman V.

Table 2. Calculated Drought Factor Index (DFI) values of drought sensitive Cappelle Desprez and drought tolerant Plainsman V cv. under medium to severe drought (*dpws- days post water stress*).

	Secondary Leaves (DFI)			Flag Leaves (DFI)		
Wheat cv. / Drought stress	Medium *7- 14 (dpws)*	Severe *14- 20 (dpws)*	Senescence *20- 27 (dpws)*	Medium *14- 20 (dpws)*	Severe *20- 27 (dpws)*	Senescence *27- 35 (dpws)*
Cappelle Desprez	-0.0659	0.1629	0.1870	0.0994	-0.2096	-0.1364
Plainsman V	-0.2548	-0.3489	-0.4978	0.3952	0.7427	0.3099

Interestingly, the DFI values of the flag leaves show an opposite trend with positive DFI for the Plainsman and negative DFI for the Cappelle Desprez cv. Again, this behavior is consistent with the higher grain yield of Plainsman V. as compared to the Cappelle Desprez cv. under drought stress.

3.1.6. Chlorophyll content on drought stressed wheat cv.

Chl a, Chl b, Chl a + b and carotenoid contents were found to be significantly higher in 10% watered Cappelle Desprez wheat cv. compared to 10% watered Plainsman V wheat cv. based on the measurements carried out in the later stages (22^{nd} day of drought treatment) of secondary leaves (Table 3). This very well correlates with the increased biomass, higher photosynthetic activity, WUE and delayed senescence characteristics exhibited by drought stressed Cappelle Desprez wheat cv.

No changes in pigment contents was observed between plants in well watered conditions (Table 3).

Table 3. Leaf Chlorophyll and carotenoid contents determined on wheat cv. Cappelle Desprez and Plainsman V from the secondary leaves on 22nd day of drought and from flag leaves of Cappelle Desprez cv. on 40th day of drought. Sampling was carried out. Data are mean ± SE of three to four independent plants per treatment. Statistically significant events between the well watered and drought stressed plants in each variety **P<0.01 and *P<0.05 are indicated.

22nd day of drought	*Chl a*	*Chl b*	*Chl (a+b)*	*Car (x+c)*
	Secondary leaves (μg/cm²)			
10%W Cappelle	**17.36±1.3	**6.07±0.4	**23.13±1.8	3.72±0.3
60%W Cappelle	9.84±0.8	*3.09±0.2	12.8±1.1	2.45±0.2
10%W Plainsman	9.98±0.9	3.82±0.3	13.62±1.2	2.64±0.2
60%W Plainsman	10.98±0.7	4.02±0.2	14.81±0.8	2.58±0.1
40th day of drought	*Flag leaves (μg/cm²)*			
10%W Cappelle	35.64±2.4	12.8±1.2	47.83±3.5	7.54±0.5
60%W Cappelle	36.68±0.2	12.99±0.1	49.1±0.2	7.78±0.1

Note: Due to early senescence, flag leaves of Plainsman V were not available for sampling.

In flag leaves of Cappelle Desprez, we could find that Chl contents did not decrease in response to water stress for a prolonged period (40 days post water stress) where as flag leaves of Plainsman V got dried off due to early senescence similar to what was reported in Gouth (2009).

3.1.7. Drought induced CEF-PSI

A characteristic response of drought stressed wheat plants is the induction of CEF around PSI (Johnson 2011; Zivcak 2013; Zivcak 2014), which directs electrons from the acceptor side of PSI back to the PQ pool. This effect is considered as a defense mechanism against oxidative stress that develops under conditions of limited availability of CO_2 as final electron acceptor due to stomatal closure (Golding & Johnson, 2003; Zulfugarov 2010). Evidence for cyclic flow at high light exists in all the plants to a greater or lesser extent (Kono 2014). Since under conditions of CEF part of the electrons which arise from PSII circulate around PSI, the rate of electron

flow though PSII (ETR (II)) and PSI (ETR(I)) are different. One way to assess the efficiency of cyclic electron flow is to follow the changes in the ETR(I)/ ETR(II) ratio.

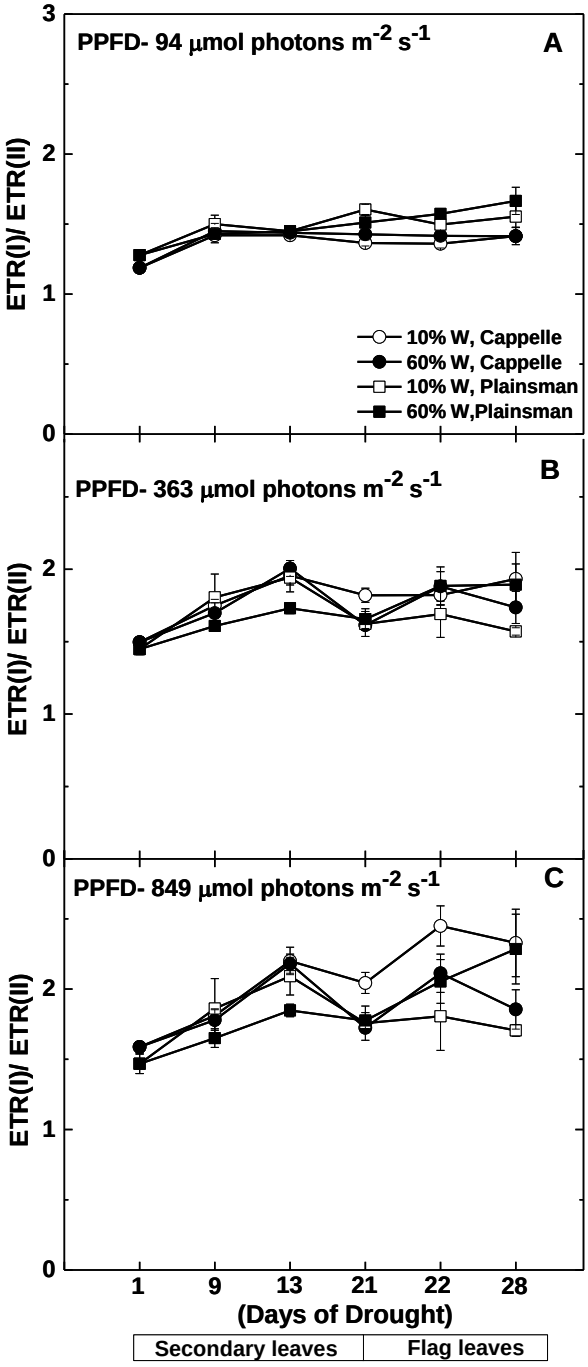

Figure 15. Changes in the ETR(I)/ ETR(II) ratio. Electron transport rates through PSI (ETR(I)) and PSII (ETR(II) were measured in leaves of well watered (*60% W- filled symbols*) and severe drought stressed (*10% W- open sysmbols*) Cappelle Desprez (*circles*) and Plainsman V (*squares*) cv. wheat seedlings at different light intensities of 94, 363 and 849 μmol photons m^{-2} s^{-1}. The values, which are shown as a function of the duration of drought treatment, represent the mean ± SE of five plants per treatment.

As shown in (Fig. 15) the ETR(I)/ ETR(II) ratio does not show significant differences between the different wheat cultivars either in the control or in drought stress conditions in the biomass accumulation period at various grow light regimes (94 - 849 µmol photons m^{-2} s^{-1}). Only in the well watered Plainsman V was the ETR(I)/ ETR(II) ratio somewhat lower under medium and high light regimes (Fig. 15B and 15C). However, the ETR(I)/ ETR(II) ratio increased in drought stressed Cappelle Desprez cv. during grain filling period at medium (363 µmol photons m^{-2} s^{-1}) and high (849 µmol photons m^{-2} s^{-1}) light regimes, respectively (Fig. 15B and 15C).

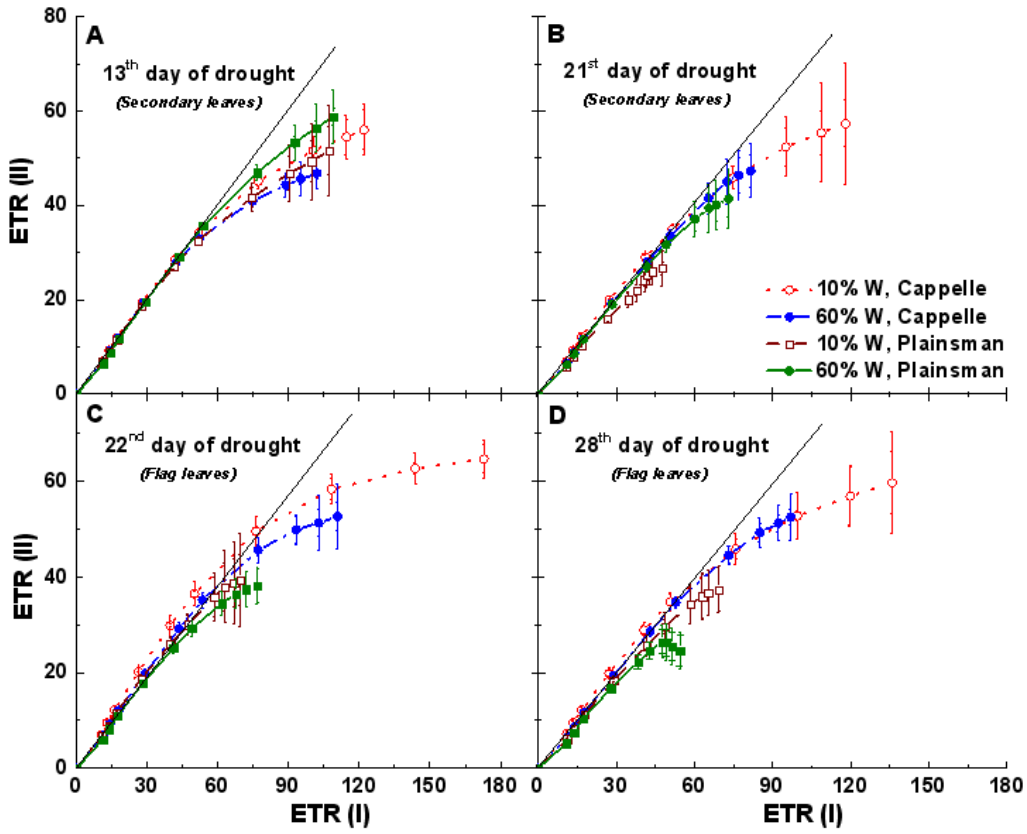

Figure 16. Relationship between PSII and PSI electron transport rates. ETR(II) and ETR(I) were measured as a function of light intensity, and the ETR(II) values were plotted as a function of the corresponding ETR(I) values. Measurements were done in in leaves of well watered (*60% W- filled symbols*) and drought stressed (*10% W- open symbols*) Cappelle Desprez (*circles*) and Plainsman V (*squares*) cv. wheat plants, respectively. Data represent the means ± SE of five plants per treatment.

The relationship between ETR(I) and ETR(II) can also be analyzed by looking at the linearity of ETR(II) as a function of ETR(I). When only linear electron flow dominates there is a linear relationship between ETR(II) and ETR(I). However, after the onset of cyclic flow ETR(I) increases faster than ETR(II) and the linear relationship breaks down at high light (Johnson, 2011). During the early days of drought (13^{th} day) cyclic flow sets in under similar conditions, ETR(I) ≈ 60 μmol/m^2s, in all treatments (Fig. 16A), but as the drought progresses they show divergent responses. On the 21 days of drought there is a tendency for the maximum ETR(I) to increase while the maximum ETR(II) does not change much in the Cappelle cv. (Fig. 16B) implying that linear electron transport is not much affected by the drought treatment while cyclic electron flow around PSI is increasing in the secondary leaves. Similar tendency is seen in the flag leaves after 22 and 28 days of drought stress (Fig. 16C and 16D). In contrast drought stressed Plainsman showed a tendency of smaller cyclic flow in the later phases of drought stress (Fig. 16C and 16D). Thus we could observe that as the drought progresses cyclic electron flow is losing in Plainsman, while it is enhancing in Cappelle.

During light-saturated photosynthetic ETR under drought stress conditions, excess ETR(I) is produced which drives cyclic electron flow (Laisk 2008). In our experiment, we could find that as the severity of drought progressed to the third week (21^{st} – 28^{th} day of drought) enhancement of cyclic electron flow through ETR(I) in Cappelle Desprez and losing of ETR(I) in Plainsman V occurred during both biomass accumulation and grain filling period (Figs. 16B- 16D).

3.1.8. Linear electron transport through PSI

Light responses of PSI parameters obtained from P700 signals were further analyzed (Fig. 17). The fraction of overall P700 that is kept in the oxidized state, Y(ND), was significantly increased with the increase of PPFD in secondary and flag leaves of drought stressed Plainsman V from the end of the second week of water withdrawal with respect to Cappelle cv. in both 60% and 10% field capacity (Fig. 17B and 17C).

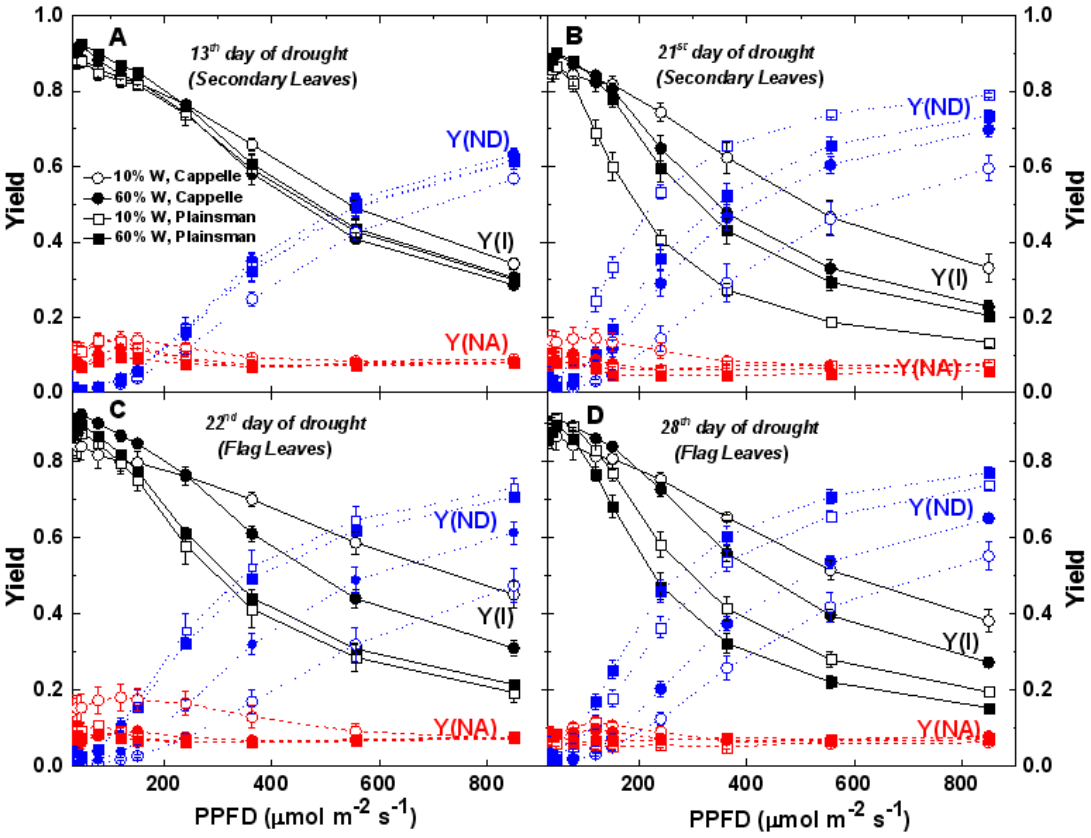

Figure 17. Light response of quantum yield parameters of PSI photochemistry in secondary and flag leaves measured at variable light intensities to different days of drought. P700 kinetics were recorded in Cappelle Desprez (*circles*) and Plainsman V (*squares*) cv. plants in well watered (*60% W- closed symbols*) and drought stressed (*10% W-open symbols*) conditions. Y(I), the effective quantum yield of PSI; Y(ND), the quantum yield of non-photochemical energy dissipation due to the donor-side limitation; Y(NA)), the quantum yield of non-photochemical energy dissipation due to the acceptor-side limitation are plotted as a function of light intensity. Data represent the means ± SE of five plants per treatment.

Higher values of Y(ND) indicates that a major fraction of overall P700 is in the oxidized state during illumination due to limitation of electron flow from PSII towards PSI under severe drought condition. Y(NA) represents the fraction of overall P700 that cannot be oxidized by a saturation pulse in a given state due to a lack of oxidized PSI acceptors (Singh 2014). A substantial increase of Y(NA) was observed in the flag leaves of drought stressed Cappelle Desprez cv. (Fig. 17C), which correlates with the lower CO_2 uptake rate of these leaves, that creates a limitation of reduced acceptors at the acceptor side of PSI at lower light intensities (Zivcak 2013). Y(NA) of Cappelle Desprez cv. was greater than Y(ND) at PPFDs <250 μmole photons m^{-2} s^{-1}, while, above this level, Y(NA) decreased and Y(ND) of drought stressed Plainsman V increased. Higher effective quantum yield of PSI, Y(I) was observed for drought-stressed Cappelle Desprez cv. in both biomass accumulation as well as grain filling period in comparison to plants of all other treatment conditions (Fig. 17A-D).

3.1.9. NPQ regulation for excess energy utilization

Activation of non-photochemical quenching NPQ by generating a proton gradient across thylakoid membrane (ΔpH) (Miyake 2005; Joliot & Johnson, 2011) is one of the alternative protective mechanisms used by plants under drought stress in combination with cyclic electron flow (Zivcak 2013). NPQ is an effective short-term mechanism that provides protection for PSII against excessive irradiation and allows excess excitation energy to be harmlessly dissipated as heat (Foyer 2012). During early stages of drought there were no significant differences in the reversible NPQ status in either variety. As the severity of drought increased an increase of reversible NPQ was observed in secondary leaves of the Cappelle variety on the 21st day (Fig.

18B). While NPQ was found to be lower in the flag leaves of drought stressed Plainsman on the 22nd day of drought (Fig. 18C). This clearly indicates higher NPQ during biomass accumulation in secondary leaves (21st day) during daily illumination of drought tolerant Plainsman V. While it is lowered in the flag leaves during grain filling time (22nd day) along with lowered reversible NPQ induction measured in the dark (Fig. 18B and 18C).

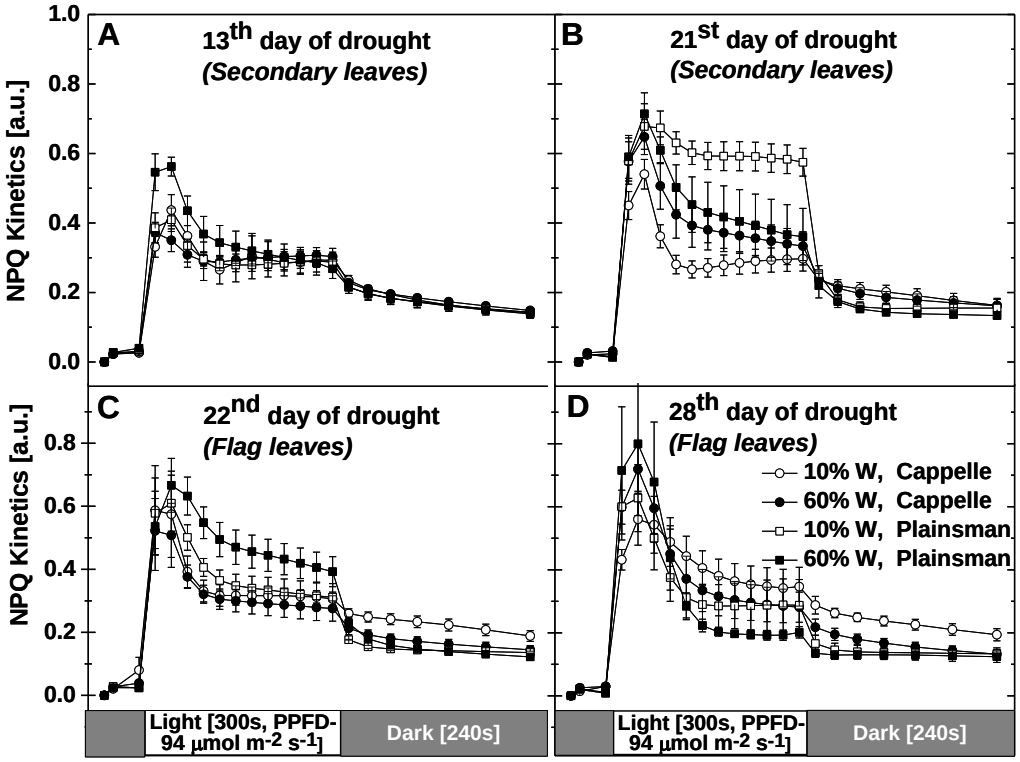

Figure 18. NPQ assayed in leafs of well-watered wheat seedlings Cappelle Desprez (circle symbols) and Plainsman V. (square symbols) cv. subjected to drought stress (10% W) and well watered (60% W). Performance of gross non-photochemical quenching (NPQ) were assayed on the first fully developed composite leaf from the top of plant at 4 hours after turning the light with Dual PAM-100. For measurement plants were adapted to dark for 20 minutes and then stimulated with repeated light pulses of actinic light (94 PPFD) for 5 minutes and once again subjected to dark for 6 minutes. Each point represents the mean ±SE (n = 5). Symbols used are 10% W Cappelle Desprez (*open circle*), 60% W Cappelle Desprez (*closed circle*), 10% W Plainsman V. (*open square*) and 60% W Plainsman V (*closed square*).

Cappelle Desprez shows increased reversible NPQ both in flag leaves in the grain filling period. (Fig. 18B- D).

3.2. Prediction of synergistic effects of drought and salt using high throughput plant phenotyping tools

3.2.1. Effect of salt and drought stress on green biomass and grain yield

Conventional destructive samplings do not allow a dissection of the three mechanisms of salinity tolerance: Na^+ exclusion, Na^+ tissue tolerance and osmotic tolerance (Rajendran 2009).

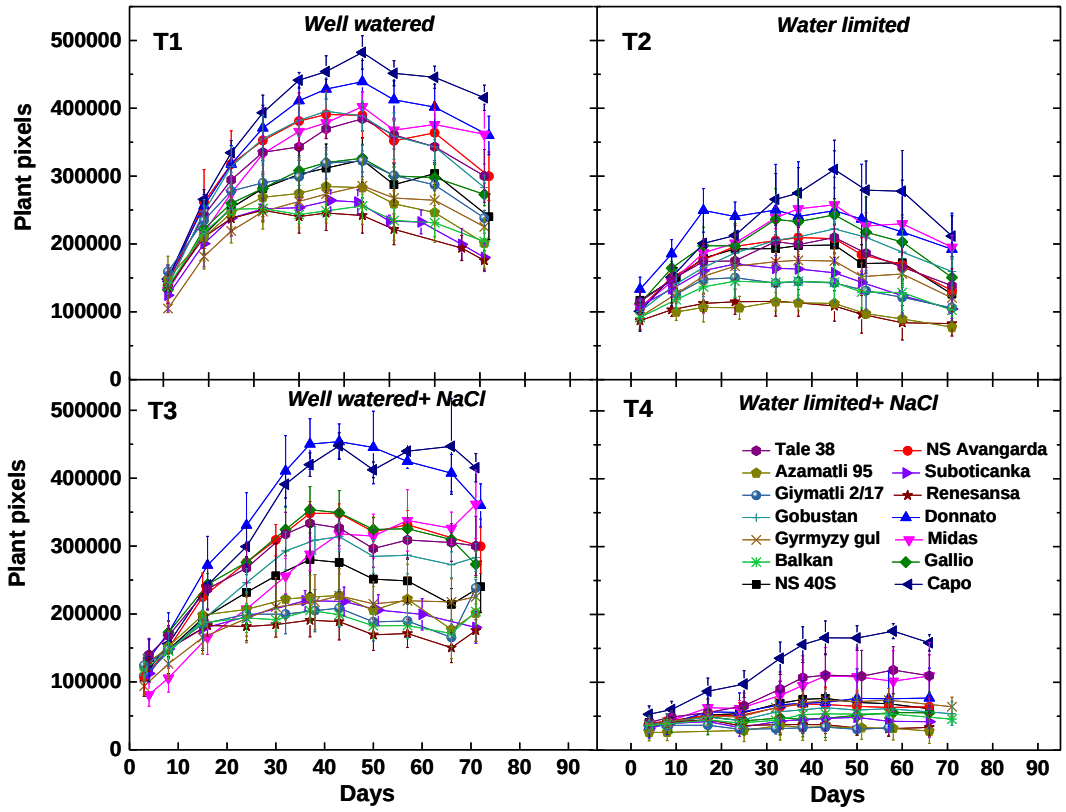

Figure 19. Effect of salt and drought stress on green biomass (*plant pixels*) in various wheat cultivars were measured using digital phenotyping. A, T1; B, T2; C, T3 and D, T4 were shown. Data shown are mean± SE (n=5) plants/treatment.

Shoot biomass in wheat seedlings under various stress treatment conditions were monitored for 80 days (Fig 19). Capo (DT) showed the highest green pixel area of 4.82 pixels*10^5 on the 44th day while Azamatli 95 (DT) was the lowest observed with 1.73 pixels*10^5 on the 74th day under control conditions (Fig 19A). Drought stress drastically reduced the biomass pixels in all the cultivars. Drought impact on

biomass was pre-dominant and completely stunted in Azamatli 95 (DT) and Renesansa wheat cultivars throughout the experimental period (Fig 19B). Green biomass in general was not significantly affected by salt stress under well-watered conditions. However, when salt was applied together with drought stress the green biomass decreased drastically to ca. 30% of the well-watered no salt control. According to our observations wheat cultivars in salt stress alone maintained similar biomass (min. 1.76 pixels*10^5 in Renesansa cv.) as that of the control (Fig 19C). A significant suppression of biomass growth was observed when drought stress was applied alone, while drought and salt stress in combination had the worst impact on biomass. Azamatli-95 recorded ca. 84% decline in biomass under the synergistic combination with respect to control (Fig 19D).

3.2.1.1. Direct measurements of actual mass

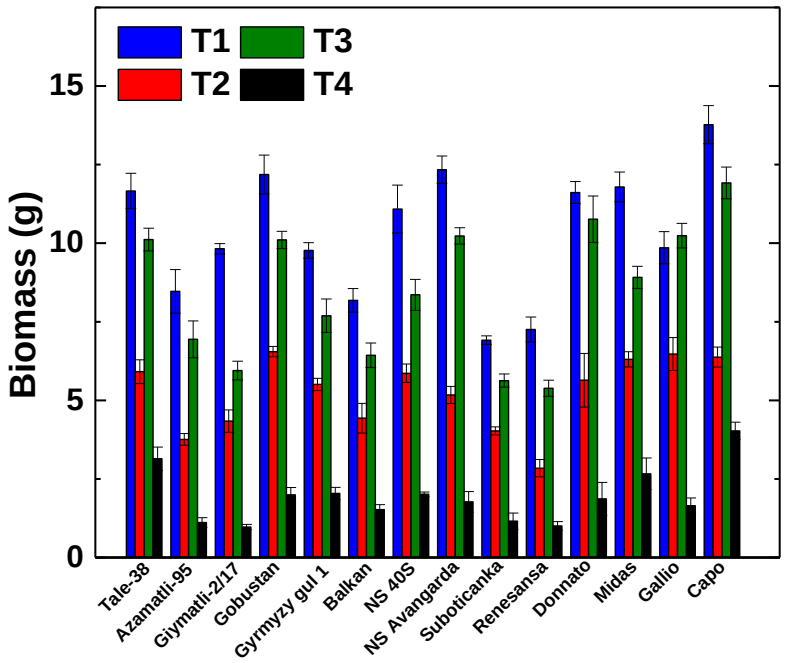

Figure 20. Biomass measured at the end of the experiment. Data are means±SE of five plants/ treatment.

Early responses to mild salinity stress through changes in gene expression have an influence on the acquisition of stress tolerance and improvement in biomass accumulation (Takahashi 2015). The results have shown that salt stress (2g NaCl/ kg soil) and drought stress when applied separately caused a retardation of water uptake and green biomass, but the negative effects of these treatments were not very strong. However, when both stresses were applied together these parameters were dramatically decreased (Fig. 19).

3.2.1.2. Grain yield determination

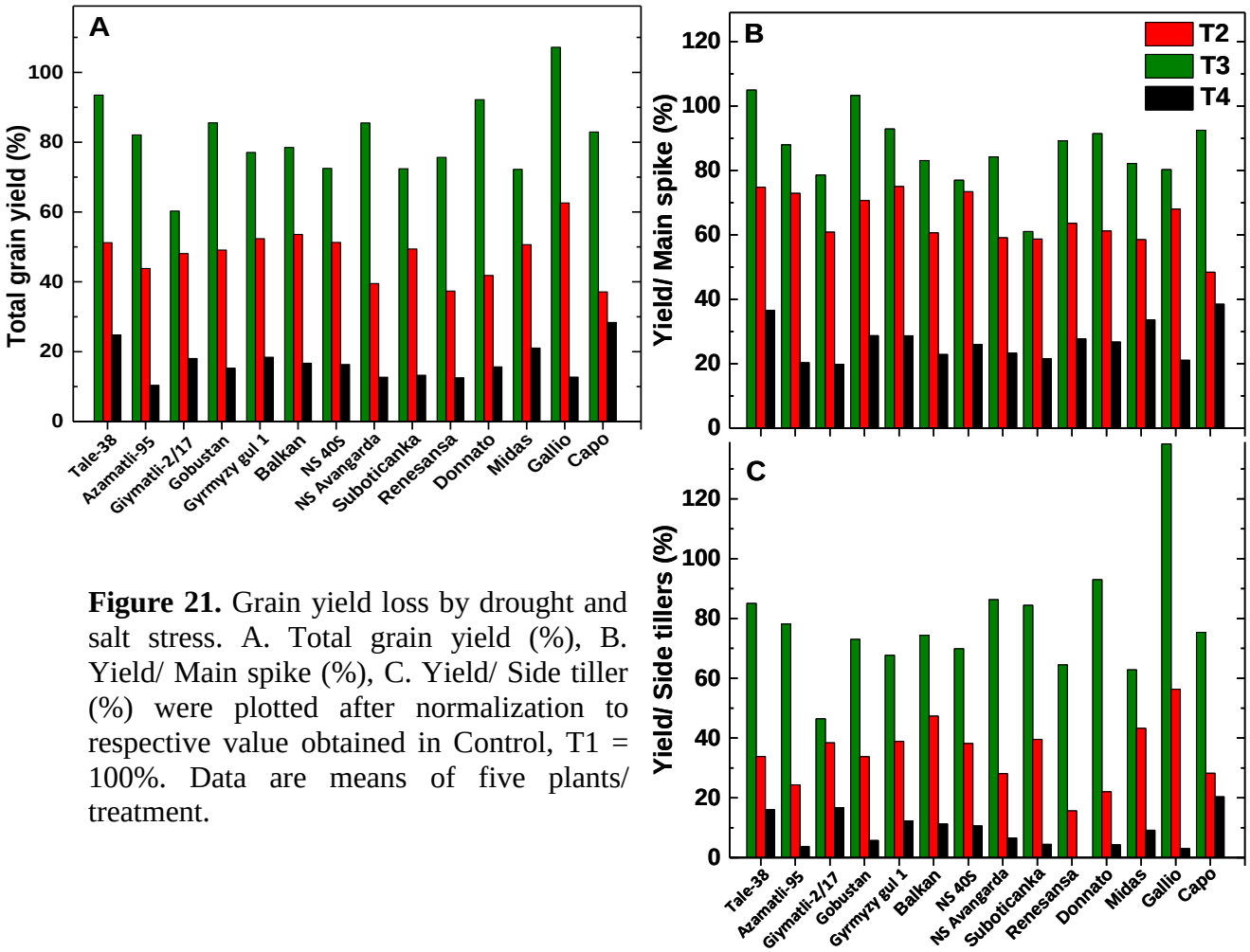

Figure 21. Grain yield loss by drought and salt stress. A. Total grain yield (%), B. Yield/ Main spike (%), C. Yield/ Side tiller (%) were plotted after normalization to respective value obtained in Control, T1 = 100%. Data are means of five plants/ treatment.

Grain yield had a significant response in all the cultivars for various treatment conditions. Yield/main spike as well as the yield/ side tillers or their sum which makes the total grain yield showed similar pattern of stress responses. As a matter of agricultural importance, total grain yield could be considered. With respect to control, 15-20% affect on total grain yield for salt stress under well-watered conditions, while 50% decline in water limited seedlings and 75- 90% affect when salt stress was combined with limited water availability (Fig. 21A). Also in contrast to these results, we observed similar or relatively higher grain yield responses for salt stress under well-watered conditions in certain wheat (Tale 38, Gobustan and Gallio) cultivars (Fig. 21B and 21C).

Regarding the grain yield the cultivars had different reactions to applied treatments. The most salt sensitive cultivar was Azerbaijan cv. Giymatli-2/17, while the most salt tolerant was Austrian cv. Galio. All other cultivars had very similar reactions to salt stress. Drought stress had stronger negative effect to the grain yield, but most of the cultivars had similar level of drought tolerance. In case when both stresses were applied together the best grain yield had *cvs*. Capo and Tale 38, while the cv. Azamatli-95 had the lowest yield. Combination of double stress had a very drastic effect on the relative yield (%) obtained from side tillers (Munns and Tester 2008; Rajendran 2009) which goes lower than 10% in most of the cultivars irrespective of the geographical location (Fig. 21C).

3.2.2. Gas exchange measurements

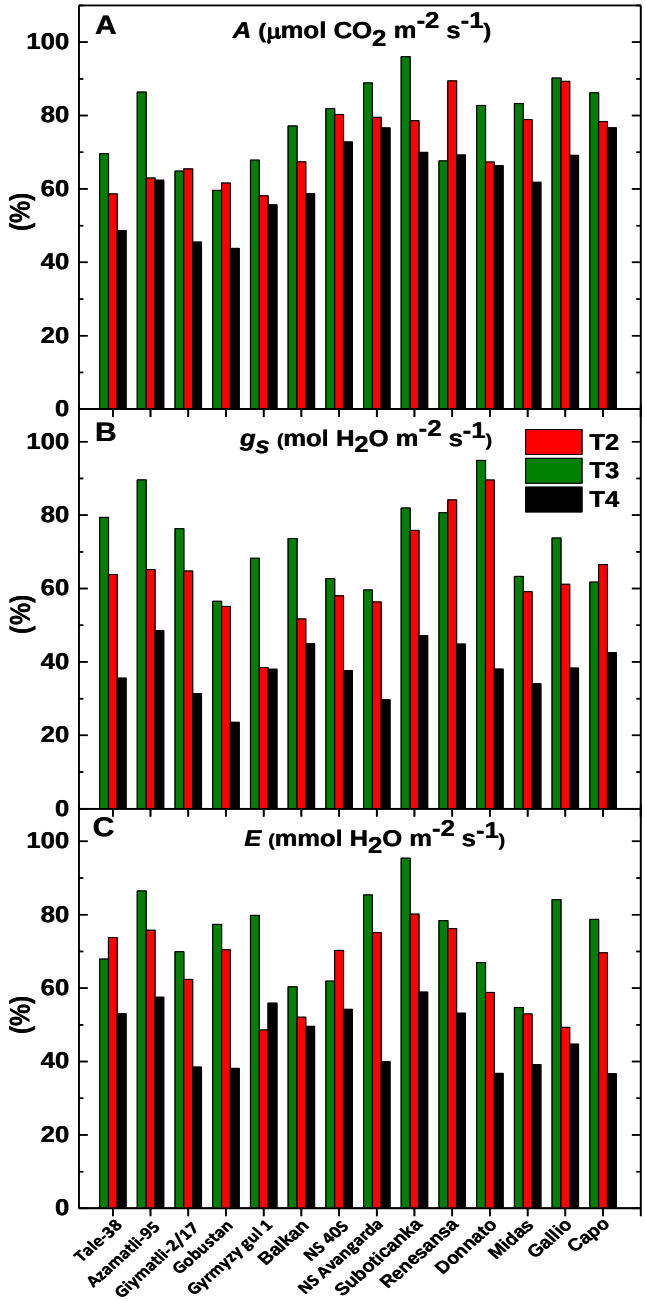

Figure 22. Effect of salt and drought stress on gas exchange parameters. A. The rate on net photosynthesis, measured by CO_2 gas exchange, *A*; B. Stomatal conductance, *gs* and C. Transpiration rate, E were plotted after normalization to respective value obtained in Control, T1 = 100%. Data are based on means of five plants/ treatment.

Salinity had no effect on the rate of A_{CO2}, *gs*, E and WUE prior to the beginning of the drought period. It is generally accepted that the main damaging

factors at the cellular level in drought and salinity are the osmotic and toxic effects of salt (Zhu 2002). Our experiments demonstrate that the supply of salt to the soil leads to a slower decrease in the photosynthetic capacity. We could observe that the net CO_2 uptake rate was not so much affected in (T3) well hydrated salt stress condition (Fig. 22A). High CO_2 uptake was detected in genotypes Azamatli-95, NS Avangardo, Suboticanka, Gallio and Capo. More profound reductions in *A* under water stress was observed in genotypes of Tale-38, Azamatli-95, Giymatli-2\17, Gobustan, Gyrmyzy gul 1 and Donnato. Reductions in CO_2 uptake rate was not strong in genotypes of NS 40S, NS Avangarda, Suboticanka, Renesansa, Midas, Gallio and Capo. Similar values of *A* were observed under T3 and T2 in genotypes of Giymatli-2/17, Gobustan, NS 40S and Gallio. The strongest reductions in *A (*~50%- 55%) under double stress (drought & salinity) was observed in genotypes of Tale-38, Gobustan, Giymatli 2/17, while the reductions was about 25-30% in genotypes of NS 40S, NS Avangardo, Suboticanka (Fig. 22A).

Stomatal conductance was reported to be a useful indicator of genetic variation in lasting growth differences (Rahnama 2010). In comparison with *A*, the reductions in stomatal conductances of wheat genotypes were stronger. Stomata close in response to stress conditions, but tolerant genotypes continue their gas exchange by regulating stomata closing and opening. Lowest g_s under T3 and T2 treatments was observed in genotypes of Gobustan, NS 40S, NS Avangardo, Midas, Gallio and Capo. Reductions in g_s was close to 40% in genotypes of Tale-38, Azamatli-95 and Giymatli-2/17, was less than 20% in genotypes of Renesansa and Donnato (Fig. 22B). It is considered that tolerant genotypes retain their water status by strong reduction of *gs*. Reductions in *gs* more affected on E than A. The transpiration rates of genotypes Tale-38, Azamatli-95, Gobustan, NS Avangardo, Suboticanka, Renesansa and Capo

was about 30% of non-stressed plants. The lowest E under T4 treatment was observed in genotypes Giymatli-2\17, Gobustan, NS Avangardo, Donnato, Midas, Gallio and Capo (Fig. 22C).

3.2.3. Proline accumulation

Previous studies suggest that proline accumulation as a defence response to salt stress is specific for the cultivar, irrespective of species (Plazek 2013). Proline accumulation is one of the common characteristics in many monocotyledons under water deficit. A significant increase of proline was detected under water stress condition, especially in genotypes of Tale-38, Azamatli-95, Giymatli-2/17, Gobustan, NS Avangardo, Renesansa and Gallio (Fig. 23).

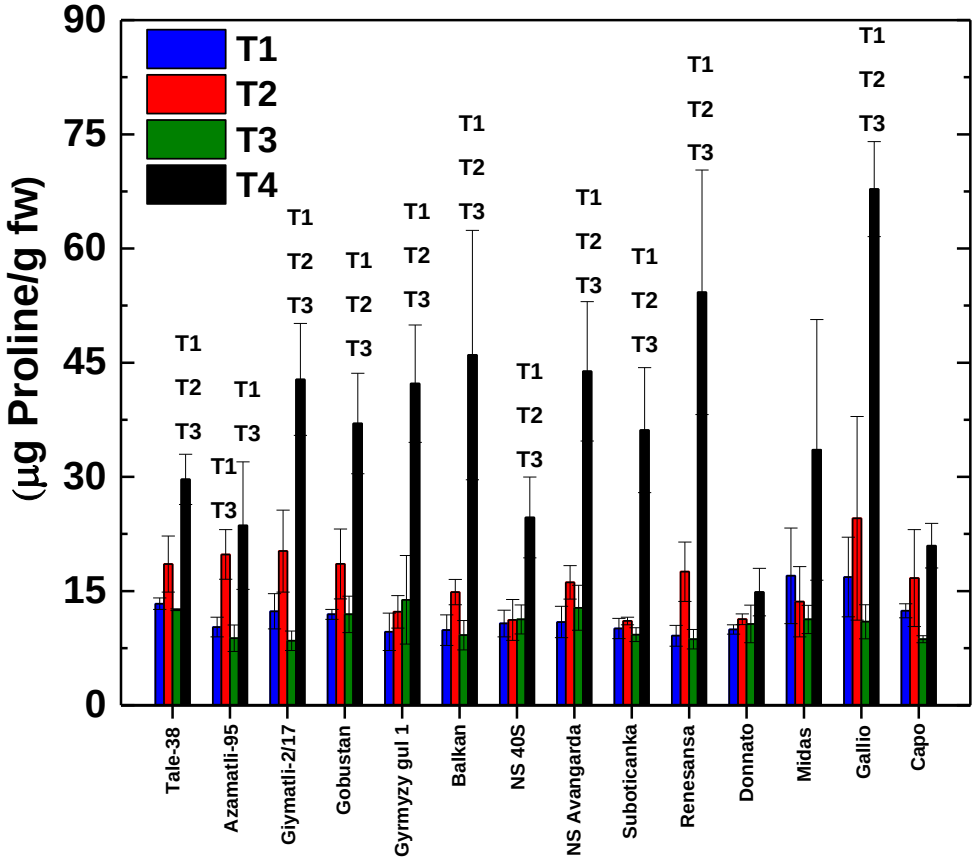

Figure 23. Effect of salt and drought stress on proline accumulation. Data are means of five plants/ treatment. Statistical significance of T4 (20% water limited+ 0.2% NaCl) with respect to other treatment conditions T1, T2 and T3 were indicated.

Significant increase of proline under double stress (drought and salinity) treatment with comparison to T1 (control) treatment was 2-fold higher in Tale-38, about 3-fold higher in genotypes of Giymatli-2/17, Gobustan, Gyrmyzy gul 1, Balkan, NS Avangardo, and more than 4 fold higher in genotype Gallio (Fig. 23). It is assumed that the accumulation of proline improves cell turgor, gas exchange and water status of plants. Irrespective of drought tolerance efficiency, both sensitive as well as tolerant wheat varieties responded with proline accumulation in the double stress combination.

3.2.4. Plot of Grain yield vs. Biomass

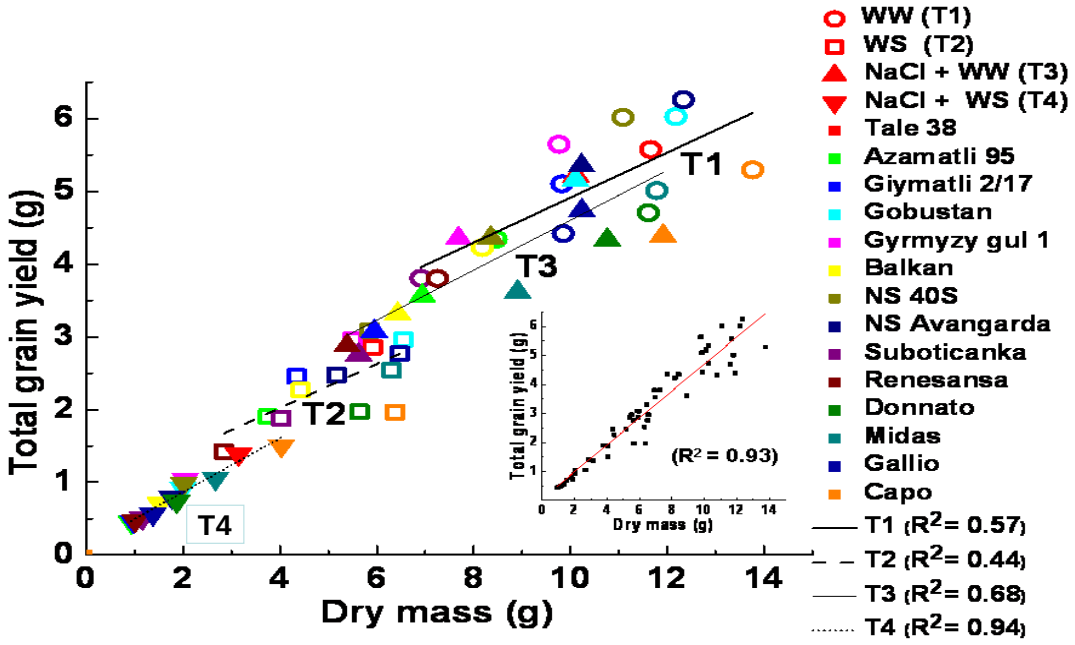

Figure 24. Correlation of grain yield and biomass are plotted. Each data point shown were means of five plants/ treatment. Symbols indicate (*open circle*) WW- T1, (*open square*) WS- T2, (*upward pointing triangle*) WW+SS- T3 and (*downward pointing triangle*) WS+SS- T4 were indicated respectively for all the cultivars. The linear (Pearson) correlation coefficient of determination R^2 was calculated as described by Zwart (2011).

Several plant breeding programs are focused to predict the grain yield from dry mass. In Fig. 24, we establish the correlation of total grain yield obtained with dry mass during various stress combinations of drought and salt stress. Significant positive correlations (R^2= 0.93) existed between dry mass and grain yield production under various treatment conditions (*Inset graph in Fig. 24*). We can find the correlation in well watered control (T1, R^2= 0.57) was significantly lower compared to salt stress under irrigated status which is (T3, R^2= 0.68). The least significance in the biomass-grain yield correlation was observed in drought stress alone (T2, R^2= 0.44) condition. We can find that both of the two stress factors drought and salt separately or their combination show reduction in biomass as well as grain yield in comparison to WW controls. Drought stress alone and its combination with salt stress significantly declined in all the wheat cultivars while salt stress in normal irrigated condition was not that much affected. The ratio of the grain yield and dry biomass remained practically constant even under the combined effect of salt stress and water-withdrawal (Fig. 24). Among the cultivars, Austrian cv. Donnato and Capo deviated from the correlation in T1, T2 and T3 conditions while Azerbaijani cv. Tale-38 and Gobustan showed best correlation under various treatment conditions. Serbian wheat cultivars showed significant correlation of biomass and grain yield in all the treatments.

3.2.5. Correlation of ETR(II) and grain yield

In Fig 25, we try to establish a correlation between grain yield obtained from main tiller spike and electron transport rate of PSII measured from main tiller flag leaves.

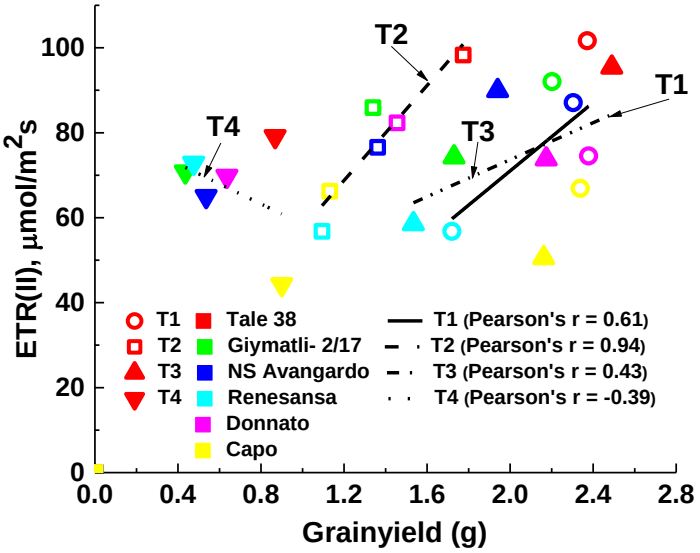

Figure 25. Relationship between grain yield/main spike and ETR(II) measured at grow light PPFD 381 µmol photons m^{-2} s^{-1} on flag leaves. Data are calculated from means of five plants/ treatment. The linear (Pearson) correlation coefficient r was calculated as described by Zwart (2011).

ETR(II) obtained from grow light PPFD 381 µmol photons m^{-2} s^{-1} was used for the study. We observed a clear positive correlation of (Pearson's r = 0.94) for T2 (*drought stress- open squares*) and ETR(II) even though the same wheat cultivars showed a correlation of (Pearson's r = 0.61) for T1 (*well watered control- open circles*); lower (Pearson's r = 0.43) for T3 (*well watered control- upward pointing triangles*) and negative correlation (Pearson's r = -0.39) in T4 (*double stress- downward pointing triangles*) (Fig. 25).

3.2.6. Correlation of biomass and grain yield with CO_2 fixation rates

In Fig 26, correlation calculations were carried out to understand the effect of drought and salinity in the biomass and grain yield production as derived from CO_2 fixation rate and stomatal conductance. We observed significant decline of biomass and grain yield in plants under double stress T4 condition (*downside pointing triangle*) as indicated by the lowest values of net CO_2 photosynthesis rate and stomatal conductance (Fig. 26A-D).

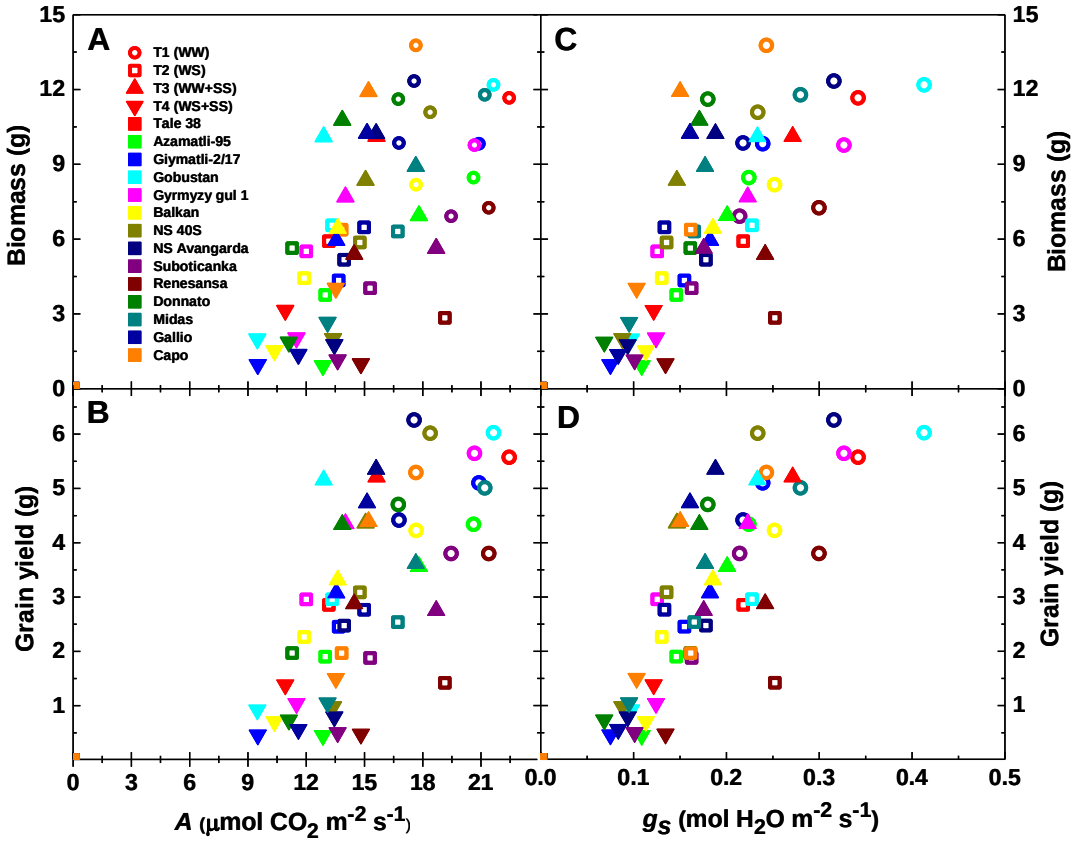

Figure 26. Correlation of biomass and grainyield with CO_2 assimilation and stomatal conductance were plotted. A and B, CO_2 assimilation rate '*A*' with biomass and grainyield; C and D, Stomatal conductance 'g_s' with biomass and grainyield. Data are calculated from means of five plants/ treatment.

Stomatal closure affecting both biomass and grain yield production is evident in T2 condition due to drought stress (*open square*) (Fig. 26A-D). Salinity reduces the ability of plants to take up water, and this quickly causes reductions in growth rate, along with a suite of metabolic changes identical to those caused by water stress (Munns 2002). In our study we could find that majority of the wheat cultivars in T3 salinity condition (*upside pointing triangles*) performs photosynthetic and other physiological functions similar to T1 well watered control series (*open circles*) for a prolonged period (Fig. 26). They are able to retain biomass stability in the source region and there by contribute for better carbon partitioning to grain production.

3.3. Differences in the electron flow responses in two ecotypes of the resurrection plant *Haberlea rhodopensis* during desiccation and rehydration

Shade ecotype **Sun ecotype**

(*Photos from Dr.Adam Solti*)

3.3.1. Leaf water content

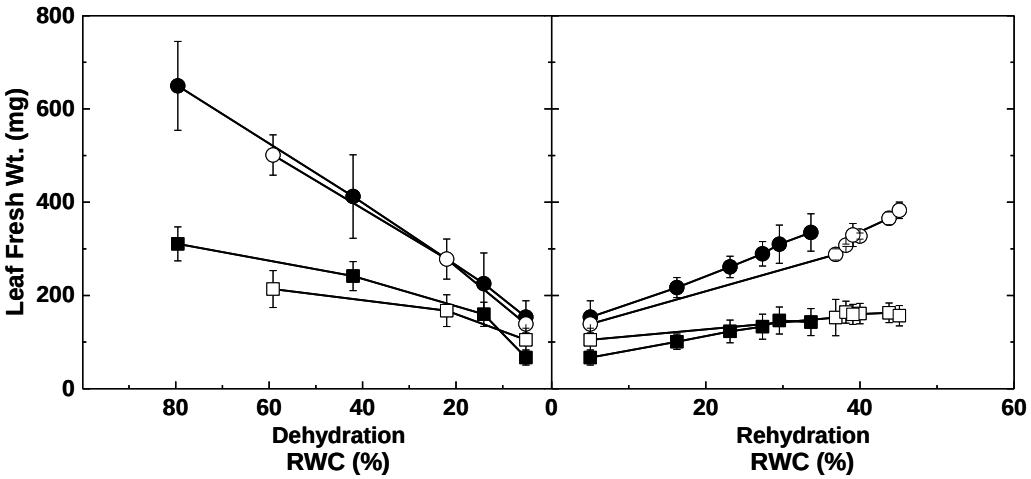

Figure 27. Leaf fresh weight (mg) with respect to RWC% was determined in shade (*filled circle*) and sun (*open circle*) ecotypes during desiccation and rehydration of *Haberlea rhodopensis* plants. Leaves kept in cuvette were represented as square boxes: Shade (*filled square*) and Sun (*open square*) ecotypes respectively. The rehydration started when leaves reached the air-dry stage (last data point in the dehydration process). Data represent the means±SE of three independent leaves/ treatment.

Processes under desiccation and rehydration of shade and sun ecotypes *H. Rhodopensis* leaves were monitored by one day measuring frequency. The desiccation

of the shade leaves proved to be a slower process due to their larger size and their somewhat higher initial net water content (Fig. 27). Thus, shade leaves desiccated to air-dry state in a three-day time, whereas the desiccation of sun leaves required only two days. The rehydration started from this air-dry stage. The first data points in each data series were registered after one day of rehydration.

3.3.2. Electron transport rate of PSI and PSII

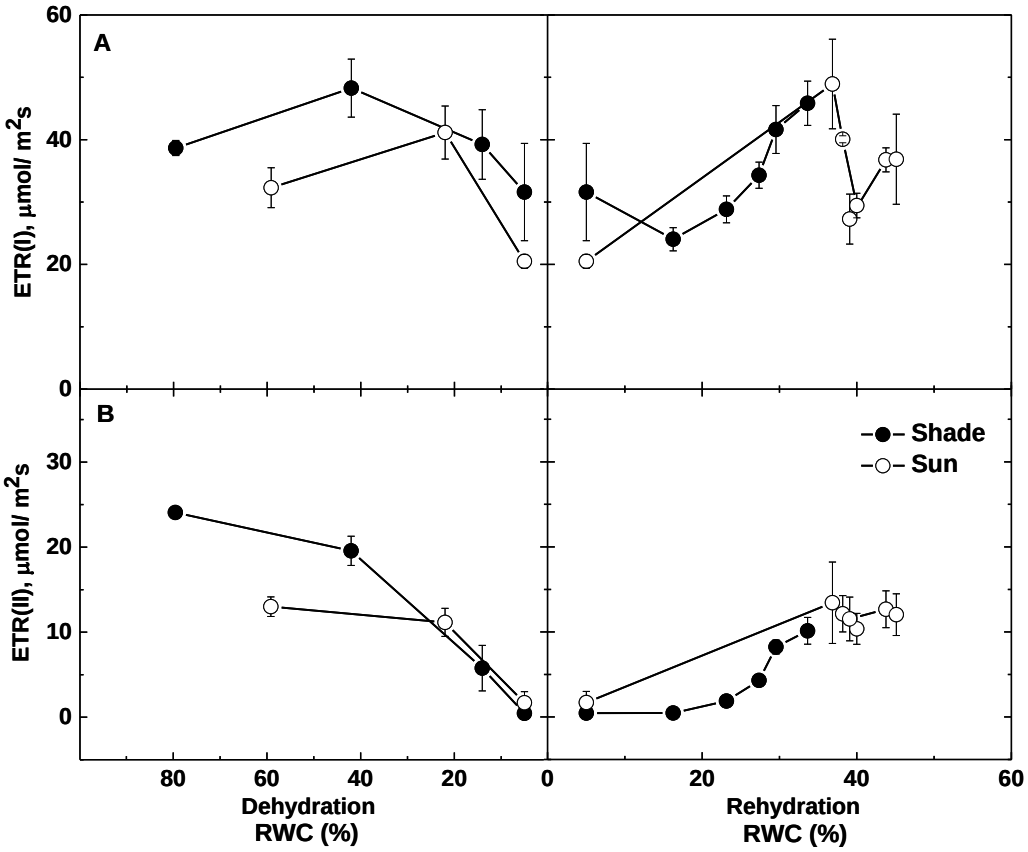

Figure 28. Photosynthetic ETRs of PSI and PSII measured in *Haberlea rhodopensis* leaves as a function of PPFD at 849 µmole photons m^{-2} s^{-1} for sun (*open circle*) and 540 µmole photons m^{-2} s^{-1} for shade (*filled circle*) ecotypes, respectively during desiccation and recovery measurements. The values represent the mean ± SE (n = 3).

We observed maximum light saturation efficiency at 849 µmole photons m^{-2} s^{-1} for sun and at 540 µmole photons m^{-2} s^{-1} for shade ecotype, respectively. Photosynthetic electron transport rates of PSI and PSII showed significant responses

to desiccation and recovery measurements in *H. rhodopensis* leaves of sun and shade ecotypes (Fig 28). During desiccation, ETR of PSI and PSII for sun ecotype declined severely to 20.5 and 1.7 μmoles m^{-2} s^{-1}, respectively, while it reached 31.6 and 0.45 μmoles m^{-2} s^{-1}, respectively, for shade ecotype until desiccating to ~5% of RWC (Fig 28A and B). A rapid rise to 48.9 and 13.4 μmoles m^{-2} s^{-1} in ETR(I) and ETR(II), respectively was observed in sun ecotype during rehydration without retaining stability. In contrast, the recovery was gradual for shade leaves and ETR(I) and ETR(II) increased significantly slower (Fig 28).

3.3.3. Linear relationship between ETR(II) and ETR(I)

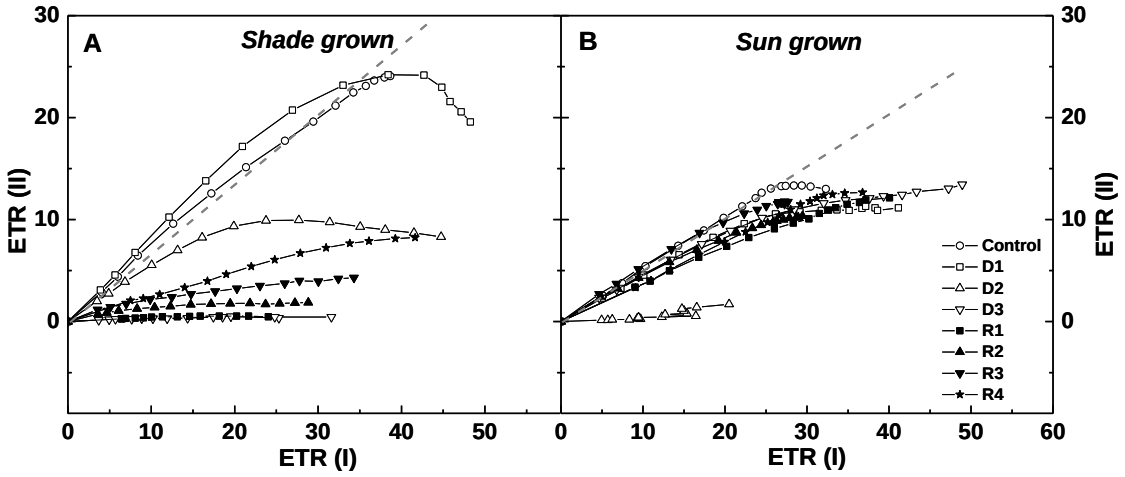

Figure 29. Plot of linearity of the relationship between PSI and PSII derived light response curves in *H. rhodopensis* leaves of sun and shade ecotypes were subjected to desiccation and recovery measurements at laboratory conditions. Data shown are leaves as a function of light saturation PPFD upto A. 540 μmol photons m^{-2} s^{-1} for shade and B. 849 μmol photons m^{-2} s^{-1} for sun grown plants respectively. In figure, D1, D2 and D3 (*open symbols*) represent desiccation and R1, R2, R3 and R4 (*filled symbols*) indicate recovery processes with respect to ETR(I) and ETR(II) on a linear scale. The values represent means of n = 3 leaves per treatment.

To reveal the differences in the light response, and to evaluate disproportionality between ETR(I) and ETR(II), which indicates the onset of CEF, ETR(I) and ETR(II) were compared on linear plots (Fig 29). The direct

proportionality of ETR(II) and ETR(I), which is shown by a linear correlation with a slope of 1 breaks down during the desiccation of the shade leaves. This is shown either by deviation of ETR(II) from the straight line at higher ETR(I) values, or by close to linear correlation, but with significantly smaller slope than one. This phenomenon shows that although electron transfer from PSII becomes limited PSI still has significant electron flow, which circulates around the PSI complex. An extreme case is seen in the strongly desiccated leaves (downward-facing open triangles in Fig. 29A) where significant ETR(I) is measured in the almost complete absence of ETR(II). During the rehydration process the slope of the ETR(II) *versus* ETR(I) curve increases, which shows the gradual decline of cyclic electron flow. Deviation from the direct linearity was much significant in the in sun leaves, and it has recovered almost completely during rehydration (Fig. 29B). Though both the ETR(II) and ETR(I) decreased under the desiccation in the shade as well as sun ecotype, the balance between the two photosystems showed differences among the ecotypes. The linear plots of ETR(II) and ETR(I) indicated, that in sun leaves, there was an imbalance between the two electron transport rates only in the D2 during the desiccation, ETR(I) was predominant only in the D3 stage.

3.3.4. Cyclic Electron Flow (CEF)

We estimated the CEF as the difference in ETR(I) and ETR(II) measured at PPFD 849 μmol photons m^{-2} s^{-1} and at PPFD 540 μmol photons m^{-2} s^{-1} in sun and shade ecotype, respectively (Fig. 30). Shade leaves showed different CEF responses during desiccation and recovery compared to the sun ecotype.

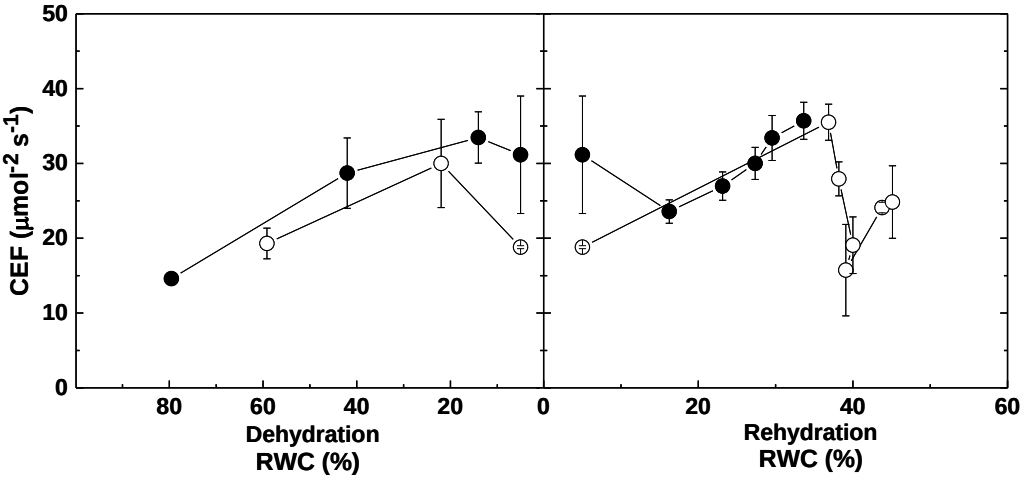

Figure 30. Activity of CEF in desiccating leaves of *Haberlea rhodopensis* ecotypes sun (*open circle*) and shade (*filled circle*) during desiccation and recovery measurements at laboratory conditions. Data shown are leaves as a function of the PPFD of 849 µmol photons m^{-2} s^{-1} for sun and 540 µmol photons m^{-2} s^{-1} for shade grown plants respectively. The rehydration started when leaves reached the air-dry stage, last data point in the dehydration process. The values represent the mean ± SE (n = 3).

In shade leaves, the activity of CEF had a peak in the terminal stage of desiccation, at 14% RWC. During the rehydration, the CEF activity showed a gradual and slow increase that only reached it maximum at around 40% RWC of leaves. In contrast, sun leaves showed a peak in the CEF activity around 40% RWC that declined during the terminal stage of the desiccation to 5% RWC. Nevertheless, the sun ecotype showed significantly more intensive CEF responses in the initial phases of the recovery. The CEF activity reached a peak during the rehydration to 20% RWC. Thereafter, the participation of CEF decreased together with the stabilization of the PSII linear electron transfer pathway (Fig. 30). Taken together, the CEF also plays a protective role in *H. rhodopensis* that finally terminates by acceptor-side limitation processes. Nevertheless, the CEF peak at higher RWC values in the sun ecotype underlines that acclimation mechanisms also affect the capability for the protection of the photosynthetic apparatus.

3.3.5. Quantum yields of PSII and PSI photochemistry

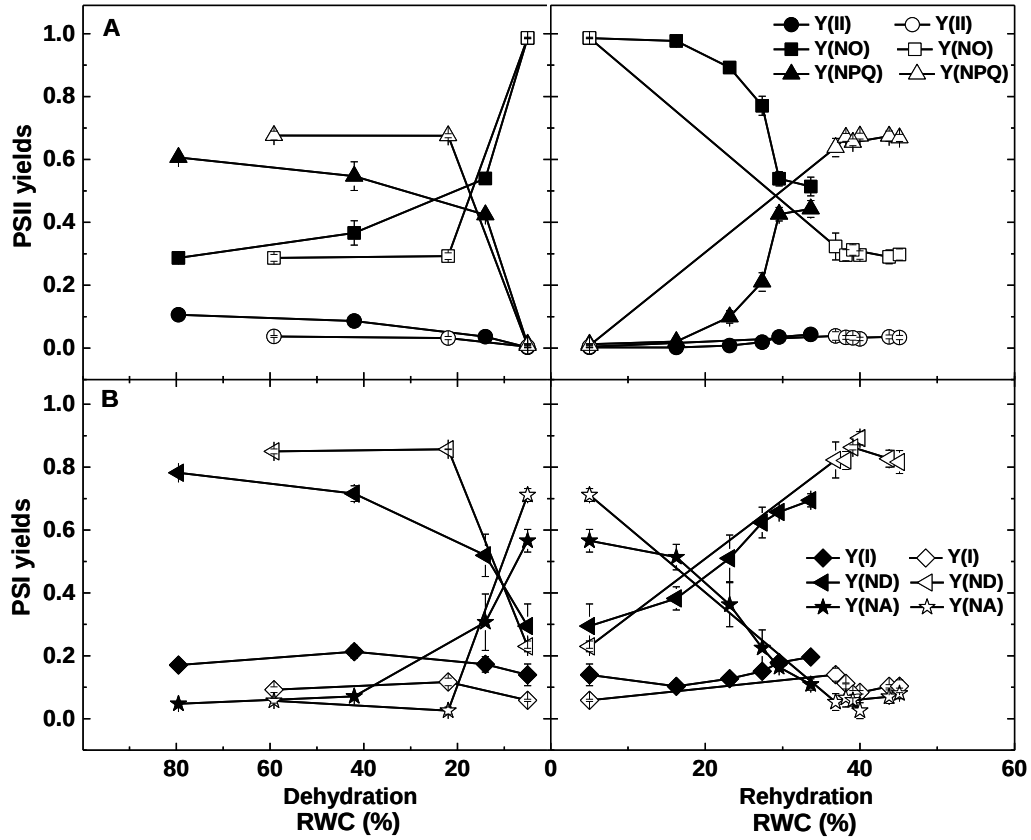

Figure 31. Changes in quantum yields of (A) PSII and (B) PSI in *Haberlea rhodopensis* leaves of shade (*closed symbols*) and sun (*open symbols*) ecotypes subjected to desiccation and recovery measurements respectively under laboratory conditions. Quantum yield were measured at saturating PPFD: 540 µmol photons m^{-2} s^{-1} (shade leaves) and 849 µmol photons m^{-2} s^{-1} (sun leaves). The rehydration started when leaves reached the air-dry stage, last data point in the dehydration process. **A.** The effective PSII quantum yield, Y(II) (*circle*), the non-regulated energy dissipation, Y(NO) (*square*), and the quantum yield of regulated energy dissipation, Y(NPQ) (*triangle*); **B.** The quantum yield of the PSI photochemistry, Y(I) (*diamond*), the quantum yield of non-photochemical energy dissipation due to the donor-side limitation, Y(ND) (*left pointing triangle*), and the energy dissipation due to the acceptor-side limitation, Y(NA) (*star*), are indicated. The values represent the mean± SE (n = 3) leaves per treatment. The small insertion show (a) Y(II) and (b) Y(I) separately.

PSI and PSII parameters were obtained from simultaneous measurements of Chl *a* fluorescence and P700 signals (Fig. 31). Y(I) and Y(II) showed mild desiccation-induced responses in leaves of both ecotypes (Fig. 31 A and B). In the leaves of shade ecotype, a significant increase in Y(NO) and Y(NA) was observed

with decline of Y(NPQ) and Y(ND) during severe desiccation at PPFD of 540 μmol photons m^{-2} s^{-1} (Fig. 31A and B). A similar tendency was observed in the leaves of sun ecotype. Characteristic differences were seen in the rapid response in the sun ecotype under recovery processes (Fig. 31A and B).

In the PSI electron flow, the donor side limitations are more important in the well-hydrated and mild desiccated stages, whereas the acceptor side limitations, such as inhibition in the carbon fixation but even a decrease in the antioxidative defence mechanisms become prominent under severe desiccation. Decrease in the defence mechanisms such as water-water cycle (Asada, 2000; Miyake, 2010) may contribute to the elevated malondialdehyde content measured previously in desiccated *H. rhodopensis* leaves compared to well-hydrated ones (Solti 2014a). Nevertheless, the acceptor-side limitation became prominent at around 50% RWC in the sun ecotype, whereas only below 10% RWC in the shade ecotype, that underlines the importance of the previously reported acclimation of the sun ecotype to the environmental stresses (Sárvári 2014; Georgieva 2016), but also indicate the importance of PSII inactivation in the protection of the photosynthetic apparatus and that of the PSI function preparing for the severe desiccation. A similar phenomenon was observed in the desiccation tolerant macroalga *Ulva prolifera* under water loss (Gao 2014), where the oxidation of PSI was significantly affected by osmotic stress and the higher quantum yield of non-photochemical energy dissipation in PSI was also due to acceptor-side limitation, Y(NA). Nevertheless, the PSI function was more retained until reaching the terminal desiccation. In *H. rhodopensis*, the ETR(II) decreased also faster than ETR(I) under strong water loss.

3.3.6. PSII maximum quantum yield efficiency

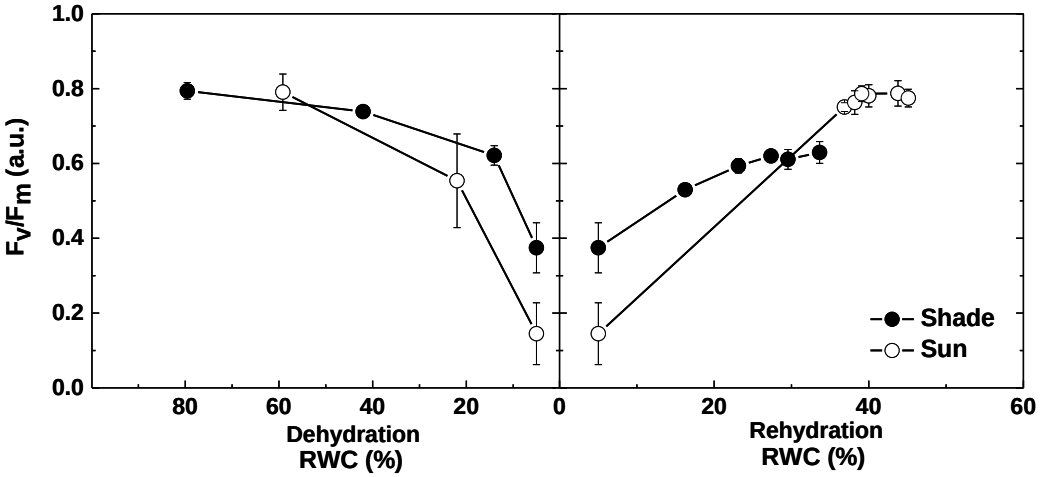

Figure 32. Changes in the PSII maximum quantum yield efficiency determination in *Haberlea rhodopensis* leaves of shade (*filled circle*) and sun (*open circle*) ecotypes during desiccation and recovery measurements at laboratory conditions. The rehydration started when leaves reached the air-dry stage, last data point in the dehydration process. The values represent the mean, n = 3 leaves per treatment.

In the maximum quantum efficiency of PSII reaction centres, a 42% and 65% decline was observed during the desiccation of shade and sun ecotypes to 5-10% RWC, respectively (Fig. 32). Even though the desiccation extent in F_v/F_m on the sun ecotype was severe, recovery processes could retain complete 96-99% resurrection rapidly, within 24 hours (45% RWC). The shade ecotype leaves recovered slowly and could retain back 84% within whole recovery regime in five days (Fig. 32). Solti (2014) indicated that in the initial stage of water loss, the maximal quantum efficiency of PSII reaction centres decreased gradually in both shade and sun leaves. Nevertheless, shade ecotype could not perform a significant antennae-based excitation energy quenching, thus the PSII inactivation was faster and more pronounced.

3.3.7. Initial amplitude of flash induced Chl fluorescence

The initial amplitude indicates the maximal fluorescence yield of Q_A^- reduction (Fig 33). Although the shade ecotype leaves reached the same level of RWC

with one day delay the intial amplitude of the flash induced fluorescence signal, reflecting the amount of functional PSII, had same at amplitude of 0.1 in both two ecotypes (Fig 33).

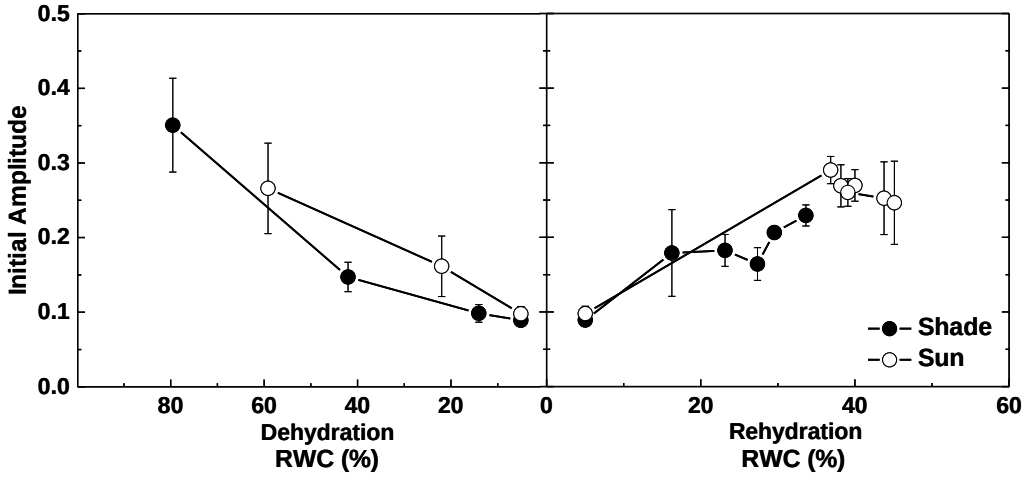

Figure 33. Maximal fluorescence yield obtained from Q_A^- reoxidation kinetics in *Haberlea rhodopensis* leaves of sun (*open circle*) and shade (*filled circle*) ecotypes during desiccation and recovery measurements at laboratory conditions. Leaves under treatment were kept inside a cuvette throughout the experiment. The rehydration started when leaves reached the air-dry stage, last data point in the dehydration process. The values represent the mean± SE (*n = 3*) leaves per treatment.

Nevertheless, a rapid and stable recovery process was observed in the sun ecotype leaves in comparison to the delayed response of the shade ones (Fig 33). Since shade ecotype leaves exhibited higher amplitude compared to its well-hydrated control staged, it could not gain a complete recovery.

3.3.8. Q_A relaxation kinetics

According to the Q_A relaxation kinetics, the effect of desiccation was different in the magnitude of perturbation in the PSII electron transport processes among the two ecotypes.

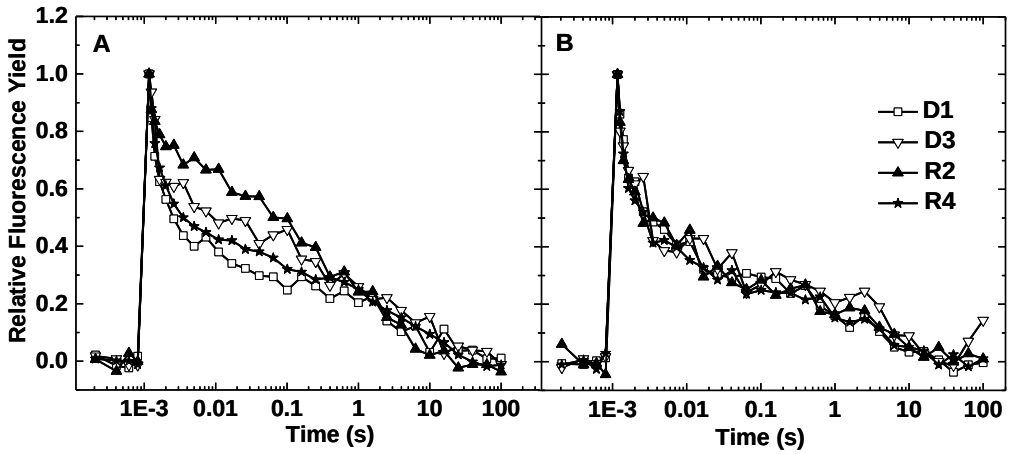

Figure 34. Q_A relaxation kinetics in leaves of *Haberlea rhodopensis* sun and shade ecotype. Leaves were subjected to desiccation and recovery treatments at laboratory conditions. D1, D3 (*open symbols*) represent stages of the desiccation while R2, R4 (*filled symbols*) indicate that of the recovery measurements.

Shade ecotype leaves show clear separation in the relaxation kinetics during desiccation and recovery processes with respect to its well-hydrated control stage, while sun ecotype leaves were unshaken and relaxed similar to its corresponding well-hydrated initial control stage (Fig 34 A and B).

The relaxation slowed especially in the few millisecond middle phase in severely desiccated and initially rehydrated leaves of the shade ecotype, reflecting on that the reoxidation of Q_A^- is mainly influenced by the oxidized PQ binding to the PSII (Vass 1999; de Wijn and Gorkom, 2001). As we found no significant changes in the F_J in the OJIP-tests, not the bound PQ acceptors (Tóth 2007) but rather the replacement of PQ acceptors from the oxidized quinone-pool inhibited the Q_A^- reoxidation in the shade ecotype under low RWCs. Thus, the availability of oxidized PQ molecules may decrease in the shade ecotype under low RWC that can also inhibit the linear electron transport even under the rehydration process.

3.3.9. OJIP Chl *a* fluorescence transients

Concerning the PSII reaction centre processes, the OJIP fluorescence induction kinetics showed gradual changes in both the shade and sun ecotype leaves of *H. rhodopensis* (Fig 35).

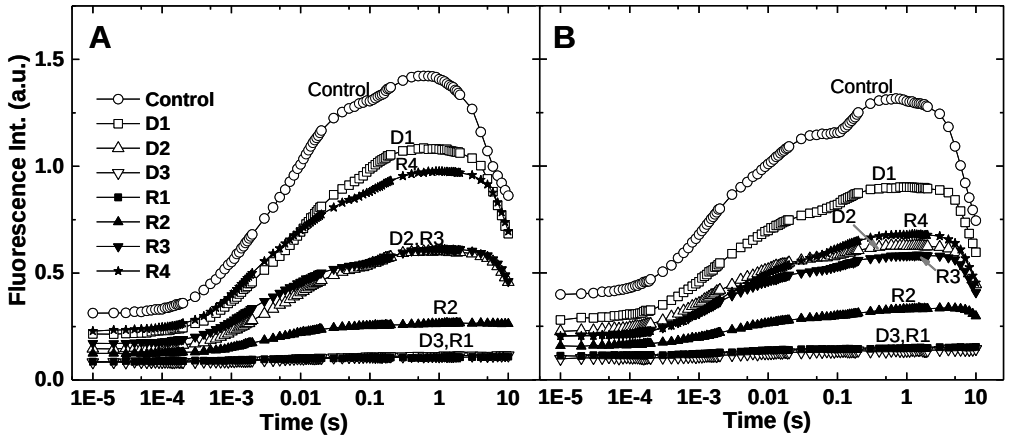

Figure 35. OJIP Chl *a* fluorescence transients in leaves of *Haberlea rhodopensis* shade and sun ecotypes subjected to desiccation and rehydration. Control refers to the well-hydrated initial control stage, D1, D2 and D3 (*open symbols*) represent stages of the desiccation while R1, R2, R3 and R4 (*filled symbols*) indicate those of the rehydration. The values represent the mean±SE (*n = 3*) leaves per treatment.

No significant differences were found between the changes in the OJIP transient in the two ecotypes during the desiccation and the rehydration. Desiccation caused a gradual decrease in the peak fluorescence, but together with the desiccation, the F_o fluorescence also showed a slight decrease in both tow ecotypes. During rehydration the fluorescence yield recovered. Nevertheless, the peak fluorescence did not reached the value of the corresponding well-hydrated initial stage. Similarly to other parameters the OJIP transients also indicate faster recovery of sun leaves compared to shade ones.

The decrease in the PSII maximal quantum efficiency is caused by the decrease of the P fluorescence (F_m) level during desiccation of both ecotypes. The tendentious decrease of the F_o in both ecotypes may correspond to an antenna

dissociation from the PSII reaction centres (Zhang and Xu, 2003; Johnson 2011) and thus contribute to the higher antennae-based non photochemical quenching during the mild desiccation that was reported previously (Solti 2014b). The increase in I–P amplitude of the OJIP fluorescence induction kinetics reflects the size of the terminal electron acceptor pool of PSI (Strasser 2004; Schansker 2005; Tsimilli-Michael and Strasser 2008), while a faster J-I phase indicate less functional PSII activity and less fraction of PSI content (Ceppi 2012). The rise of the I-P amplitude in the D1 and R4 levels of shade ecotype leaves was well correlated with a higher PSI activity and increased ETR-PSI observed in Fig 29A. The CEF was further confirmed in the D1 and R4 levels of shade ecotype leaves using OJIP fluorescence transient.

3.4. Photosynthetic efficiency of tetraploid willow genotypes

3.4.1. Pigment content determination: Field and greenhouse

Leaf Chl content is a key parameter for characterization of physiological performance of plants including the determination of vegetation indices in woody species as well (Lu 2015). Under greenhouse conditions leaves of the tetraploid plants contained significantly higher amounts of Chls and carotenoids than the diploid plants (Table. 3). The field grown willow plants synthesized more pigments in their leaves than the greenhouse grown plants in case of all studied lines. Elevated amounts of these pigments were also detectable in the tetraploid variants in the field grown leaves relative to the diploid ones but these differences did not reach the statistically significant levels.

Table 4. Leaf Chlorophyll and carotenoid contents determined from tetraploid plants grown under field and greenhouse conditions. Sampling was carried out from the 5^{th}/ 6^{th} fully developed younger leaves (from top). Data are mean ± SE of six to seven independent plants per genotype. Statistically significant events between the diploid and tetraploid lines ***P<0.001, **P<0.01, *P<0.05 are indicated.

Sample	Chl a	Chl b	Chl (a+b)	Car (x+c)	Chl a	Chl b	Chl (a+b)	Car (x+c)
	(μg/cm^2)							
	Field grown plants				Greenhouse grown plants			
Diploid	48.68 ±1.4	17.47 ±0.5	65.32 ±1.9	12.15 ±0.25	18.50 ± 0.48	5.3 ± 0.24	23.56 ± 0.58	3.84 ± 0.13
PP-E6	51.60 ±1.3	18.49 ±0.5	69.22 ±1.7	12.38 ±0.22	22.02 ± 0.58 ***	6.5 ± 0.19 **	28.17 ± 0.75 ***	4.45 ± 0.12 *
PP-E7	49.71 ±1.5	18.50 ±0.4	67.35 ±1.8	12.07 ±0.22	22.66 ± 0.94 **	6.6 ± 0.32 **	28.96 ± 1.25 **	4.58 ± 0.16 **
PP-E13	49.84 ±2.2	18.17 ±0.8	67.15 ±3.0	11.74 ±0.33	23.34 ± 0.71 ***	6.6 ± 0.25 **	29.59 ± 0.91 ***	4.62 ± 0.12 **

Higher Chl (a+b) contents (25-30%) in greenhouse grown leaves (Table 3) can be a sign for a more efficient light utilization. Differences between diploid and tetraploid plants in the chlorophyll content were not statistically significant under field conditions.

3.4.2. Calculated Chl *a* fluorescence parameters: Field and greenhouse

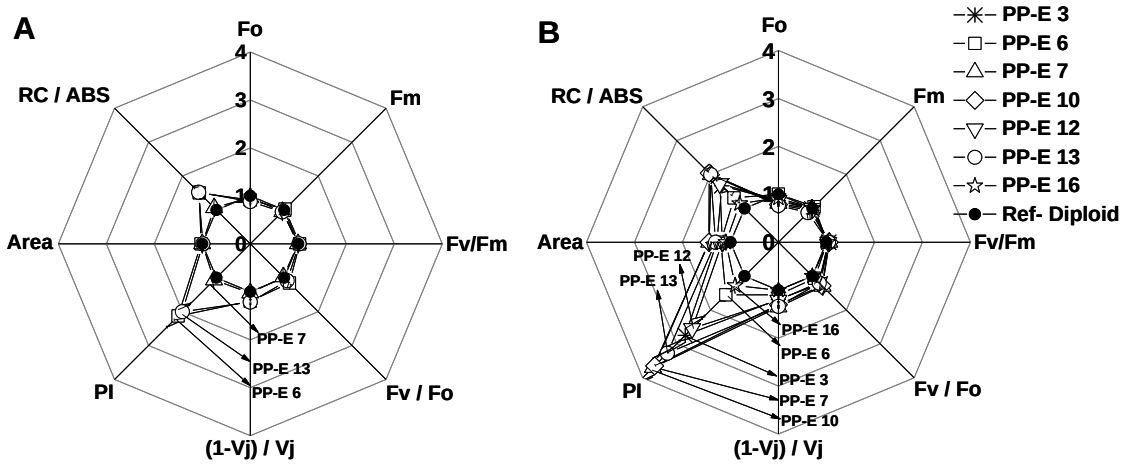

Figure 36. Spider plot of chl fluorescence parameters in leafs of tetraploid willow plants grown in A, Field and B, Greenhouse conditions. The figure shows the values measured on 5^{th} / 6^{th} young fully developed leaves from apical shoot. The data are shown for the tetrapliod lines (*open symbols*) after normalization to respective value obtained in the diploid line (*closed symbol*). Data are mean±SE of six to seven independent plants per genotype.

The so called OJIP chlorophyll fluorescence transient reflects electron transport through redox components of PSII and PSI (Strasser 2004). Chlorophyll fluorescence parameters are mostly used as indicators for monitoring stress response even in tree species (Desotgiu 2012). We compared the physiological responses of tetraploid willow seedlings grown in greenhouse and field conditions using fast fluorescence kinetics approach (Fig. 36). Among the deduced biophysical parameters, Performance Index (PI) and RC/ABS showed more sensitivity in tetraploid lines. Based on PI values PP-E7, E13, E12 plants exhibited the highest leaf photosynthetic

activities. 2. Dissipated energy flux per active reaction centers RC/ABS) values were higher in leaves of some tetraploid lines (PP-E13, E7) (Fig. 36B).

3.4.3. Electron transfer efficiency: Field and greenhouse

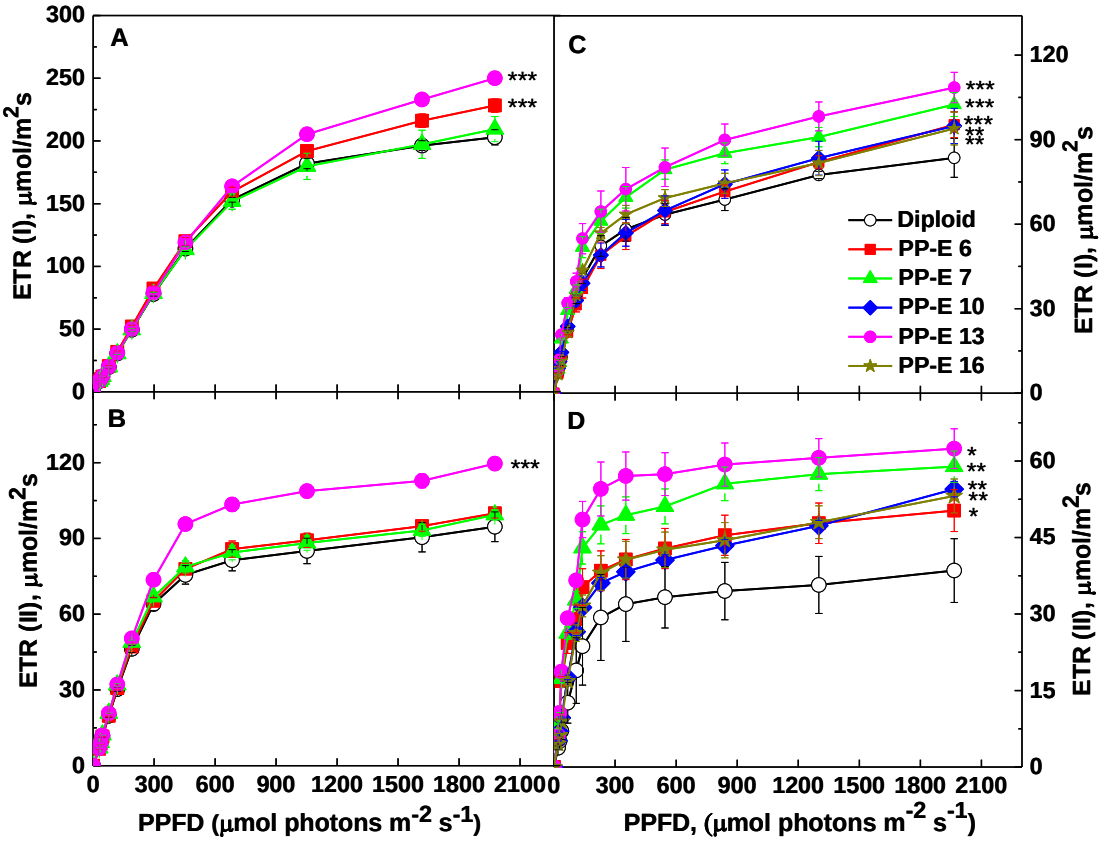

Figure 37. Photosynthetic ETRs of PSI and PSII measured on leafs of tetraploid willow plant samples. Simultaneous light response curves of ETR(I) and ETR(II) were measured in the dark-adapted 5th/ 6th fully developed young leaves (from top) for both field and greenhouse genotypes using Dual PAM- 100 instrument. A, ETR (I) under field conditions. B, ETR(II) under field conditions. Leaves of field-grown plants were collected in wet tissue and kept in an ice box, and ETR measurements were carried out within 2h of sample collection. C, ETR(I) under greenhouse conditions. D, ETR(II) under greenhouse conditions. Tetraploid willow genotypes are indicated as *closed symbols* and the diploid genotype by *open symbols*. Data are means±SE of six independent plants per genotype. Based on Welch's t test, statistically significant events compared with diploids are indicated next to corresponding data points as ***, P< 0.01, **, P<0.05 and *, P<0.1. (for the highest photosynthetic photon flux density [PPFD] measurement).

Since the ETR is an estimation of the number of electrons passing through photosystem I and II therefore these associated parameters could be used for prediction of the photosynthetic capacity in leaves of different willow genotypes. (Fig. 37). We have applied Pulse Amplitude Modulation (PAM) based chlorophyll fluorescence and P700 absorbance using Dual-PAM-100 (Walz GmbH) to determine ETR through PSII and PSI, respectively in dark adapted leaves of both field and greenhouse grown willow plants.

Light saturation curves show increased rates of ETR(I) in tetraploid genotypes PP-E13 and PP-E6 under field conditions at higher light intensities (Fig. 37A). ETR (II) was significantly higher in PP-E13 and getting increased from PPFD 450 µmol photons m^{-2} s^{-1} (Fig. 37B). ETR(I) and ETR(II) values were generally lower in leaves of greenhouse grown plants. Under these circumtances the photosynthetic capacities of tetraploid variants were found to be improved as indicated by both ETR(I) and ETR(II) values (Fig. 37C and D). In field conditions, we observed significantly higher electron transport rate of PSI in PP-E13 and PP-E6 while ETR(II) was also found to be higher for PP-E13 (Fig. 37A and B).

3.4.4. Net CO_2 assimilation and transpiration rates of tetraploid willows

Efficiency in uptake of the atmospheric CO_2 by plants and of its photosynthetic assimilation into organic compounds, the building blocks of biomass has major impact on capacity of wood production and reduction of environmental concerns. In photochemical reactions, PSII utilize light energy to extract electrons from water and release O_2. Electrons are transferred to PSI, and ultimately produce NADPH. While the protons which are pumped into the thylakoid lumen during

electron transport are used in ATP production, which together with NADPH is the driving force of CO_2 assimilation in the Calvin-Benson cycle.

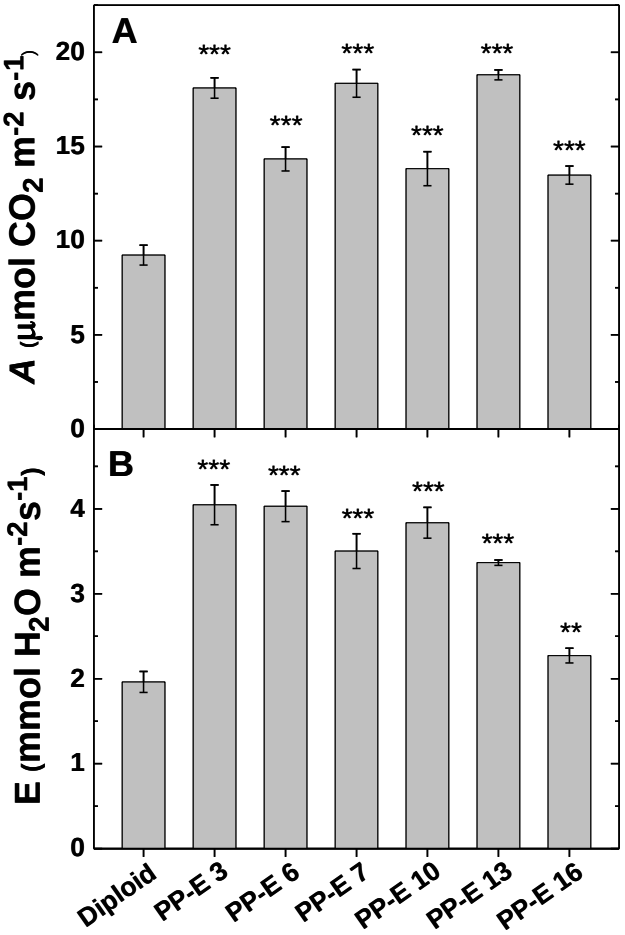

Figure 38. CO_2 uptake and transpiration rate in leaves of tetraploid lines.The measurements were recorded in air CO_2 concentration of 400 ppm, leaf temperature of 22°C, and PAR of 400- 430 µmol photons m^{-2} s^{-1} (n=5) plants/ treatment. Based on Welch's *t*-test, statistically significant events compared to diploids are indicated above the sample labels as ***P<0.01 and ** P<0.05.

In accordance with the stomatal conductance data several tetraploid plants showed enhanced CO_2 assimilation rate (Fig. 38A). Tetraploid willows were found to transpire more water from leaves (Fig. 38B). Net photosynthetic CO_2 uptake rate per unit leaf area has a positive linear relatioanship with the quantum yield of PSII or electron transfer rate (ETR) as shown by Kubota and Yoshimura (2002).

4. CONCLUSIONS

- **Characterization of biomass and grain yield to severe drought**

- We could characterize biomass accumulation in the vegetative phase from early developing 'secondary leaves' and grain yield in the grain filling period from 'flag leaf' under drought conditions. We could find that Green biomass and grain yield may respond differentially to drought stress. Grain yield optimization of wheat can not be based on green biomass phenotyping alone.
- Cappelle Desprez variety exhibits an early ground cover, growth habit and higher cyclic electron flow around PSI (CEF-PSI) along with secondary trait associated mechanisms like delayed senescenece and enhanced water use efficiency for increased biomass while early spiking and prolonged transpiration rate through flag leaf was observed in Plainsman V for grain yield.
- It is also concluded that increase in drought factor (DFI) and performance (PI) indices calculated from variable chlorophyll fluorescence parameters of secondary leaves was correlated for increased biomass observed in drought sensitive Cappelle Desprez cv. In drought tolerant Plainsman V, increase in DFI and PI through flag leaf during early phases of grain filling period also contribute to grain yield stability.

- **Synergistic effects of drought and salt using high throughput plant phenotyping tools**

- Salt stress induces more severe effects under water limitation than under well-watered conditions. Water use efficiency remains unaffected by salt stress in well performing wheat lines, but drops significantly in salt sensitive lines.

- The ratio of the grain yield and dry biomass remained practically constant even under the combined effect of salt stress and water limitation, showing that carbon partitioning to grains is not affected specifically by the salt + water stress.
- Biomass and grain yield were significantly reduced in T2 (drought) as well as T4 (drought and salt stress combination) due to stomatal closure in the source region and less carbon partitioning to the sink region respectively.
- Higher proline content during double stress (drought & salinity) act as a defense mechanism. Grain yield effect was noted to be 75-90% on T4 (double stress), 50% affect on T2 (drought stress) and 20% affect on T3 (salt stress) conditions. Our data show that substantial crop loss due to salinity stress could be avoided by providing irrigation measures on time.

➢ **Differences in the electron flow responses in two ecotypes of the resurrection plant Haberlea rhodopensis during desiccation and rehydration**

- Compared to the thoroughly investigated, more common shade acclimated ecotype, the high irradiance acclimated ecotype of *Haberlea rhodopensis* performs more effective protective mechanism in its photosynthesis.
- Under severe desiccation, the PSII becomes inactive and acceptor-side limitation factors start to inhibit the PSI function in the high irradiance acclimated ecotype. In the early phase of rehydration, the photosynthetic function recovers rapidly together with an increase in cyclic electron flow for sun ecotype.

- In contrast, the shade ecotype only showed an increased cyclic electron flow under severe desiccation and upon rewatering, all the recovery processes proved to be slower. Therefore, growth conditions and acclimation processes in the natural habitat strongly influence the desiccation tolerance.

➢ **Photosynthetic efficiency of tetraploid willow genotypes**

- Morphological and physiological growth traits of the tetraploid lines are significantly correlated with photosynthetic parameters.
- Broader leaf area and biomass helps the tetraploids to regulate better radiation use efficiency in the reaction centers of photosynthetic apparatus. This will regulate better water splitting on the donor side of PSII, enhancing electron transport rates, higher energy production in the form of ATP and NADPH; increase CO_2 fixation rates thereby increasing dry matter accumulation.
- Photosynthetic characterization of tetraploid energy willow lines show increased CO_2 fixation rate and better photosynthetic efficiency as compared to the control diploid line.

5. LIST OF REFERENCES

Ahad MA.1986. Growth analysis of Rice bean (Vigna umbellata Thunb.) under different management practices and their agronomic appraisal. Ph.D. Dissertation in Agronomy.

Alamillo JM and Bartels D. 2001. Effects of desiccation on photosynthesis pigments and the ELIP-like dsp 22 protein complexes in the resurrection plant *Craterostigma plantagineum*. *Plant Sci*. 160: 1161–1170.

Alpert P. 2005. The limits and frontiers of desiccation tolerant life. *Integr. Comp. Biol*. 45: 685–695.

Asada K. 2000. The water-water cycle as alternative photon and electron sinks. *Phil.Trans*. *Biol*. *Sci*. 355: 1419-1431.

Asada K. 2006. Production and scavenging of reactive oxygen species in chloroplasts and their functions. *Plant Physiology*. 141: 391–396.

Ashraf M .1994. Breeding for salinity tolerance in plants. *Crit. Rev. Plant Sci.* 13:17–42.

Ashraf M and Ali Q. 2008. Relative membrane permeability and activities of some antioxidant enzymes as the key determinants of salt tolerance in canola (*Brassica napus L.*). *Environ*. *Exp*. *Bot*. 63: 266-273.

Babic L, Babic M, Turan J, Matic-Kekic S, Radojcin M, Mehandzic-Stanisic S, Pavkov I and Zoranovic M. 2011. Physical and stress–strain properties of wheat (*Triticum aestivum* L) kernel. *J. Sci Food Agric*. 91: 1236–1243.

Babayev HG, Bayramov Sh. M, Mehvaliyeva UA, Aliyeva MN, Guliyev NM, Huseynova IM and Aliyev JA. 2013. Activities of C4-photosynthetic enzymes in different wheat genotypes under continuous soil drought conditions. *Journal of Biochemistry Research*. Vol. 1 (1), pp.7-16.

Baker NR and Rosenqvist E. 2004. Applications of chlorophyll fluorescence can improve crop production strategies: an examination of future possibilities. *Journal of Experimental Botany,* Vol. 55, No. 403, pp. 1607–1621.

Bandurska H. 2000. Does proline accumulated in leaves of water deficit stressed barley plants confine cell membrane injury? I. Free proline accumulation and membrane injury index in drought and osmotically stressed plants. *Acta Physiol Plant*. 22: 415.

Barbour MM, Warren CR, Farquhar GD, Forrester G, and Brown H. 2010. Variability in mesophyll conductance between barley genotypes, and effects on transpiration efficiency and carbon isotope discrimination. *Plant Cell Environ.* 33:1176-1185.

Bartels D. 2005. Desiccation tolerance studied in the resurrection plant *Craterostigma plantagineum*. *Integr. Comp. Biol*. 45: 696–701.

Bates LS, Waldren RP, Teare ID. 1973. Rapid determination of free proline for water-stress studies. *Plant and Soil.* 39: 205–207

Bensen RJ, Boyer JS & Mullet JE.1988. Water deficit induced changes in abscisic acid, growth, polysomes, and translatable RNA in soybean hypocotyls. *Plant Physiology*. 88: 289–294.

Berger B, Parent B,Tester M. 2010. High-throughput shoot imaging to study drought responses. *Journal of Experimental Botany*. 61: 3519-3528.

Bernacchia G., F. Salamini, and D. Bartels. 1996. Molecular characterization of the rehydration process in the resurrection plant Craterostigma plantagineum. Plant Physiol. 111:1043–1050.

Bilger W, Bjorkman O. 1990. Role of the xanthophyll cycle in photoprotection elucidated by measurements of light-induced absorbance changes,

fluorescence and photosynthesis in leaves of *Hedera canariensis*. *Photosynthesis Research*. 25: 173-185.

Björkman O, Demmig B. 1987. Photon yield of O_2 evolution and chlorophyll fluorescence characteristics at 77 K among vascular plants of diverse origins. *Planta*. 170: 489-504.

Boyer JS. 1982. Plant productivity and environment. *Science* 219, 443-448.

Boyer JS, Westgate ME. 2004. Grain yields with limited water. *Journal of Experimental Botany*. 55: 2385-2394.

Bradford KJ and Hsiao TC. 1982. Physiological response to moderate stress. In Encyclopedia of plant physiology. Physiological plant ecology II. Water relations and carbon assimilation. Eds. Lange OL, Nobel PS, Osmond CB and Ziegler H. Heidelberg Springer, Newyork, Berlin. pp.263- 324.

Bray EA, Bailey-Serres J, Weretilnyk E. (2000) Responses to abiotic stresses. W. Gruissem, B. Buchannan, R. Jones (Eds.), Biochemistry and Molecular Biology of Plants, American Society of Plant Biologists, Rockville, MD**:** 158–1249.

Brestic M, Zivcak M .2013. PSII fluorescence techniques for measurement of drought and high temperature stress signal in crop plants: protocols and applications. In: Rout GR, Das AB (eds) Molecular stress physiology of plants. Springer, Dordrecht, pp 87–131.

Campos H, Trejo C, Peña-Valdivia CB, García-Nava R, Conde-Martínez FV, Cruz-Ortega MR. 2014. Photosynthetic acclimation to drought stress in *Agave salmiana* Otto ex Salm-Dyck seedlings is largely dependent on thermal dissipation and enhanced electron flux to photosystem I. *Photosynthesis Research*. 122: 23-39.

Chaves MM, Flexas J, Pinheiro C. 2009. Photosynthesis under drought and salt stress: regulation mechanisms from whole plant to cell. *Annals of Botany*. 103: 551–560.

Cornic G, Briantais JM .1991. Partitioning of photosynthetic electron flow between CO_2 and O_2 reduction in a C3 leaf (*Phaseolus vulgaris* L.) at different CO_2 concentrations and during water stress. *Planta* 183: 178–184.

Ceppi MG, Oukarroum A, Çiçek N, Strasser RJ, Schansker G. 2012. The IP amplitude of the fluorescence rise OJIP is sensitive to changes in the photosystem I content of leaves: a study on plants exposed to magnesium and sulfate deficiencies, drought stress and salt stress. *Physiol Plant*. 144: 277-288.

Congming Lu, Vonshak A. 2002. Effects of salinity stress on photosystem II function in cyanobacterial Spirulina platensis cells. *Physiol Plant.* 114(3): 405- 413.

Cseri A, Sass L, Törjék O, Pauk J, Vass I, Dudits D. 2013. Monitoring drought responses of barley genotypes with semi-robotic phenotyping platform and association analysis between recorded traits and allelic variants of some stress genes. *Australian Journal of Crop Science*. 7: 1560-1570.

Cuellar-Ortiz SM, De La Paz Arrieta-Montiel M, Acosta-Gallegos J, Covarrubias AA. 2008. Relationship between carbohydrate partitioning and drought resistance in common bean. *Plant Cell Environment*. 31: 1399-1409.

Dhondt S, Wuyts N, Inzé D. 2013. Cell to whole-plant phenotyping: the best is yet to come. *Trends Plant Science*. 18: 428-439.

Daskalova E, Dontcheva S, Yahoubian G, Minkov I, Toneva V. 2011. A strategy for conservation and investigation of the protected resurrection plant *Haberlea rhodopensis* Friv. *BioRisk*. 6: 41–60.

Davies WJ, Zhang J .1991. Root signals and the regulation of growth and development of plant in drying soil. *Annu. Rev. Plant Physiol. Plant Mol. Biol.* 42: 55–76.

Dencic. S, Kastori R, Kobiljski B & Duggan B. 2000. Evaluation of grain yield and its components in wheat cultivars and landraces under near optimal and drought conditions. *Euphytica*. 113: 43–52.

de Wijn, R., van Gorkom, H.J. 2001. Kinetics of electron transfer from Q_A to Q_B in photosystem II. *Biochemistry*. 40: 11912-11922.

Dimitrijevic M, Petrovic S, Mladenov N, Belic M, Hristov N, Banjac B and Vukosavljev M. 2009. *Genetika*. 41 (2): 169 -177.

Dudits D, Török K, Cseri A, Paul K, Nagy AV, Nagy B, Sass L, Ferenc G, Vankova R, Dobrev P, Vass I and Ayaydin F. 2016. Response of organ structure and physiology to autotetraploidy in early development of energy willow *Salix viminalis* L. *Plant Physiology.* Vol. 170, pp. 1504–1523**.**

Duysens LNM, Sweers HE. 1963. Mechanism of two photochemical reactions in algae as studied by means of fluorescence. In *Studies on Microalgae and Photosynthetic Bacteria*. Edited by the Japanese Society of Plant Physiologists pp. 353-372. University of Tokyo Press, Tokyo, Japan.

Elmore CD. 1980. The paradox of no correlation between leaf photosynthetic rates and crop yields. In: Hesketh JD and Jones JW (eds) Predicting Photosynthesis for Ecosystem Models, Vol II, pp 155-167. Boca Raton, FL: CRC Press.

Eppler U and Petersen J-E. 2007. Short Rotation Forestry, Short Rotation Coppice and energy grasses in the European Union: Agro-environmental aspects, present use and perspectives. EEA Specific Contract No 2

3604/B2006/EEA.52793 - Deliverable Task 2b: Background report on current SRF/SRC cropping patterns in Europe.

Erdei N, Barta C, Hideg É, Böddi B. 2005. Light-induced wilting and its molecular mechanism in epicotyls of dark-germinated pea (*Pisum sativum* L.) seedlings. *Plant and Cell Physiology*. 46: 185-191.

Errabii T, Gandonou CB, Essalmani H, Abrini J, Idaomar M, Skali- Senhaji N. 2006. Growth, Proline and ion accumulation in Sugarcane callus cultures under drought-induced osmotic stress and its subsequent relief. *Afr. J. Biotechnol*. 5(6): 1488-1493.

Evans LT, Bingham J, Johnson P and Sutherlands J. 1972. Effect of awns and drought on the supply of photosynthate and its distribution within wheat ears. *Ann. Appl. Biol*. 70: 67–76.

Fábián A, Jäger K, Rakszegi M, Barnabás B. 2011. Embryo and endosperm development in wheat (*Triticum aestivum* L.) kernels subjected to drought stress. *Plant Cell Reports*. 30: 551-563.

Fan D-Y. 2007. Quantification of cyclic electron flow around Photosystem I in spinach leaves during photosynthetic induction. *Photosynthesis Research*. 94: 347-357.

Farquhar GD, Richards RA. 1984. Isotopic composition of plant carbon correlates with water-use efficiency of wheat genotypes. *Australian Journal of Plant Physiology*.11: 539-552.

Fehér-Juhász E, Majer P, Sass L, Lantos C, Csiszár J, Turóczy Z, Mihály R, Mai A, Horváth GV, Vass I, Dudits D, Pauk J. 2014. Phenotyping shows improved physiological traits and seed yield of transgenic wheat plants expressing the alfalfa aldose reductase under permanent drought stress. *Acta Physiol.Plant*.

36: 663-673.

Flexas J, Bota J, Loreto F, Cornic G, Sharkey TD. 2004. Diffusive and metabolic limitations to photosynthesis under drought and salinity in C_3 plants. *Plant Biology*. 6: 269–279.

Flexas J, Diaz-Espejo A, Galmes J, Kaldenhoff R, Medrano H, Ribas-Carbo M. 2007. Rapid variations of mesophyll conductance in response to changes in CO2 concentration around leaves. *Plant, Cell & Environment*. 30: 1284–1298.

Flowers TJ and Yeo AR. 1995. Breeding for salinity resistance in crop plants: Where next? *Aust. J. Plant Physiol*. 22: 875–884.

Gaff DF. 1971. Desiccation-tolerant flowering plants in southern Africa. *Science.* 174: 1033–10343.

Gao S, Shen S, Wang G, Niu J, Lin A, Pan G. 2011. PSI-driven cyclic electron flow allows intertidal macro-algae *Ulva* sp. (Chlorophyta) to survive in desiccated conditions. *Plant Cell Physiol*. 52: 885–893.

Gao S, Wang G. 2012. The enhancement of cyclic electron flow around photosystem I improves the recovery of severely desiccated *Porphyra yezoensis* (Bangiales, Rhodophyta). *J. Exp. Bot.* 63: 4349–4358.

Gao S, Zheng Z, Gu W, Xie X, Huan l, Pan G, Wang G. 2014. Photosystem I shows a higher tolerance to sorbitol-induced osmotic stress than photosystem II in the intertidal macro-algae *Ulva prolifera* (Chlorophyta). *Physiol Plant.* 152: 380–388.

Gechev TS, Benina M, Obata T, Tohge T, Sujeeth N, Minkov I and Toneva V. 2013. Molecular mechanisms of desiccation tolerance in the resurrection glacial relic Haberlea rhodopensis. *Cellular and Molecular Life*

Sciences. *70*(4): 689-709. 10.1007/s00018-012-1155-6.

Genty B, Briantais J-M, Baker NR. 1989. The relationship between the quantum yield of photosynthetic electron transport and quenching of chlorophyll fluorescence. *Biochimica et Biophysica Acta* 990: 87-92.

Georgieva K, Doncheva S, Mihailova G, Petkova S. 2012. Response of sun- and shade-adapted plants of *Haberlea rhodopensis* to desiccation. *Plant Growth Regul*. 67: 121–132.

Georgieva K, Lenk S, Buschmann C. 2008. Responses of the resurrection plant *Haberlea rhodopensis* to high irradiance. *Photosynthetica* 46: 208-215.

Georgieva K, Maslenkova L. 2006. Thermostability and photostabitity of PSII in leaves of resurrection plant *Haberlea rhodopensis* studied by means of chlorophyll fluorescence. *Z Naturforsch*. 61c: 234-240.

Georgieva K, Szigeti Z, Sárvári É, Gáspár L, Maslenkova L, Peeva V, Péli E, Tuba Z. 2007. Photosynthetic activity of homoiochlorophyllous desiccation tolerant plant *Haberlea rhodopensis* during dehydration and rehydration. *Planta*. 225: 955-964.

Georgieva K, Rapparini F, Bertazza G, Mihailova G, Sárvári É, Solti Á, Keresztes Á. 2016. Alterations in the sugar metabolism and in the vacuolar system of mesophyll cells contribute to the desiccation tolerance of *Haberlea rhodopensis* ecotypes. *Protoplasma*. DOI 10.1007/s00709-015-0932-0.

Golding AJ, Johnson GN. 2003. Down-regulation of linear and activation of cyclic electron transport during drought. *Planta*. 218: 107-114.

Golzarian MR, Frick RA, Rajendran K, Berger B, Roy S, Tester M, Lun DS. 2011. Accurate inference of shoot biomass from high-throughput images of cereal plants. *Plant Methods*.7.

Gosse G. 1995. Environmental Issues and Biomass, Biomass for Energy, Environment, Agriculture and Industry, *Proceedings of the 8th European Conference.* Vol. 1: 52 - 62.

Govindjee and Veit W. 2010. Z-Scheme of electron transport in photosynthesis. (http://www.life.illinois.edu/govindjee/Z-Scheme.html)

Grant OM, Chaves MM and Jones HG. 2006. Optimizing thermal imaging as a technique for detecting stomatal closure induced by drought stress under greenhouse conditions. *Physiologia Plantarum* 127: 507–518.

Guóth A, Tari I, Gallé Á, Csiszár J, Pécsváradi A, Erdei L. 2009. Comparison of the drought stress responses of tolerant and sensitive wheat cultivars during grain filling: Changes in flag leaf photosynthetic activity, ABA levels, and grain yield. *J.Plant Growth Regul*. 28: 167-176.

Hafsi M, Akhter J, Monneveux J. 2007. Leaf senescence and carbon isotope discrimination in durum wheat (*Triticum durum Desf*.) under severe drought conditions. *Cereal Res. Commun*. 35: 71-80.

Hamdani S, Qu M, Xin C-P, Li M, Chu C, Govindjee, Zhu X-G. 2015. Variations between the photosynthetic properties of elite and landrace Chinese rice cultivars revealed by simultaneous measurements of 820 nm transmission signal and chlorophyll *a* fluorescence induction. *Journal of Plant Physiology*.177: 128-138.

Harb A, Krishnan A, Ambavaram MMR, Pereira A. 2010. Molecular and physiological analysis of drought stress in *Arabidopsis* reveals early responses leading to acclimation in plant growth. *Plant Physiology*. 154: 1254-1271.

Harley PC, Loreto F, Di Marco G, and Sharky TD. 1992. Theoretical considerations when estimating the mesophyll conductance to CO_2 flux by analysis of the response of photosynthesis to CO_2. *Plant Physiol.* 98:1429-1436.

Hartmann A, Tobias Czauderna, Roberto Hoffmann, Nils Stein and Falk Schreiber .2011. HTPheno: An image analysis pipeline for high-throughput plant phenotyping. *BMC Bioinformatics*. 12:148.

Hassan IA. 2006. Effects of water stress and high temperature on gas exchange and chlorophyll fluorescence in *Triticum aestivum* L. *Photosynthetica*. 44(2): 312-315.

He T & Cramer GR. 1996. Abscisic acid concentrations are correlated with leaf area reductions in two salt-stressed rapidcycling *Brassica* species. *Plant and Soil*. 179: 25–33.

Hinchee M, Rottmann W, Mullinax L, Zhang CS, Chang SJ, Cunningham M, Pearson L, Nehra N. 2009. Short-rotation woody crops for bioenergy and biofuels applications. In Vitro Cellular & Developmental Biology-Plant 45: 619–629.

Hoekstra FA, Golovina EA, Buitink J. 2001. Mechanisms of plant desiccation tolerance. *Trends Plant Sci*ence, 6: 431-438

Huang W, Yang S-J, Zhang S-B, Zhang J-L, Cao K-F. 2012. Cyclic electron flow plays an important role in photoprotection for the resurrection plant *Paraboea rufescens* under drought stress. *Planta*. 235: 819–828.

Huseynova IM, Suleymanov SY, Aliyev JA. 2007. Structural–functional state of thylakoid membranes of wheat genotypes under water stress. *Biochimica et Biophysica Acta*. 1767; 869–875.

Ingram J, Bartels D. 1996. The molecular basis of dehydration tolerance in plants. *Annu.Rev.Plant Physiol.Mol.Biol*. 47: 377-403.

Jacobsen SE, Rosenqvist E, Bendevis M. 2012. Chlorophyll extraction with dimethylformamide DMF. PrometheusWiki. http://prometheuswiki. publish.csiro.au/tikicitation.php?page=Chlorophyll%20extraction%20with %20Dimethylformamide%20DMF (August 13, 2015).

Jäger K, Fábián A, Eitel G, Szabó L, Deák C, Barnabás B, Papp I. 2014. A morpho-physiological approach differentiates bread wheat cultivars of contrasting tolerance under cyclic water stress . *Journal of Plant Physiology*. 171: 1256-1266.

Johnson E. 2009. Goodbye to carbon neutral: Getting biomass footprints right. *Environmental Impact Assessment Review* 29: 165–168.

Johnson GN. 2011. Physiology of PSI cyclic electron transport in higher plants. *Biochimica et Biophysica Acta*. 1807: 384-389.

Joliot P and Joliot A. 2002. Cyclic electron transfer in plant leaf. *Proc. Natl. Acad. Sci.USA* 99: 10209-10214.

Jureková Z, Dražić G. eds., 2011. External and internal factors influencing the growth and biomass production of short rotation woods genus Salix and perennial grass Miscanthus. Beograd: Fakultet zaprimenjenu ekologiju Futura. 176 pp.

Kana R, Vass I. 2008. Thermoimaging as a tool for studying light-induced heating of leaves. Correlation of heat dissipation with the efficiency of photosystem II photochemistry and non-photochemical quenching. *Environ.Exp.Bot*. 64: 90-96.

Kalaji HM, Govindjee, Bosa K, Koscielniak J, Zuk-Gołaszewskae K. 2011. Effects of salt stress on photosystem II efficiency and CO2 assimilation of two Syrian barley landraces. *Environmental and Experimental Botany*. 73: 64–72.

Klughammer C, Schreiber U. 1994. An improved method, using saturating light pulses, for the determination of photosystem I quantum yield via $P700^{+}$-absorbance changes at 830 nm. *Planta*. 192: 261-268.

Kono M, Noguchi K, Terashima I. 2014. Roles of the cyclic electron flow around PSI (CEF-PSI) and O_2-dependent alternative pathways in regulation of the photosynthetic electron flow in short-term fluctuating light in *Arabidopsis thaliana*. *Plant and Cell Physiology*. 55: 990-1004.

Kusumi K, Hirotsuka S, Kumamaru T, Iba K. 2012. Increased leaf photosynthesis caused by elevated stomatal conductance in a rice mutant deficient in SLAC1, a guard cell anion channel protein. *Journal of Exp. Botany*. 63: 5635-5644.

Kubota HF, Yoshimura Y. 2002. Estimation of photosynthetic activity from the electron transport rate of photosystem II in film-sealed leaf of sweet potato, *Ipomoea batatas* Lam. *Photosynthetica*. 40: 337–341.

Laisk A, Oja V, and Eichelmann H. 2008. Alternative and cyclic electron flow: Rate and role in potato leaves. In J. F. Allen, J. H. Gantt, J. H. Golbeck, and B. Osmond [eds.], Photosynthesis. Energy from the Sun: *14th International Congress on Photosynthesis* 913-916. Springer Netherlands.

Levitt J. 1980. Responses of plants to environmental stresses. Water, radiation, salt and other stresses Vol. II. Academic Press, New York. pp. 93-128.

Long SP, Farage PK, Garcia RL. 1996. Measurement of leaf and canopy photosynthetic CO_2 exchange in the field. *Journal of Experimental Botany*. 47: 1629-1642.

Lovelli S, Perniola M, Ferrara A, Di Tommaso T. 2007. Yield response factor to water (Ky) and water use efficiency of *Carthamus tinctorius* L. and *Solanum melongena* L. *Agricultural Water Management* 92: 73-80.

Lu C, Zhang J. 1999. Effects of water stress on photosystem II photochemistry and its thermostability in wheat plants. *Journal of Experimental Botany* 50: 1199-1206.

Lu S, Lu X, Zhao W, Liu Y, Wang Z and Omasa K. 2015. Comparing vegetation indices for remote chlorophyll measurement of white poplar and Chinese elm leaves with different adaxial and abaxial surfaces. PMID: 26034132, *J Exp Bot.* doi:10.1093/jxb/erv270.

Maggio A, Miyazaki S, Veronese P, Fujita T, Ibeas JI, Damsz B, Narasimhan M.L, Hasegawa PM, Joly RJ, Bressan RA. 2002. Does proline accumulation play an active role in stress-induced growth reduction. Plant J, 31: 699-712.

Mahajan S, Tuteja N. 2005. Cold, salinity and drought stresses: an overview. Arch Biochem Biophys 444: 139-158.

Marcelis LFM, Heuvelink E, Baan Hofman-Eijer LR, Den Bakker J, Xue LB. 2004. Flower and fruit abortion in sweet pepper in relation to source and sink strength. *Journal of Experimental Botany* 55: 2261-2268.

Marco G, Massacci A and Gabrielli R. 1988. Drought effects on photosynthesis and fluorescence in hard wheat cultivars grown in the field. *Physiologia Plantarum.* 74(2): 385–390.

Marschner H .1995. Mineral Nutrition of Higher Plants, Academic Press, London.

Maser P. 2002. Altered shoot/root Na^+ distribution and bifurcating salt sensitivity in Arabidopsis by genetic disruption of the Na^+ transporter AtHKT1. *FEBS Letters*. 531, 157–161.

McKendry P. 2002. Energy production from biomass (part 1): overview of biomass. *Bioresource Technology*. 83 : 37–46.

Mehta P, Jajoo A, Mathur S, Bharti S. 2010. Chlorophyll a fluorescence study revealing effects of high salt stress on Photosystem II in wheat leaves. *Plant Physiology and Biochemistry* 48: 16-20.

Milovanovic J, Dražic G, Ikanovic J, Jurekova Z, Rajkovic S. 2012. Sustainable production of biomass through Miscanthus giganteus plantantion development. *Annals of Faculty Engineering Hunedoara - International Journal of Engineering.* 10 (1) ISSN 1584- 2665, pp 79-82.

Miyake C, Miyata M, Shinzaki Y,Tomizawa K-I. 2005. CO_2 response of cyclic electron flow around PSI (CEF-PSI) in tobacco leaves-relative electron fluxes through PSI and PSII determine the magnitude of non-photochemical quenching (NPQ) of Chl fluorescence. *Plant and Cell Physiology* 64: 629-637.

Miyake, C. 2010. Alternative electron flows (water–water cycle and cyclic electron flow around PSI) in photosynthesis: molecular mechanisms and physiological functions. *Plant Cell Physiol*. 51: 1951–1963.

Moss DN and Musgrave RB. 1971. Photosynthesis and crop production. In: Brady NC (ed) *Advances in agronomy*, 23: 317-336. New York: Academic Press.

Munekage Y. 2002. PGR5 is involved in cyclic electron flow around photosystem I and is essential for photoprotection in Arabidopsis. Cell 110, 361–371.

Munekage Y, Hashimoto M, Miyake C, Tomizawa KI, Endo T, Tasaka M, Shikanai T .2004. Cyclic electron flow around photosystem I is essential for photosynthesis. *Nature*. 429: 579–582.

Munns R, Guo J, Passioura JB & Cramer GR. 2000. Leaf water status controls day-time but not daily rates of leaf expansion in salt-treated barley. *Australian Journal of Plant Physiology* **27**, 949–957.

Munns R. 2002. Comparative physiology of salt and water stress. *Plant, Cell and Environment.* 25: 239–250.

Munns R & James RA .2003. Screening methods for salinity tolerance: a case study with tetraploid wheat. *Plant and Soil.* 253: 201–218.

Munns R and Tester M. 2008. Mechanism of salinity tolerance. *Annu Rev Plant Biol.* 59: 651–681.

Naidu CV and Swamy PM. 1995. Seasonal pattern of photosynthetic rate and its relationship with chlorophyll content, ribulose-l,5-bisphosphate carboxylase activity and biomass production. *Biologia Plantarum.* 37(3): 349-354.

Nicolas ME, Munns R, Samarakoon AB, Gifford RM.1993. Elevated CO_2 improves the growth of wheat under salinity. *Australian Journal of Plant Physiology*. 20, 349–360. doi:10.1071/PP9930349.

Oukarroum A, Madidi SE, Schansker G, Strasser RJ. 2007. Probing the responses of barley cultivars (*Hordeum vulgare* L.) by chlorophyll a fluorescence OLKJIP under drought stress and re-watering. *Environ*. *Exp*. *Bot*. 60: 446.

Parida AK, Mittra B, Das AB. 2005. High salinity reduces the content of a highly abundant 23-kDa protein of the mangrove *Bruguiera parviflora*. *Planta*. 221: 135-140.

Paul MJ and Foyer CH. 2001. Sink regulation of photosynthesis. *Journal of Experimental Botany*. 52: 360, pp. 1383-1400, ISSN 1460-2431.

Petrova G, Moyankova D, Nishii K, Forrest L, Tsiripidis I, Drouzas AD, Djilianov D, Möller M. 2015. The European paleoendemic *Haberlea rhodopensis* (Gesneriaceae) has an oligocene origin and a pleistocene diversification and occurs in a long-persisting refugial area in Southeastern Europe. *Int. J. Plant Sci.* 176: 499–514.

Pfündel EE. 2009. Deriving room temperature excitation spectra for photosystem I and photosystem II fluorescence in intact leaves from the dependence of F_V/F_M on excitation wavelength. *Photosynthesis Research* 100, 163–177.

Płazek A, Tatrzanska M, Maciejewski M, Koscielniak J, Gondek K, Bojarczuk J and Dubert F. 2013. Investigation of the salt tolerance of new Polish bread and durum wheat cultivars. *Acta Physiol Plant*. 35:2513–2523, DOI 10.1007/s11738-013-1287-9.

Price AH, Cairns JE, Horton P, Jones HG,Griffiths H. 2002. Linking drought-resistance mehcanisms to drought avoidance in upland rice using a QTL approach: progress and new opportunities to integrate stomatal and mesophyll responses. *Journal of Experimental Botany*. 53: 989-1004.

Rahnama A, James RA, Poustini K, Munns R. 2010. Stomatal conductance as a screen for osmotic stress tolerance in durum wheat growing in saline soil. *Functional Plant Biology*. 37: 255-263.

Rajendran K, Tester M, Roy SJ. 2009. Quantifying the three main components of salinity tolerance in cereals. Plant, Cell Environ 32(3): 237–249.

Rengasamy P .2006. World salinization with emphasis on Australia. *Journal of Experimental Botany*. 57, 1017–1023. doi:10.1093/jxb/erj108.

Rengasamy, North and Smith. 2010. Diagnosis and management of sodicity and salinity in soil and water in the Murray Irrigation region. The University of Adelaide, SA.

Roy SJ, Negrao S and Tester M. 2014. Salt resistant crop plants. *Current Opinion in Biotechnology* 2014, 26: 115–124.

Sairam RK and Tyagi A. 2004. Physiology and molecular biology of salinity stress tolerance in plants. *Current Science*, 86: 407–421.

Sárvári É, Mihailova G, Solti Á, Keresztes Á, Velitchkova M and Georgieva K. 2014. Comparison of thylakoid structure and organization in sun and shade *Haberlea rhodopensis* populations under desiccation and rehydration. *J. Plant Physiol.* 171:1591–1600.

Schansker G, Tóth SZ and Strasser RJ. 2005. Methylviologen and dibromothymoquinone treatments of pea leaves reveal the role of photosystem I in the Chl *a* fluorescence rise OJIP. *Biochimica et Biophysica Acta.* 1706: 250-261.

Schansker G, Tóth SZ, Holzwarth AR and Garab G. 2014. Chlorophyll a fluorescence: beyond the limits of the Q_A model. *Photosynth. Res.* 120: 43–58.

Schreiber U. 2004. Pulse-Amplitude-Modulation (PAM) fluorometry and saturation pulse method: an overview. Chlorophyll a Fluorescence 279-319. Springer, Netherlands.

Secenji M, Hideg É, Bebes A,Györgyey J. 2010. Transcriptional differences in gene families of the ascorbate–glutathione cycle in wheat during mild water deficit. *Plant Cell Reports* 29: 37-50.

Sedjo. 2013. Comparative life cycle assessments: Carbon neutrality and wood biomass energy. RFF DP 13-11. *Resources for the Future.* Washington DC.

Sharma DK, Andersen SB, Ottosen CO, Rosenqvist E. 2015. Wheat cultivars selected for high Fv/Fm under heat stress maintain high photosynthesis, total chlorophyll, stomatal conductance, trandspiration and dry matter. *Physiologia Plantarum.* 153:2, pp. 284-298.

Singh R, Naskar J, Pathre UV, Shirke PA. 2014. Reflectance and cyclic electron flow as an indicator of drought stress in cotton (*Gossypium hirsutum*). *Photochemistry and Photobiology* 90: 544-551.

Solti Á, Lenk S, Mihailova G, Mayer P, Barócsi A, Georgieva K. 2014. Effects of habitat light conditions on the excitation quenching pathways in desiccating *Haberlea rhodopensis* leaves: an Intelligent FluoroSensor study. *J. Photochem. Photobiol.* 130: 217-225.

Solti A, Müller B, Czech V, Sárvári É, Fodor F. 2014a. Functional characterization of the chloroplast ferric chelate oxidoreductase enzyme. *New Phytologist.* 202(3):920-928. doi: 10.1111/nph.12715.

Solti A, Mihailova G, Sárvári1 É, Georgieva K. 2014b. Antioxidative defence mechanisms contributes to desiccation tolerance in Haberlea rhodopensis population naturally exposed to high irradiation. *Acta Biol Szeged*. 58(1):11-14.

Strasser RJ, Srivastava A, and Tsimilli-Michael M. 2000. The fluorescence transient as a tool to characterize and screen photosynthetic samples. In M. Yunus and U. V. Pathre [eds.], Probing photosynthesis: Mechanisms regulation and adaptation 443-480. Taylor & Francis, New York.

Strasser RJ, Tsimilli-Michael M, and Srivastava A. 2004. Analysis of the chlorophyll *a* fluorescence transient. In G. C. Papageogriou and Govindjee [eds.], Chlorophyll Fluorescence: A Signature of Photosynthesis 321-362. Springer Netherlands.

Strasser RJ, Tsimilli-Michael M, Qiang S, Goltsev V. 2010. Simultaneous in vivo recording of prompt and delayed fluorescence and 820-nm reflection changes during drying and after rehydration of the resurrection plant Haberlea rhodopensis. *Biochim Biophys Acta* 1797: 1313–1326.

Strauss AJ, Krüger GHJ, Strasser RJ,Van Herdeen PDR. 2006. Ranking of dark chilling tolerance in soybean genotypes probed by the chlorophyll *a*

fluorescence transient O-J-I-P. *Environ. Exp. Bot.* 56: 147-157.

Stirbet A and Govindjee. 2011. On the relation between the kautsky effect (chlorophyll a fluorescence induction) and photosystem II: basics and applications of the ojip fluorescence transient. *J. Photoch. Photobio. B.* 104: 236–257.

Szalonek M, Sierpien B, Rymaszewski W, Gieczewska K, Garstka M, Lichocka M, Sass L, Paul K, Vass I, Vankova R, Dobrev P, Szcsesny P, Marczewski W, Krusiewicz D, Strzelczyk-Zyta D, Hennig J,Konopka-Postupolska D. 2015. Potato annexin STANN1 promotes drought tolerance and mitigates light stress in transgenic *Solanum tuberosum* L. plants. *PloS One* 10: e0132683. doi:10.1371/journal.pone.0132683.

Takahashi F, Tilbrook J, Tritterman C, Berger B, Roy SJ, Seki M, Shinozaki K, Tester M. 2015. Comparison of leaf sheath transcriptome profiles with physiological traits of bread wheat cultivars under salinity stress. *PLoS One*. 10(8): e0133322. doi:10.1371/journal.pone.0133322.

Talai JM .2010. Biological and economic peculiarities of newly developed wheat varieties. *Proceedings of ANAS (Biological Sciences)*, 65(5-6): 216-223.

Taiz L, Zeiger E. 2010. *Plant Physiology*. Response and Adaptation to Abiotic Stress. Sinauer Associates, Inc. Publishers, Sunderland, MA. ISBN 978-0-87893-866-7.

Teizer B .2010. Novel selection criteria for drought tolerant winter wheat genotypes and their correlations to drought stress indicators, crop development, plant morphology, yield and quality parameters. Master / Diploma Thesis - Institut für Pflanzenbau und Pflanzenzüchtung (IPP), BOKU-Universität für Bodenkultur, pp 95.

Tsimilli-Michael M and Strasser R J. 2008. In vivo assessment of stress impact on plant's vitality: Applications in detecting and evaluating the beneficial role of mycorrhization on host plants. Mycorrhiza. *State of the Art, Genetics and Molecular Biology, Eco-Function, Biotechnology, Eco-Physiology, Structure and Systematics,* 679-703. Springer , Berlin Heidelberg.

Toldi O, Tuba Z, Scott P. 2009. Vegetative desiccation tolerance: Is it a goldmine for bioengineering crops? *Plant Science*. 176: 187-199.

Tóth SZ, Schansker G, Strasser RJ. 2007. A non-invasive assay of the plastoquinone pool redox state based on the OJIP-transient. *Photosynth. Res.* 93: 193–203.

Trtilek M, Kramer DM., Koblizek M, Nedbal L. 1997. Dual-modulation LED kinetic fluorometer. *J. Lumin.* 72-74:597-599.

Van Loon CD. 1981. The effect of water stress on potato growth, development and yield. *American Potato Journal*. 58: 51- 69.

Vass I, Kirilovsky D, Etienne A-L. 1999. UV-B radiation-induced donor- and acceptor-side modifications of photosystem II in the cyanobacterium *Synechocystis* sp. PCC 6803. *Biochemistry.* 38: 12786-12794.

Wang W, Vinocur B, Altman A .2003. Plant responses to drought, salinity and extreme temperatures: towards genetic engineering for stress tolerance. *Planta.* 218: 1–14.

Wellburn AR. 1994. The spectral determination of chlorophylls a and b, as well as total carotenoids, using various solvents with spectrophotometers of different resolution. *J. Plant Physiol*ogy.144: 307–313.

Xoconostle-Cazares B, Ramirez-Ortega FA, Flores-Elenes L and Ruiz-Medrano R. 2011. Drought tolerance in crop plants. *American Journal of Plant Physiology*. DOI: 10.3923/ajpp.2011.

Yamori W, Shikanai T and Makino A. 2015. Photosystem I cyclic electron flow via chloroplast NADH dehydrogenase-like complex performs a physiological role for photosynthesis at low light. *Scientific Reports.* 5:13908; DOI: 10.1038/srep13908.

Yan K, Shao H, Shao C, Zhao S, Brestic M. 2013. Dissection of photosynthetic electron transport process in sweet sorghum under heat stress. *Plos One* 8: e62100. doi:10.1371/journal.pone.0062100.

Yancey PH, Clark ME, Hand SC, Bowlus RD, Somero GN. 1982. Living with water stress: Evolution of osmolyte systems. *Science* 217: 1214-1222.

Yancey PH.1994. Compatible and counteracting solutes, In Cellular and Mol. Physiol. of Cell Volume. Edited by Strange K. Boca Raton: CRC Press, pp. 81-109.

Yordanov I, Velikova V & Tsone V. 2000. Plant response to drought, acclimatation and stree tolerance. *Photosynthetica.* 30: 171-186.

Yordanov I, Velikova V, Tsonev T. 2003. Plant responses to drought and stress tolerance. *Bulgarian Journal of Plant Physiology. Special Issue* 187-206.

Zhang H-B, Xu D-Q. 2003. Role of light-harvesting complex 2 dissociation in protecting the photosystem 2 reaction centres against photodamage in soybean leaves and thylakoids. *Photosynthetica* 41: 383-391.

Zhu JK. 2002. Salt and Drought Stress Signal Transduction in Plants. *Annual Review of Plant Biology*, 53, 247-73.

Zivcak M, Brestic M, Olsovska K, Slamka P. 2008. Performance index as a sensitive indicator of water stress in *Triticum aestivum* L. *Plat Soil Environ.* 54: 133-139.

Zivcak M, Brestic M, Balatova Z, Drevenakova P, Olsovska K, Kalaji HM, Yang X, Allakhverdiev SI. 2013. Photosynthetic electron transport and specific photoprotective responses in wheat leaves under drought stress. *Photosynthesis Research* 117: 529-546.

Zivcak M, Kalaji HM, Shao H-B, Olsovska K, Brestic M. 2014. Photosynthetic proton and electron transport in wheat leaves under prolonged moderate drought stress. *J.Photochem.Photobiol.B.* 137: 107-115.

Zulfugarov IS, Mishra SR, Lee C-H. 2010. Quantitative analysis of cyclic electron flow in rice plants (*Oryza sativa L*.) lacking PsbS protein of Photosystem II. *Proc.ANAS (Biological Sciences)* 65: 90-95.

Zwart A and PrometheusWiki contributors, "r and R^2," PrometheusWiki, http://www.publish.csiro.au/prometheuswiki/tiki-pagehistory.php?page=r and R2&preview=12 (accessed March 22, 2016).

6. SUMMARY OF FINDINGS

Our primary interest in the present work was to correlate natural variations of physiological responses using photosynthetic and plant phenotyping tools. Our correlations and characterisation can be useful for the breeders who could select the varieties according to the stress resistance related beneficial properties plants. The results obtained by the application of our low cost stress diagnostic system will also be useful for taking precautionary measures against various stresses before visual symptoms appear.

- **Characterization of biomass and grain yield under severe drought**

Non-invasive photosynthetic measurements provide highly useful tools for making reliable predictions of physiological traits of wheat and other plants. Our findings demonstrate that the agronomically highly important traits of biomass and grain yield are not necessarily correlated in wheat and possibly in other cereal crops. Therefore, phenotyping of biomass responses alone is not sufficient for predictions of grain yield changes. As a consequence, phenotyping protocols should include grain yield assessment when the aim is the optimization of grain yield and grain yield stability under stress conditions.

Our results support the importance of cyclic electron flow in drought stress tolerance. We can also conclude that changes in physiological parameters show different responses to drought stress depending on the developmental stage of leaves in the case of the studied two cultivars. Flag leaves, which serve as grain supporting leaves show similar response in their CO_2 fixation, drought factor index, and electron transport parameters as the grain yield, whereas the secondary leaves, which support overall green biomass growth show similar responses as biomass accumulation. These

findings are warranted by the presented results for the Cappelle Desprez and Plainsman V cultivars.

- **Characterization of biomass and grain yield traits under salinity and drought**

The responses of wheat to different stress conditions have been analysed and revealed differences in the effects of salt and drought stress in various wheat cultivars from different geographical regions (Azerbaijan, Serbia and Austria).

The rate on net photosynthesis, measured by CO_2 gas exchange, was also affected most significantly by the combination of salt stress and water limitation. Accumulation of the osmoprotectant proline, was affected only to a small extent by water limitation and salt stress when applied separately, but proline was induced significantly by the combined application of the two stress factors. At the same time, biomass and grain yield were significantly reduced in drought as well as drought plus salt stress combination due to stomatal closure in the source region and decreased carbon partitioning from the sink region, respectively. But the minor effect of salt stress under well watered condition shows that agricultural crop loss due to salinity could be prevented by providing normal irrigation.

- **Electron transport responses in desiccating *Haberlea* ecotypes**

Compared to the widely investigated, more common shade acclimated one, the high irradiance acclimated ecotype of *Haberlea rhodopensis* performs more effective protective mechanism in its photosynthesis. Under drought stress, the CEF is enhanced together with constant thermal energy dissipation of the PSII, whereas under severe desiccation, the PSII complex becomes inactive and acceptor-side

limitation factors start to inhibit the PSI function. Under rehydration, the photosynthetic function recovers rapidly together with an increase in the CEF that may contribute to the energy-dependent recovery processes in the metabolism. In contrast, the shade ecotype showed these protective mechanisms only under severe desiccation and upon rewatering, all the recovery processes proved to be slower resulting in a significantly delayed restoration of the photosynthetic functions. Therefore, growing conditions and acclimation processes on the natural habitat strongly influence the desiccation tolerance of this homoiochlorophyllous resurrection plant species.

- **Photosynthetic efficiency of willows developed by genome duplication**

Higher net CO_2 uptake rate and increased transpiration through leaves of tetraploid willows plays a significant role in enhanced growth and biomass production for the energy willow *Salix viminalis* L. Light response curves of PSI and PSII revealed higher electron trnasport rates in the tetraploid leaves analyzed from plants grown under both field and greenhouse conditions. Chlorophyll and carotenoid levels were observed to be significantly higher in tetraploid willow genotypes grown in field conditions, which substantiate the functional characteristics for photosynthetic efficacy.

7. ÖSSZEFOGLALÁS

Munkánk célja a növényi biomassza-növekedés jellemzése volt fotoszintetikus mérések és komplex fenotipizálási megközelítés alkalmazásával. Az általunk felderített összefüggések és stresszindikátorok fontos alkalmazást nyerhetnek fokozott stressztoleranciával rendelkező növényi vonalak kiválasztásában.

- **A biomassza és terméshozam jellemzése búzanövényekben szárazságstressz alatt**

A nem invazív fotoszintézis mérési módszerek hatékony eszközt biztosítanak a búza és egyéb növények fiziológiai sajátságainak jellemzésére. A Cappelle Desprez és Plainsman V modell búzafajtákon végzett vizsgálataink eredményei azt mutatják, hogy olyan mezőgazdaságilag is fontos tulajdonságok, mint a biomassza és terméshozam nem feltétlenül függenek össze a búzában és egyéb gabonanövényekben. Ezért a biomassza-válaszok fenotipizálása önmagában nem elegendő a terméshozamban bekövetező változások előrejelzésére. Ennek következtében a fenotipizálási protokolloknak tartalmazniuk kell a terméshozam-felmérést is, ha a cél a hozam optimalizálása és stabilitás biztosítása stresszkörülmények között.

Az eredmények megerősítik a ciklikus elektrontranszport-folyamatok jelentőségét a szárazságtűrésben. Azt is megállapíthatjuk, hogy az élettani paraméterek változásai különböző válaszokat mutatnak a levelek fejlettségi állapotától függően. A magfejlődést közvetlenül meghatározó zászlóslevelek élettani jellemzőinek (széndioxid-fixáció, szárazságfaktor index, elektrontranszport paraméterek) változásai összefüggést mutatnak a terméshozammal. Ugyanakkor a

másodlagos levelek jellemzői hasonló összefüggéseket mutatnak a zöld biomassza felhalmozódásának tekintetében.

- **A biomassza és terméshozam tulajdonságainak jellemzése búzanövényekben só- és szárazságstressz alatt**

A növényi stresszválaszok komplex jelemzésére kifejlesztett módszer feltárta a búzanövényekben só- és szárazságstressz által okozott hatásokban mutatkozó eltéréseket a különböző földrajzi területekről (Azerbajdzsán, Szerbia és Ausztria) származó fajták esetén. A nettó fotoszintézis mértéke, a Co2 gázcserét vizsgálva, szintén érzékenynek mutatkozott a só- és szárazságstressz kombinációjára. A prolin, ozmotikus védő fehérje, felhalmozódását a külön külön alkalmazott só- és szárazságstressz nem befolyásolta számottevően, ellenben amikor a két stresszfaktor egyszerre volt jelen a prolin termelődés jelentősen nőtt. A biomassza-produkció és a terméshozam jelentős csökkenést mutatott szárazság esetén és kombinált só- és szárazság stressz körülményei között, aminek oka a sztómazáródás miatt csökkent mértékű CO_2-fixálás, illetve a csökkent mennyiségű szervesanyag-allokáció a magok irányába. A megfelelő talajnedvesség mellett elhanyagolható hatást okozó sóstressz arra utal, hogy megfelelő öntözéssel megelőzhető a talaj magas sótartalma miatt bekövetkező termésveszteség.

- **Elektrontranszport válaszok alacsony és magas fényintenzitásokhoz adaptálódott *Haberlea* ökotípusokban**

A *Haberlea rhodopensis* növények rendelkeznek azzal a kölönleges tulajdonsággal, hogy víztartalmuk 95 %-ának elvesztése után is képesek fotoszintetikus és fiziológiai aktivitásuk visszaállítására. Eredményeink szerint a gyakrabban vizsgált és elterjedtebb árnyékos fényviszonyokhoz adaptálódott

Haberlea rhodopensis ökotípussal szemben a magasabb fényintenzitásokhoz akklimatizálódott *Haberlea* ökotípus sokkal hatékonyabb fotoszintézis védelmi mechanizmusokkal rendelkezik. Szárazságstressz hatására a lineáris elektrontranszport folyamatok fokozatosan gátlódnak, ezzel párhuzamosan a fotoprotektív ciklikus elektron transzport (CEF) hatékonysága megnövekszik. Rehidratáció alatt a fényadaptált ökotípus esetén a fotoszintetikus funkciók gyorsan visszaállnak hidratált levelekre jellemző értékekre. Ezzel ellentétben az árnyékadaptált ökotípus esetén a regenerációs lépesek lassabbnak bizonyultak, ami a fotoszintetikus funkciók késleltetett visszaállítását jelentette.

- **Tetraploid energiafűz fotoszintetikus hatékonyságának jellemzése**

A tetraploid fűzvonalak magasabb nettó CO_2-felvételéről és levél gázcsere-értékeiről kimutattuk, hogy jelentős szerepet játszanak a fás szárú *Salix Viminalis* gyorsabb növekedésében és hatékonyabb biomassza-termelésében. A PSI és PSII fotokémiai rendszerek hatékonysága magasabb a tetraploid vonalak leveleiben a kontroll diploid vonalakhoz képest mind szántóföldi, mind üvegházi körülmények között. A tetraploid fűz genotípusokban megfigyelhető klorofill- és karotinoid-tartalom is lényegesen magasabb volt, mint a diploid kontrollban, ami a fotoszintetikus hatékonyság funkcionális alapjának lényeges eleme.

PUBLICATION LIST (MTMT ID: 10031509)

8.1. Publications related to the Phd thesis:

- **Paul K**, Pauk J, Deák Z, Sass L, Vass I. 2016. Contrasting response of biomass and grain yield to severe drought in Cappelle Desprez and Plainsman V wheat cultivars. *PeerJ*. 4:e1708; DOI 10.7717/peerj.1708. **IF: 2.1**
- Dudits D, Török K, Cseri A, **Paul K**, Nagy AV, Nagy B, Sass L, Ferenc G, Vankova R, Dobrev P, Vass I and Ayaydin F. 2016. Response of organ structure and physiology to autotetraploidy in early development of energy willow *Salix viminalis* L. *Plant Physiology.* Vol. 170, pp. 1504–1523**. IF: 6.84**

8.2. Other peer-reviewed publications:

- Szalonek M, Sierpien B, Rymaszewski W, Gieczewska K, Garstka M, Lichocka M, Sass L, **Paul K**, Vass I, Vankova R, Dobrev P, Szcsesny P, Marczewski W, Krusiewicz D, Strzelczyk-Zyta D, Hennig J, Konopka-Postupolska D. 2015. Potato annexin STANN1 promotes drought tolerance and mitigates light stress in Transgenic Solanum tuberosum L. plants *PLoS ONE* 10(7): e0132683. doi:10.1371/journal.pone.0132683. **IF: 3.23**
- Vass IZ, Deák Z, **Paul K**, Kovács S, Vass I. 2015. Interaction of nanoparticles with biological systems. *Acta Biol Szeged* Volume 59 (Suppl.2): 225-245.
- **Paul K**, Deák Z, Csösz M, Purnhauser L and Vass I. 2011. Characterization and Early detection of Tan Spot Disease in Wheat *in vivo* with Chlorophyll Fluorescence Imaging. *Acta Biologica Szegediensis*; Volume 55(1): 87-90.

8.3. Manuscripts under preparation

- **Paul K,** Vass I and Solti A. 2016. Ecotype-level differences in the electron flow under desiccation and rehydration of the resurrection plant *Haberlea rhodopensis*. (*manuscript submitted*)
- **Paul K**, Pauk J, Kondic-Spika A, Cseri A, Grausgruber H, Allahverdiyev T, Deák Z, Sass L and Vass I. 2016. Synergistic effects of salt and drought stress in wheat studied by high throughput phenotyping and photosynthetic measurements. (*manuscript under preparation*)
- **Paul K**, Großkinsky D, Vass I and Roitsch T. 2016. Silver nanoparticles mitigates the *Arabidopsis thaliana- Pseudomonas syringae* infection. (*manuscript under preparation*)
- Keller B, Muller O, Matsubara S, Kolber Z, **Paul K**, Pieruschka R, Vass I, Rascher U. Electron transport time constants derived by light induced fluorescence transient (LIFT) method were validated and revealed cold response in the dark before photo inhibition took place. (*manuscript under preparation*)
- Digruber T, Sass L, Cseri A, **Paul K**, Nagy AV, Remenyik J, Molnár I, Vass I, Toldi O, Gyuricza C and Dudits D. 2016. Stimulation of biomass productivity of short rotation energy willow by pre-plantation treatment of stem cuttings with triacontanol or seeweed extract. (*manuscript under preparation*)
- Pesti R, Molnár J, **Paul K**, Vass I, Tusnády GE, Zoltán H and Várallyay E. Investigation of gene expression changes in virus infected tobacco and tomato plants. (*manuscript under preparation*)

9. CONFERENCE ABSTRACTS

9.1. Oral presentations

- **Paul K,** Vass I and Solti A. Photosynthetic electron transport responses in detached leaves of two ecotypes of the resurrection plant *Haberlea rhodopensis* grown under natural habitat. Plant Biology Europe FESPB/EPSO 2016 Congress, 26 - 30th June 2016, Prague, Czech Republic.
- **Paul K,** Pauk J, Deák Z, Sass L, Vass I - Non-invasive plant phenotyping using photosynthetic tools to characterise 'biomass and grainyield' under water stress in wheat, COST FA 1306, Ist General meeting, June 22-24, 2015, IPK Gatersleben, Germany, pp.40.
- **Paul K**, Sass L, Cseri A, Deák Z, Pauk J, Kondic Spika A, Dudits D, Vass I. Plant phenotyping as a tool in optimizing crop productivity. Plant Biology Europe FESPB/EPSO 2014 Congress, 22nd - 26th June 2014, Dublin, Ireland, pp.94. (O103)
- **Kenny Paul*** - Application of various imaging techniques in plant stress diagnostics. Szegedi Biológus Doktorandusz Konferencia, 19- 20 May, 2014, Szeged, Hungary.
- **Paul K,** Deák Z, Sass L and Vass I. Application of non-invasive phenotyping approaches to characterize responses of wheat plants to water stress. Phenodays Conference, October 16th to 18th 2013, Kasteel Vaalsbroek, Netherlands, pp.30.
- **Kenny Paul*** - Testing leaf infections of wheat by digital photography and chlorophyll fluorescence imaging. Workshop on complex plant stress diagnostics "Improvement of cereals for conventional production and

biofarming" Biocereal HUSRB/1002/214/045/02, 25th September 2013, Biological Research Centre, Szeged, Hungary.

- **Kenny Paul*** - Practical demonstrations on (i) Measurement of photosynthetic electron transport by Dual PAM (PSII + PSI) and (ii) Measurement of photosynthetic parameters by portable Chl fluorometers and Chl fluorescence imaging. June 30th -July 7th 2013, EPPN Summer School on Plant Phenotyping, Szeged, Hungary.
- **Paul Kenny*** - Application of imaging techniques for characterization and early detection of fungal infections in wheat leaves. 2nd ITC Alumni Conference on "Multidisciplinary Approaches to Biological Problems", 1-3rd September 2011, Biological Research Centre- HAS, Szeged, Hungary, pp.37.

9.2. Poster presentations

- **Paul K**, Vass I and Solti A. Electron flow responses in the ecotype level differences under desiccation and rehydration of the resurrection plant *Haberlea rhodopensis.* 2nd general COST MEETING. 18th - 20th of April 2016. Copenhagen, Denmark.
- Pesti R, **Paul K**, Vass I, Zoltán H and Várallyay É. A vírusfertőzés tüneteinek kialakulásában szerepet játszó génexpressziós változások vizsgálata. a 62. Növényvédelmi Tudományos Napok 2016, február 16. A Magyar Növényvédelmi Társaság 8. közgyűlésére, Széchenyi István tér 9, 1051 Budapest, pp.25.
- Vass I, **Paul K**, Pauk J, Kondic-Spika A, Grausgruber H, Allahverdiyev T, Deák Z, Sass L (2015) Synergistic effects of salt and drought stress on the

growth and photosynthetic parameters of wheat. COST FA 1306, Ist general meeting, June 22-24, 2015, IPK Gatersleben, Germany. pp.52.

- **Paul K,** Deák Z, Sass L and Vass I. Non invasive plant phenotyping by using photosynthetic tools. 3rd International Plant Phenotyping Symposium 17- 19 February 2014, Chennai, India, pp.40. (S 01)
- Digruber T, Sass L, **Paul K**, Molnár I, Vass I, Gyuricza C, Dudits D. Development of stimulation technologies to increase the biomass production of energy willow plants (*Salix* sp.). A Magyar Növénybiológiai Társaság XI. Kongresszusa 2014. Augusztus 27 - Augusztus 29. Szeged, MTA Szegedi Biológiai Kutatóközpont, pp.10.
- **Paul K**, Deák Z, Csösz M, Purnhauser L and Vass I. Application of chlorophyll fluorescence imaging for early plant disease diagnosis. 29 July to 3 August 2012, FESPB/EPSO Plant Biology Congress 2012, Freiburg, Germany. (P520)
- **Kenny P**, Deák Z, Csösz M, Purnhauser L and Vass I. Characterization and Early detection of Tan Spot Disease in Wheat *in vivo* with Chlorophyll Fluorescence Imaging. A Magyar Növénybiológiai Társaság X. Kongresszusa, 31st August- 2nd September 2011, Szeged, Hungary, pp.10. (S3- P04)